

An-Najah National University

Faculty of Graduate Studies

**Improvement of Electrical Grid – Quality
Parameters by LC-Filters, at Supplying of Power
Electronics Converters**

By

Asma' Shara'b

Supervisor

Prof. Marwan M. Mahmoud

**This Thesis is Submitted in Partial Fulfillment of the Requirements
for the Degree of Master of Electrical Power Engineering, Faculty of
Graduate Studies, An-Najah National University, Nablus-Palestine.**

2018

**Improvement of Electrical Grid-Quality Parameters
by LC-Filters, at Supplying of Power Electronics
converters**

By

Asma' Shara'b

This Thesis was Defended Successfully on 22/3/2018 and approved by:

Defense Committee Members

Signature

- | | |
|--|--------------|
| 1. Prof. Marwan M. Mahmoud / Supervisor | |
| 2. Prof. Abedl karim Daud / External Examiner | |
| 3. Dr. Moien Omar / Internal Examiner | |

III

Dedication

This thesis is dedicated to:

The sake of Allah, my creator and my master,

My great teacher and messenger, Mohammed (May Allah bless and grant him), who taught us the purpose of life,

My homeland Palestine, the warmest womb,

The great martyrs and prisoners, the symbol of sacrifice,

An -Najah University, my second magnificent home,

My great parents, who never stop giving of themselves in countless ways,

My beloved brothers and sisters, who stand by me when things look bleak,

To all my family, the symbol of love and giving,

My friends who encourage and support me, all the people in my life who touch my heart, I dedicate this research.

Acknowledgments

By the Name of Allah, the Most Merciful, the Most Compassionate. All praise be to Allah, the Lord of the world. Prayers and peace be upon Mohammed; his servant and messenger.

First and foremost, praises and thanks to the God, the Almighty, for His showers of blessings throughout my research work to complete this thesis successfully.

I would like first to express special appreciation and my deepest sense of gratitude to my advisor Professor **Marwan Mahmoud** for his dynamism, vision, sincerity and motivation he has deeply inspired in me. He has taught me the methodology to carry out the thesis and to present the research work as clearly as possible. It was a great privilege and honor to work and study under his guidance. I am extremely grateful for what he has offered me. I would also like to thank him for his friendship and empathy. His guidance helped me through research and writing of this thesis. I could not have imagined having a better advisor and mentor for my study.

I owe a deep debt in gratitude to our university for giving us an opportunity to complete this work.

Last, but not least, I would thank my family. Words cannot express how grateful I am to them for their generous support; they provided me throughout my entire life and particularly through the process of pursuing my Master's degree. Because of their unconditional love, I have got the chance to complete this thesis.

Unfortunately, I cannot thank everyone by name because it would take a lifetime but, I just want you all to know that you count so much. Had it not been for all your prayers and benedictions; were it not for your sincere love and help, I would never have completed this thesis, so thank you all.

الإقرار

أنا الموقع أدناه مقدم الرسالة التي تحمل العنوان:

Improvement of Electrical Grid – Quality Parameters by LC-Filters, at Supplying of Power Electronics Converters

أقر بأن ما اشتملت عليه هذه الرسالة هو نتاج جهدي الخاص، باستثناء ما تمت الإشارة إليه حيث ورد، وأن هذه الرسالة ككل أو أي جزء منها لم يقدم من قبل لنيل أي درجة أو لقب علمي أو بحثي لدى أي مؤسسة تعليمية أو بحثية أخرى.

Declaration

The work provided in this thesis, unless otherwise referenced, is the researcher's own work, and has not been submitted elsewhere for any other degrees or certifications.

Student's Name:

أسم الطالب:

Signature:

التوقيع:

Date:

التاريخ:

VII
Table of Contents

No	Subject	Pages
	Dedication	III
	Acknowledgments	IV
	Declaration	VI
	List of Tables	X
	List of Figures	XII
	List of Abbreviations	XX
	Abstract	XXII
	Chapter One: Introduction	1
1.1	Project Background	1
1.2	Objectives of the Study	5
1.3	Thesis Outline	5
	Chapter Two: Problem Statement	7
2.1	Power Electronic Conversion	7
2.2	Converters Classification	8
2.3	AC-DC Converters	8
2.4	Uncontrolled Full Wave Bridge Rectifier	9
2.5	Single Phase Full Wave Bridge Diode Rectifier	11
2.5.1	Effects of the rectifier on AC mains	12
2.5.2	System simulation	15
2.5.3	Performance parameters	17
2.6	Controlled Full Wave Bridge Rectifiers	19
2.6.1	RL - load, continuous current	20
2.6.2	System simulation	22
2.6.3	Determination of the circuit parameters	27
2.6.4	Representation in decibel form (dB)	32
	Chapter Three: Background and Literature Review	36
3.1	Power Quality	36
3.2	Nonlinear Loads	37
3.3	Basic Harmonic Concepts	38
3.3.1	Types of harmonics	39
3.3.2	Causes and sources of harmonics	41
3.3.2.1	Causes	41
3.3.2.2	Soures	43
3.3.3	Types of harmonic sources	44
3.3.4	How harmonics are generated	46
3.3.5	Harmonic mitigation measures	50
3.3.6	Harmonics impacts on power system components	50
3.3.7	Harmonic limit standards	50
3.3.8	Total harmonic distortion	52
3.3.9	Harmonics and system power factor	52
3.3.9.1	Power factor in systems with only linear loads	52

3.3.9.2	Power factor in power system with nonlinear loads	53
3.4	Power Filter Topologies	55
3.5	Harmonic Filter	55
3.5.1	Passive Filter	57
3.5.1.1	Passive shunt filters	58
3.5.1.2	Passive series filters	60
3.6	Passive Filters Configuration	61
3.6.1	Low-pass filters	61
3.6.2	High-pass filters	62
3.6.3	Band-pass filters	63
3.6.4	Band-stop filters	64
3.7	Selection of Power Filters	65
3.8	Passive Filter for Different Circuits	66
3.8.1	Rectifier with resistive load	66
3.8.2	Rectifier with capacitive filter in the output side	67
3.8.3	Rectifier with LC- filter in the output side	67
3.8.4	Rectifier with series resonant filter	68
3.8.5	Rectifier with parallel resonant filter	69
3.8.6	Rectifier with improved passive wave shaping filter	70
3.8.7	Rectifier with AC-side inductor	73
3.8.8	Rectifier with shunt LC- filter	73
3.8.9	Rectifier with LCL- third order low pass filter	76
3.8.10	Rectifier with harmonic trap filter	77
	Chapter Four: Results and Analysis	79
4.1	L-Filter- First Order	80
4.1.1	System simulation using L- filter	81
4.1.2	Determination of the circuit parameters	86
4.1.3	Efficiency	90
4.1.4	Representation in decibel form (dB)	91
4.1.5	Comparison between the obtained results	92
4.1.6	Filter cost	95
4.1.7	Comparison between the costs of the filters	96
4.1.8	Reactive power	96
4.2	Series Input Resonance LC-Filter (Band Pass)	97
4.2.1	System simulation using series input resonance filter.	98
4.2.2	Determination of the circuit parameters	104
4.2.3	Efficiency	108
4.2.4	Representation in decibel form (dB)	108
4.2.5	Comparison between the obtained results	109
4.2.6	Reactive power	110
4.3	Parallel Input Resonance LC- Filter (Band Stop)	111
4.3.1	System simulation using parallel input resonance filter	112
4.3.2	Determination of the circuit parameters	116

4.3.3	Efficiency	119
4.3.4	Representation in decibel form (dB)	120
4.3.5	Comparison between the obtained results	121
4.3.6	Reactive Power	123
4.4	Parallel LC-Filter in Series with Inductance L	123
4.4.1	System simulation using parallel LC-filter in series with inductor L	124
4.4.2	Determination of the circuit parameters	127
4.4.3	Efficiency	132
4.4.4	Representation in decibel form (dB)	132
4.4.5	Comparison between the obtained results	133
4.4.6	Reactive power	135
4.5	Second Order High Pass Filter	135
4.5.1	System simulation using second order high pass filter	136
4.5.2	Determination of the circuit parameters	139
4.5.3	Efficiency	142
4.5.4	Representation in decibel form (dB)	143
4.5.5	Comparison between the obtained results	144
4.5.6	Reactive power	146
4.6	Third Order High Pass T- Filter	146
4.6.1	System simulation using third order low pass filter	147
4.6.2	Determination of the circuit parameters	151
4.6.3	Efficiency	154
4.6.4	Representation in decibel form (dB)	155
4.6.5	Comparison between the obtained results	155
4.6.6	Reactive power	158
4.7	Third Order High Pass π - Filter	158
4.7.1	Reactive power	159
4.8	Conclusion	160
4.8.1	Performance parameters	161
4.8.2	Proper selection of filter configuraion	162
4.8.3	The summarized-comparative results	166
	Chapter Five: Conclusions and Future Work	171
5.1	Conclusions	171
5.2	Recommendations and Future Work	172
	References	174
	Appendix	182
	الملخص	ب

List of Tables

No	Subject	Pages
Table 2.1	Simulation specifications of an uncontrolled single phase full wave bridge rectifier with RL-load	14
Table 2.2	Frequency spectrum of the input current	16
Table 2.3	The complete parameters for uncontrolled single phase full wave bridge rectifier with RL-load	18
Table 2.4	Simulation specifications of controlled single phase full wave bridge rectifier with RL-load	22
Table 2.5	Frequency spectrum of the input current	24
Table 3.1	IEEE 519 standards for total harmonic voltage distortion [37]	51
Table 3.2	Comparison of the results obtained from the analyzed circuits	69
Table 3.3	Calculated power factor values of different values of capacitance C_b	72
Table 3.4	Simulated results for shunt LC- filter	75
Table 3.5	Simulated comparative results	76
Table 3.6	Components and specifications used in T-Filter	77
Table 4.1	Simulation specifications of controlled single phase full wave bridge rectifier with L-filter	82
Table 4.2	Harmonic of the input current	83
Table 4.3	Examples of calculated reactive power for different values of L-filter.	97
Table 4.4	Simulation specifications of controlled single phase full wave rectifier with series input resonance filter	100
Table 4.5	Frequency spectrum of the input current	101
Table 4.6	Examples of calculated reactive power for different values of series input resonance filter	111
Table 4.7	Simulation specifications of controlled single phase full wave rectifier with parallel input resonance filter	113
Table 4.8	Frequency spectrum of the input current	113
Table 4.9	Example of calculated reactive power for different values of parallel input resonance filter.	123
Table 4.10	Simulation specifications of controlled single phase full wave bridge rectifier with parallel LC-filter in series with inductance L	124
Table 4.11	Frequency spectrum of the input current	125
Table 4.12	Calculated parameter values of different values of L_3 .	133

Table 4.13	Examples of calculated reactive power for different values of parallel LC-filter in series with inductance L	135
Table 4.14	Simulation specifications of controlled single phase full wave bridge rectifier with second order high pass filter	136
Table 4.15	Frequency spectrum of the input current	137
Table 4.16	Examples of calculated reactive power for different values of second order high pass filter.	146
Table 4.17	Simulation specifications of controlled single phase full wave bridge rectifier with third order high pass T-filter rectifier.	147
Table 4.18	Frequency spectrum of the input current	148
Table 4.19	Examples of calculated reactive power for different values of third order high pass T- filter.	158
Table 4.20	Examples of calculated reactive power for different values of third order high pass π - filter	159
Table 4.21	Comparison between the results obtained from the various analyzed circuits	160
Table 4.22	The performance parameters of controlled full wave rectifier with RL-load and different input LC-filter topologies at firing angle of $\alpha=30^\circ$	161

Table of Figures

No	Subject	Pages
Figure 2.1	Classification of uncontrolled rectifier	10
Figure 2.2	Simplified schematic of uncontrolled single phase full wave bridge rectifier with RL- Load.	11
Figure 2.3	MATLAB/Simulink implementation circuit diagram of an uncontrolled single phase full wave bridge rectifier supplying RL- load	15
Figure 2.4	Input voltage and input current waveform for uncontrolled single phase full wave bridge rectifier with RL-load	16
Figure 2. 5	Harmonic input current spectrum for the uncontrolled single phase full wave bridge rectifier with RL- load	17
Figure 2.6	Simplified schematic of single phase full wave controlled rectifier with RL-Load	20
Figure 2.7	Output voltage waveform (a) for resistive load (b) for resistive inductive load (with continuous current conduction)[12].	22
Figure 2.8	MATLAB/Simulink implementation circuit diagram of controlled single phase full wave bridge rectifiers supplying RL- load	23
Figure 2.9	Input voltage and input current waveform for controlled single phase full wave bridge rectifiers with RL- load at $\alpha=30^\circ$	23
Figure 2.10	Frequency spectrum of input current spectrum for controlled single phase full wave bridge rectifier with RL- load (a) at $\alpha=30^\circ$ (b) at $\alpha=90^\circ$ (c) at $\alpha=120^\circ$	25
Figure 2.11	(a) THD of input current; (b) power factor for controlled single phase full wave bridge rectifiers with RL- load at $\alpha=30^\circ$, 90° and 120°	26
Figure2.12	FFT analysis of the input current for controlled single phase full wave rectifier with RL – load at $\alpha=30^\circ$	29
Figure 2.13	Output voltage waveform for controlled single phase full wave bridge rectifier with RL- load at $\alpha=30^\circ$	30
Figure 2.14	Output current waveform for controlled single phase full wave bridge rectifier with RL-load at $\alpha=30^\circ$	31
Figure 2.15	Input current spectrum in dB for controlled single phase full wave bridge rectifier with RL- load at $\alpha=30^\circ$	34
Figure 3.1	Distorted composite current waveform[32].	39
Figure 3.2	:Single phase two- pulse controlled rectifier as a source of harmonic generation and harmonic power flow [28]	42

Figure 3.3	Typical current-source nonlinear load (a) thyristors rectifier for DC drives, heater drives, etc. (b) per-phase equivalent circuit of thyristors rectifier [35]	45
Figure 3.4	Typical current-source nonlinear load (a) thyristors rectifier for DC drives, heater drives, etc. (b) per-phase equivalent circuit of thyristors rectifier [35]	45
Figure 3.5	Typical voltage and current waveforms of thyristors rectifier, source voltage V_{Sa} and line current I_{La} [35]	46
Figure 3.6	Typical current and voltage waveforms of diode rectifier, line current I_L , line-to-neutral voltage V_{La} , and line-to-line voltage V_{Lab} at rectifier input [35]	46
Figure 3.7	Current waveform in a linear load	47
Figure 3.8	Current waveform in non-linear load	48
Figure 3.9	Equivalent circuit of a non-linear load [32]	49
Figure 3.10	Power Factor vectors relationship (a) for non-linear load (b) for linear load [23]	53
Figure 3.11	AC input voltage vs. current relationships [23]	54
Figure 3.12	Classifications of power filters [9]	56
Figure 3.13	Passive harmonic shunt filter [32]	59
Figure 3.14	Passive series and shunt filters [32]	59
Figure 3.15	(a) Inductive low-pass filter (b) capacitive low-pass filter	61
Figure 3.16	(a) Capacitive high-pass filter (b) inductive high-pass filter	62
Figure 3.17	System level block diagram of a band-pass filter	63
Figure 3.18	System level block diagram of a band-pass filter	63
Figure 3.19	System level block diagram of a band-stop filter	64
Figure 3.20	“Twin-T” band-stop filter	64
Figure 3.21	(a) Single phase rectifier (b) input and output waveforms	66
Figure 3.22	(a) Single phase full wave bridge rectifier (b) input and output waveforms	67
Figure 3.23	(a) Single phase full wave bridge rectifier with LC-filter in the output side (b) FFT analysis of input current waveform for series resonant filter	68
Figure 3.24	(a) Single phase full wave bridge rectifier with series resonant filter (b) FFT Analysis of input current waveform for series resonant filter	68
Figure 3.25	(a) Single phase full wave bridge rectifier with for parallel resonant filter (b) FFT analysis of input current waveform for parallel resonant filter	69
Figure 3.26	Single phase full wave bridge diode rectifier using improved passive wave shaping method [28]	71

Figure 3.27	Variation of power factor with respect to capacitance C_b	72
Figure 3.28	Rectifier with AC-side inductor and inputs waveforms[11].	73
Figure 3.29	Input filter circuit per phase [11]	74
Figure 3.30	Simulation circuits and current harmonics spectrum of shunt LC- filter [49]	75
Figure 3.31	T-Filter with rectifier circuit [11]	77
Figure 3.32	Rectifier with harmonic trap filter and inputs waveforms[47]	78
Figure 4.1	Simplified schematic of controlled single phase full wave bridge rectifier with RL-load and input L –filter	81
Figure 4.2	MATLAB/Simulink implementation circuit diagram of controlled single phase full wave bridge rectifier with RL-load and input L-filter	81
Figure 4.3	Input voltage and input current waveform for controlled single phase full wave bridge rectifier with RL-load and L-filter at $\alpha=30^\circ$.	82
Figure 4.4	Frequency spectrum of input current spectrum for controlled single phase full wave bridge rectifier with RL-load and input L-filter (a) at $\alpha=30^\circ$ (b) at $\alpha=90^\circ$ (c) at $\alpha=120^\circ$	84
Figure 4.5	Comparison among the harmonic current spectrums for single phase full wave bridge rectifier with RL-load and input L-filter and without it	85
Figure 4.6	(a) THD of input current (b) power factor for controlled single phase full bridge with RL-load and input L-filter at $\alpha=30^\circ, 90^\circ, 120^\circ$	86
Figure 4.7	FFT analysis results of the input current for controlled single phase full wave bridge rectifier with RL-load and input L-filter at $\alpha=30^\circ$	87
Figure 4.8	Output voltage waveform for controlled single phase full wave bridge rectifier with RL-load and input L-filter at $\alpha=30^\circ$	88
Figure 4.9	Output current waveform for controlled single phase full wave bridge rectifier with RL-load and input L-filter at $\alpha=30^\circ$	90
Figure 4.10	Input current spectrum in dB for controlled single phase full wave bridge rectifier with RL-load and input L- filter at $\alpha=30^\circ$	91
Figure 4.11	(a) THD of the input current (b) input current harmonic (c) output voltage for controlled single phase full wave bridge rectifier with RL-load and various L-filter values at $\alpha=30^\circ$	92

Figure 4.12	Power factor for controlled single phase full wave bridge rectifier with RL-load and various L-filter values at $\alpha=30^\circ$	93
Figure 4.13	Input current waveform for controlled single phase full wave bridge rectifier with RL-load and L-filter (1mH) at $\alpha=30^\circ$	94
Figure 4.14	Simplified schematic of controlled single phase full wave bridge rectifier with RL-load and series input resonance filter	98
Figure 4.15	MATLAB/Simulink implementation circuit diagram of controlled single phase full wave bridge rectifier with RL-load and series input resonance filter	99
Figure 4.16	Input voltage and input current waveform for controlled single phase full wave bridge rectifier with RL-load and series input resonance filter at $\alpha=30^\circ$	100
Figure 4.17	Frequency spectrum of input current for controlled single phase full wave bridge rectifier with RL-load and series input resonance filter (a) at $\alpha=30^\circ$ (b) at $\alpha=90^\circ$ (c) at $\alpha=120^\circ$	102
Figure 4.18	(a) THD of input current (b) power factor for controlled single phase full wave bridge rectifier with RL-load and series input resonance filter at $\alpha=30^\circ, 90^\circ, 120^\circ$.	103
Figure 4.19	FFT analysis results of the input current for controlled single phase full wave bridge rectifier with RL-load and series input resonance filter at $\alpha=30^\circ$	104
Figure 4.20	Output voltage waveform for controlled single phase full wave bridge rectifier with RL-load and series input resonance filter at $\alpha=30^\circ$	106
Figure 4.21	Output current waveform for controlled single phase full wave bridge rectifier with RL-load and series input resonance filter at $\alpha=30^\circ$	107
Figure 4.22	Frequency spectrum of input current in dB for controlled single phase full wave bridge rectifier with RL-load and series input resonance filter at $\alpha=30^\circ$	108
Figure 4.23	(a)THD of input current (b) input current (c) output voltage for controlled single phase full wave bridge rectifier with RL-load and various series input resonance filter values at $\alpha=30^\circ$	109
Figure 4.24	Power factor for controlled single phase full wave bridge rectifier with RL-load and various series input resonance filter values at $\alpha=30^\circ$.	110

Figure 4.25	Simplified schematic of controlled single phase full wave bridge rectifier with RL-load and parallel input resonance filter	112
Figure 4.26	Input voltage and input current waveform for controlled single phase full wave bridge rectifier with parallel input resonance filter at $\alpha=30^\circ$	113
Figure 4.27	Frequency spectrum of the input current for controlled single phase full wave bridge rectifier with RL-load and parallel input resonance filter (a) at $\alpha=30^\circ$, (b) at $\alpha=90^\circ$, (c) at $\alpha=120^\circ$	114
Figure 4.28	(a) THD of input current (b) power factor for controlled single phase full wave bridge rectifier with RL-load and parallel input resonance filter at $\alpha=30^\circ, 90^\circ, 120^\circ$	115
Figure 4.29	FFT analysis results of the input current for controlled single phase full wave bridge rectifier with RL-load and parallel input resonance filters at $\alpha=30^\circ$	116
Figure 4.30	Output voltage waveform for controlled single phase full wave bridge rectifier with RL-load and parallel input resonance filter at $\alpha=30^\circ$	118
Figure 4.31	Output current waveform for controlled single phase full wave bridge rectifier with RL-load and parallel input resonance filter at $\alpha=30^\circ$	119
Figure 4.32	Frequency spectrum of input current in dB for controlled single phase full wave bridge rectifier with RL-load and parallel input resonance filter at $\alpha=30^\circ$	120
Figure 4.33	(a)THD of input current (b) input current (c) output voltage for controlled single phase full wave bridge rectifier with RL-load and various parallel input resonance filter values at $\alpha=30^\circ$	121
Figure 4.34	Power factor for controlled single phase full wave bridge rectifier with RL-load and various parallel input resonance filter values at $\alpha=30^\circ$	122
Figure 4.35	Simplified schematic of controlled single phase full wave bridge rectifier with RL-load and parallel LC-filter in series with inductor L	124
Figure 4.36	Input voltage, input current waveform for controlled single phase full wave bridge rectifier with RL-load and parallel LC-filter in series with inductor L at $\alpha=30^\circ$.	125

Figure 4.37	Frequency spectrum of input current for controlled single phase full wave bridge rectifier with RL-load and parallel LC-filter in series with inductor L at $\alpha=30^\circ, 90^\circ, 120^\circ$	126
Figure 4.38	(a) THD of input current (b) power factor for controlled single phase full wave bridge rectifier with RL-load and parallel LC-filter in series with inductor L at $\alpha=30^\circ, 90^\circ, 120^\circ$	127
Figure 4.39	FFT analysis results of the input current for controlled single phase full wave bridge rectifier with RL-load and parallel LC-filter in series with inductor L at $\alpha=30^\circ$	128
Figure 4.40	Output voltage waveform for controlled single phase full wave bridge rectifier with RL-load and parallel LC-filter in series with inductor L at $\alpha=30^\circ$	129
Figure 4.41	Output current waveform for controlled single phase full wave bridge rectifier with RL-load and parallel LC-filter in series with inductor L at $\alpha=30^\circ$	131
Figure 4.42	Frequency spectrum of input current in dB for controlled single phase full wave bridge rectifier with RL-load and parallel LC-filter in series with inductor L at $\alpha=30^\circ$	132
Figure 4.43	(a) THD of input current (b) input current (c) output voltage for controlled single phase full wave bridge rectifier with RL-load and various parallel LC-filter in series with inductor L values at $\alpha=30^\circ$	134
Figure 4.44	Power factor for controlled single phase full wave bridge rectifier with RL-load and various parallel LC-filter in series with inductor L values at $\alpha=30^\circ$.	134
Figure 4.45	Simplified schematic of controlled single phase full wave bridge rectifier with RL-load and second order high pass filter	136
Figure 4.46	Input voltage and input current waveform for controlled single phase full wave bridge rectifier with RL-load and second order high pass filter at $\alpha=30^\circ$.	137
Figure 4.47	Frequency spectrum of the input current for controlled single phase full wave bridge rectifier with RL-load and second order high pass filter (a) at $\alpha=30^\circ$, (b) at $\alpha=90^\circ$, (c) at $\alpha=120^\circ$	138
Figure 4.48	(a) THD of input current (b) power factor for controlled single phase full wave bridge rectifier with RL-load and second order high pass filter at $\alpha=30^\circ, 90^\circ, 120^\circ$	139

Figure 4.49	FFT analysis results of the input current for controlled single phase full wave bridge rectifier with RL-load and second order high pass filter at $\alpha=30^\circ$	140
Figure 4.50	Output voltage waveform for controlled single phase full wave bridge rectifier with RL-load and second order high pass filter at $\alpha=30^\circ$	140
Figure 4.51	Output current waveform for controlled single phase full wave bridge rectifier with RL-load and second order high pass filter at $\alpha=30^\circ$	142
Figure 4.52	Frequency spectrum of input current in dB for controlled single phase full wave bridge rectifier with RL-load and second order high pass filter at $\alpha=30^\circ$	143
Figure 4.53	(a)THD of input current (b) input current (c) output voltage for controlled single phase full wave rectifier with various second order high pass filter at $\alpha=30^\circ$.	144
Figure 4.54	Power factor for controlled single phase full wave bridge rectifier with second order high pass filter at $\alpha=30^\circ$	145
Figure 4.55	Simplified schematic of controlled single phase full wave bridge rectifier with third order high pass T-filter	147
Figure 4.56	Input voltage and input current waveform for controlled single phase full wave bridge rectifier with third order high pass T- filter at $\alpha=30^\circ$.	148
Figure 4.57	Frequency spectrum of the input current for controlled single phase full wave bridge rectifier with RL-load and third order high pass T- filter (a) at $\alpha=30^\circ$, (b) at $\alpha=90^\circ$, (c) at $\alpha=120^\circ$.	149
Figure 4.58	(a) THD of input current (b) power factor for controlled single phase full wave bridge rectifier with RL-load and third order high pass T- filter at $\alpha=30^\circ, 90^\circ, 120^\circ$	150
Figure 4.59	FFT analysis results of the input current for controlled single phase full wave bridge rectifier with third order high pass T- filter at $\alpha=30^\circ$	152
Figure 4.60	Output voltage waveform for controlled single phase full wave bridge rectifier with third order high pass T-filter at $\alpha=30^\circ$	153
Figure 4.61	Output current waveform for controlled single phase full wave bridge rectifier with third order high pass T- filter at $\alpha=30^\circ$	154

Figure 4.62	Frequency spectrum of input current spectrum in dB for controlled Single phase full wave bridge rectifier with third order high pass T- filter at $\alpha=30^\circ$.	155
Figure 4.63	(a)THD of input current (b)input current (c)output voltage for controlled single phase full wave bridge rectifier with RL-load and various third order high pass T- filter values at $\alpha=30^\circ$	156
Figure 4.64	Power factor for controlled single phase full wave bridge rectifier with RL-load and third order high pass T- filter at $\alpha=30^\circ$	157
Figure 4.65	Simplified schematic of controlled single phase full wave bridge rectifier with RL-load and third order high pass π - filter	159
Figure 4.66	Variation of IDF for various input passive filter topologies	167
Figure 4.67	Variation of PF for various input passive filter topologies	168
Figure 4.68	Variation of THD for various input passive filter topologies	168
Figure 4.69	Variation of efficiency for various input passive filter topologies	169

List of Abbreviations

EPQ	Electric Power Quality
AC	Alternating Current
DC	Direct Current
THD	Total Harmonic Distortion
IDF	Input Displacement Factor
SCRs	Silicon Controlled Rectifiers
PF	Power Factor
FFT	Fast Fourier Transform
RMS	Root Mean Square
PS	Power System
PPF	Passive Power Filters
FF	Form Factor
CF	Crest Factor
RF	Ripple Factor
TUF	Transformer Utilization Factor
LC	Inductor-Capacitor
RL	Resistor-Inductor
PLL	Phase Locked Loop
dB	Decibel

**Improvement of Electric Grid-Quality Parameters by LC-Filters, at
Supplying of Power Electronics Converters**

By

Asma'Shara'b

Supervisor

Prof. Dr. Marwan M.Mahmoud

Abstract

Recently, Power electronic devices are applied in many fields, mainly in the industry and domestic appliances. The major problem that faces the power system by these devices is the generation of current harmonics. These harmonic currents act as a source of pollution to the power system as they have the major following impacts:

- Reduction of power quality parameter represented in power factor and system efficiency.
- Increment of total harmonic distortion.

This work investigates the mitigation of harmonic currents by different LC-filter configurations to improve the quality parameters of supplying electrical grid. Also it discusses the design and simulation of these LC passive filters within SCR rectifier.

The performance parameters of the controlled rectifiers, with various LC-filter configurations, for RL-load and firing angles, investigated in this

work are: input current THD, input power factor, efficiency and output voltage.

This investigation was implemented by FFT analysis tool through MATLAB/SIMULINK.

The simulation of a single phase full wave controlled rectifier with RL-load and a firing angle of $\alpha=30^\circ$ has resulted in: THD=18.04%, PF=0.804 and rectification efficiency of $\eta=73.53\%$.

Inserting a series resonance LC-filter at the input of this rectifier, the simulation resulted in THD=2.52%, PF=0.745 and $\eta=63.05\%$ the corresponding reactive power to be installed in the LC-filter amounts to $Q=39.053 \text{ kVAr}$.

Investigating the insertion of a high pass T-LC filter, the simulation results in THD=4.27%, PF=0.842, $\eta=77.87\%$ and $Q=14.96 \text{ kVAr}$. The results for the T-LC filter indicate a considerable improvement of the grid quality parameters (especially for THD) in comparison with the corresponding parameters of the rectifier without LC-filter.

In addition, five LC-filter with different topologies were inserted at the input of the rectifier and investigated in the thesis. The simulation results of all seven filters show a significant reduction in the harmonic currents represented in THD for the different filters in the range of THD = 2.522%-5.15 %.

Moreover, the rectification efficiency could be improved by a simple second order high pass LC-filter to achieve $\eta = 79.66\%$ at an installed reactive power of $Q = 10.086 \text{ kVAr}$.

The thesis compass investigating the mentioned main grid quality parameters beside other parameters for different firing angles of the above mentioned full wave controlled rectifier.

Chapter One

Introduction

1.1 Project Background

The high expense of using DC power sources [1] are the main reason of the widespread using of single phase AC/DC power converters.

These converters have been used in many fields such as industrial, commercial, residential, aerospace, and military environments. This extensive use of converters is due to its high efficiency, smaller size and weight. Meanwhile, the widespread power converters draw a pulsating current; the input current from the utility line. This does not only decline the input power factor of the convertors, but also injects a significant amount of harmonic current into the utility line [2]. In addition to that when converting AC power to DC using rectifiers, many undesirable AC components are contained called ripples. When these ripples exceed a specific value, the system is affected as follows: [1].

- Power quality problems; appearance of large values of harmonics.
- Poor power factor.
- High total harmonic distortion.
- Phase shift between current and voltage waveforms [3].

As mentioned above, the widespread of using nonlinear loads leads to raise the THD in the electrical distribution system. Current harmonics

cause serious harmonic problems in the distribution feeders for sensitive consumers.

On the other hand, the controlled rectifiers that are used to convert AC to DC consist of at least two thyristors which are nonlinear devices that generate harmonics in the power system line. Consequently, cause an increase in the level of R.M.S current, which results in an increase of power loss, heating the equipment and voltage sags [4].

In the electrical power systems, the increase of THD can raise consonant voltage and current in an electrical power system to permissible abnormal states that can aggressively affect the system. For that IEEE standards have characterized cutoff points for the harmonic voltages and the harmonic currents.

For power system engineers, THD values must be taken into consideration since it can highly affect the systems power quality (PQ) which is the main concern for those engineers nowadays.

To solve PQ issues many methods can be used. In addition, [5] various harmonic reduction techniques have been developed to meet the requirements needed by the current harmonic standards. In general, these techniques can be classified into five broad categories, as follows:

1. Passive filters (line reactors and/or DC link chokes, series, shunts, and low pass broadband filters).
2. Phase multiplication systems (12-pulse, 18-pulse rectifier systems).

3. Active harmonic compensation systems (series, parallel).
4. Hybrid systems.
5. PWM rectifiers [6].

The main purpose of using these techniques is the mitigation of the power quality problems [7] by making the input current a pure sinusoidal waveform, and reducing the overall current THD by eliminating the majority of the harmonic current orders. Passive filters can be introduced as the simplest conventional solution to eliminate the current harmonics and to improve the load power factor. The main concept of both series which can be of a purely inductive type or an LC tuned type and the shunt passive filters, is the usage of a high series impedance to block undesired harmonic current or to invert these current to a low impedance shunt path [6]. In tuned harmonic filters a combination of an inductor and capacitor are used. These two elements can be tuned so as to create a resonance [7] that can filter one specific frequency or range of frequencies out of a mix of different frequencies in a circuit [8] this tuning can reduce harmonics, compensate reactive power and eliminate undesirable harmonics [9].

Filtering characteristic of the passive filter can be affected by the following:

- System impedance that may create series or parallel resonance causing amplification of the harmonic voltage or the current at a specific frequency.
- Variability of the non-linear load operating conditions.
- The ageing of the filter capacitors will affect their performance [10].

Through mathematical calculations, and simulated results; designers can be able to choose one or more of filter configurations to meet the standard requirements. However, there are other factors to be considered when choosing the proper configuration; like the use of ready and available components to form the filter, cost optimization, and size minimization. When such factors are taken in consideration, designers are left with compromises, which will influence the design and the performance of the filter [11].

This work highlights on the improvement of electric grid quality parameters for the controlled single phase full wave bridge rectifiers supplying RL-load. Also, it presents the modeling, design and simulation of a single phase full wave bridge rectifier with input passive filter in MATLAB/SIMULINK software to compensate for the harmonic current injected. The spectral analysis of the supply current shows that the harmonics produced by the load has been successfully compensated by the passive filter. The effect of using different firing angles of SCRS on the performance of the passive filter is also discussed.

1.2 Objectives of the Study

The overall goal of this thesis can be summarized as to improve the quality parameters of the electrical grid supplying power electronic circuits. However, the objectives can be summarized as follows:

1. Improving the harmonic factor in the supplying grid by improvement for the shape of the supply current.
2. Improving the power factor of the circuit.
3. Improving the efficiency of the circuit.
4. Determining the best configuration of the compensation network through the simulation using MATLAB/SIMULINK program.
5. Determining the appropriate sizes of compensation network considering the installed reactive power of such element.
6. Determining the variation firing angle on the rated values of the selected filter network and thereby quality parameter of the grid.

1.3 Thesis Outlines

This thesis is organized into five chapters: namely, introduction, problem identification, literature reviews, results analysis, conclusion and recommendation.

Chapter 1 discusses the background, general and specific objectives with clarification in a simple way for a better understanding of the important concepts related to the study.

Chapter 2 shows problem identification via the power electronics circuits which includes controlled and uncontrolled single phase full wave bridge rectifiers; summarized results of each configuration are used in the suggested filters and also mentioned in this chapter.

Chapter 3 describes passive filters and their various types. It also accounts for different relevant literature views which would be focused on solving harmonic problems with the uncontrolled single phase full wave rectifiers.

Chapter 4 presents the simulation results and analyses for some passive filter configurations as well as the comparison of performance parameters. Moreover, it discusses the advantages and the disadvantages of each configuration.

Chapter 5 states the conclusions and the recommendations for future work and lists some tips and pieces of advice for future researchers to carry on with the same topic.

Chapter Two

Problem Statement

In order to obtain the DC voltage from an AC voltage source, power electronic converters are used mainly (rectifiers), the AC source is mainly electrical grid, by using such converters. The electrical grid can be affected with different problems such as harmonics and poor power factor hence it is essential to mitigate and reduce such problems. This thesis represents passive filters to perform that, passive filters come with different configurations so the thesis also proposes how to select the suitable filter configuration.

2.1 Power Electronic Conversion

The process of converting electric power from one form to another is treated by power electronic conversion. The power converters are the power electronic devices performing power conversion; they are often called as static power converters since they contain no moving parts.

Power conversion achievement can be done through power semiconductor devices, such as switches. These power devices are Diode, SCRs (Silicon Controlled Rectifiers, or Thyristors), TRIACS, power transistors, power MOSFETs, Insulated Gate Bipolar Transistors (IGBTs) and MCTs (MOS-Controlled Thyristors) [12].

2.2 Converters Classification

Matching the voltage and current requirements of the load to those of the source is the main objective of a power electronics circuit in the first place which converts one type or level of current waveform or a voltage to another, and consequently are called converters. Converters interfere to be the interface between the load and the source [13].

Power converters are classified generally in relationship between input and output:

- AC to DC conversion (Rectifier).
- DC to AC conversion (Inverter).
- DC to DC conversion (Chopper buck and boost converters).
- AC to AC conversion (Cycloconverter) [12].

2.3 AC-DC Converters

The AC-DC converter produces a DC output from an AC input. Average power is transferred from an AC source to a DC load. The AC-DC converter is specifically classified as a rectifier. Rectifiers can be divided into two main categories: controlled and uncontrolled rectifiers therefore, controlled rectifiers are classified into semi-controlled and fully controlled rectifiers. There are many configurations of rectifiers. The most common familiar ones are:

- Single-phase full wave uncontrolled rectifier.
- Single-phase half wave controlled rectifier.
- Single-phase semi-controlled full wave rectifier.
- Single-phase fully controlled full wave rectifier [13].

2.4 Uncontrolled Full Wave Bridge Rectifier

Turning on the diode can only be activated when its cathode voltage becomes less than anode voltage. Thus, the diode conduction time will be uncontrolled which is the main disadvantage of the diode circuits. However, the diode circuits are still used due to their simplicity, low price, ruggedness.....etc. [14].

Diodes normally conduct current in one direction and therefore, they are used in rectifier circuits. Rectification process is defined, as “Converting alternating voltages and currents into direct currents and the device is known as rectifier”. It is largely used in electrochemical processes, charging batteries, supply DC motors as well as power supply sections in industrial components [14].

The DC output voltage always remains constant if AC input voltage is constant and this happens only in an uncontrolled rectifier. There are two main groups of rectifiers, which are classified according to the type of input source as shown in Fig.(2.1).

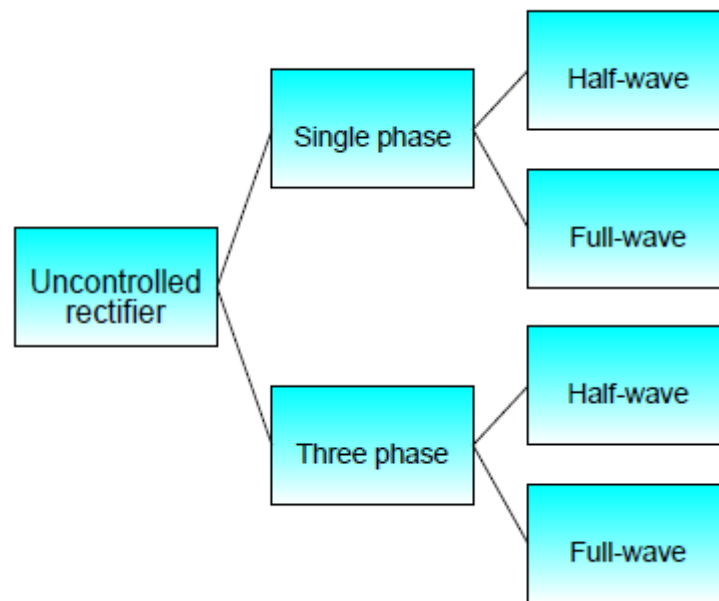


Figure 2.1: Classification of uncontrolled rectifier.

The full wave bridge type and the full wave center tapped transformer type are the types of full wave rectifiers. These rectifiers have better performances than Half Wave rectifiers. The disadvantages of half wave rectifiers are as follows:

- High ripple factor.
- Low efficiency.
- Low transformer utilization factor.
- DC saturation of transformer secondary winding [14].

2.5 Single Phase Full Wave Bridge Diode Rectifier

A single phase diode rectifier, as shown in Fig.(2.2), is used to convert an alternating current to a direct current.

Note that this rectifier is an uncontrolled one. [15].

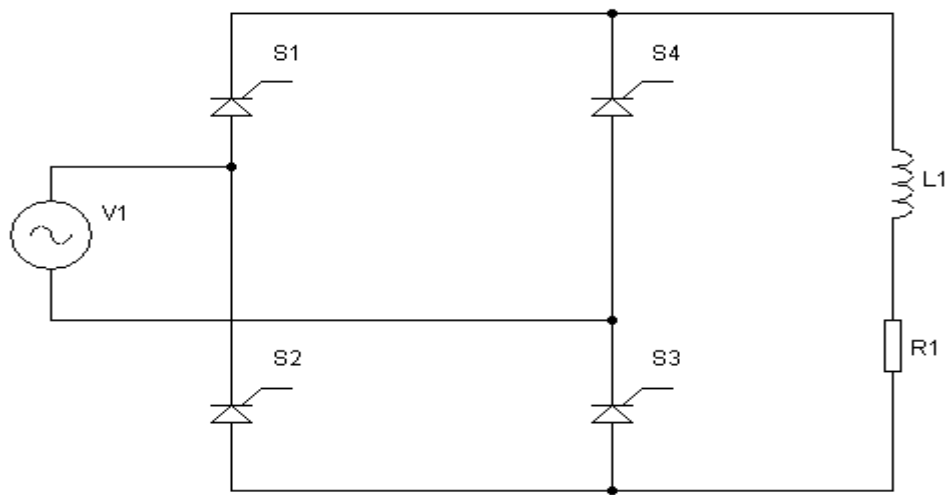


Figure 2.2: Simplified schematic of uncontrolled single phase full wave bridge rectifier with RL-Load.

Follows are the characteristics of the operation of the above-mentioned rectifier:

- Diodes D_4 and D_2 are conducting during the positive half-wave of the input voltage while , Diode D_3 and D_1 are conducting during the negative half.
- Kirchhoff's voltage law around the loop containing the source, D_2 , and D_3 reveal that D_2 and D_3 cannot be on at the same time. Similarly,

D_1 and D_4 cannot conduct simultaneously. The load current can be positive or zero but can never be negative.

- The voltage across the load is V_{out} when D_2 and D_4 are on. The voltage across the load is also V_{out} when D_1 and D_3 are on [13].

2.5.1 Effects of the rectifier on AC mains

The first stage of power supplies, which have an AC source, is a full wave rectifier resulting in the conversion of AC voltage from AC input. Within each cycle, the diodes conduct in only a short time resulting in currents that are highly non-sinusoidal. The outcome of the process is a large and total harmonic distortion of current coming from the AC [13].

The consequence is a large total harmonic distortion (THD) of current coming from the AC; a large THD corresponds to a low power factor.

In the case of pure resistive load, the current wave form is sinusoidal and the phase shift with input voltage source equals zero; this leads to total harmonic distortion THD amounting to zero, and unity power factor. Otherwise, in cases of non-sinusoidal input current waveform, with large amount of harmonics, the power factor will be less than unity, and THD greater than zero.

The non-sinusoidal current can be expressed as a fundamental current at the mains frequency with harmonics superimposed on it [16].

Pulse number determines the characteristics of current harmonics that are produced according to the following equation:

$$h_i = k * p \pm 1 \quad (2.1)$$

Where,

h_i : is the harmonic number.

K : is any positive integer 1, 2, 3, 4, etc.

p : is the pulse number of the rectifier (2).

The magnitude of the harmonic current in an idealized harmonic is given as the reciprocal of the harmonic number. i.e. $I \sim 1/h_i$ Thus,

3rd harmonic current should represent 33.33% of the fundamental current.

5th harmonic current should represent 20.00% of the fundamental current.

7th harmonic current should represent 14.29% of the fundamental current.

9th harmonic current should represent 11.11% of the fundamental current.

11th harmonic current should represent 9.09% of the fundamental current.

13th harmonic current should represent 7.69% of the fundamental current.

This means that 2-pulse (or bridge) rectifier has only odd harmonics order represented in 3rd, 5th, 7th, 11th, 13th, 15th, 17th, 19th, 23th, 25th, etc. multiplied by the fundamental component (50 Hz).

As a rough rule of thumb, the magnitudes of the harmonic currents will be the fundamental current divided by the harmonic number (e.g. the magnitude of the 5th harmonic would be about 1/5th of the fundamental current) [17].

The value of total harmonic current distortion THD must not be more than 5%. And any individual harmonic current distortion must not be more 3% of the fundamental value of the current line. In typical applications, the harmonics are measured up to 25th order, but in critical applications, they are measured up to 50th or 100th order [18].

Table 2.1: Simulation specifications of an uncontrolled single phase full wave bridge rectifier with RL-load.

Parameter Name	Symbol	Value
Input voltage (V)	V supply	220 (R.M.S)
Load resistance (Ω)	R	5
Load inductance (mH)	L	19
Supply frequency (Hz)	f	50
Load angle	ϕ	50°

Single-phase uncontrolled full wave (bridge) rectifiers of Fig.(2.1), the source is 220 V_{rms} at 50 Hz, and the load of simulation model is assumed as a series R-L combination with R = 5 Ω and L = 19 mH, the load angle

is determined from the equ. (2.2) suppose that voltage at the input of the rectifiers have sinusoidal waveforms with period $T_{\text{mains}} = 20\text{ms}$ (corresponding to $f_{\text{mains}} = 50\text{ Hz}$), through the following definition:

$$\phi = \tan^{-1} \left(\frac{\omega L}{R} \right) \quad (2.2)$$

Where,

ω : Angular velocity (rad/sec).

L: Load inductance (H).

R: Load resistance (Ω).

$$\phi = \tan^{-1} \frac{(314)(.019)}{5} = 50^\circ$$

2.5.2 System simulation

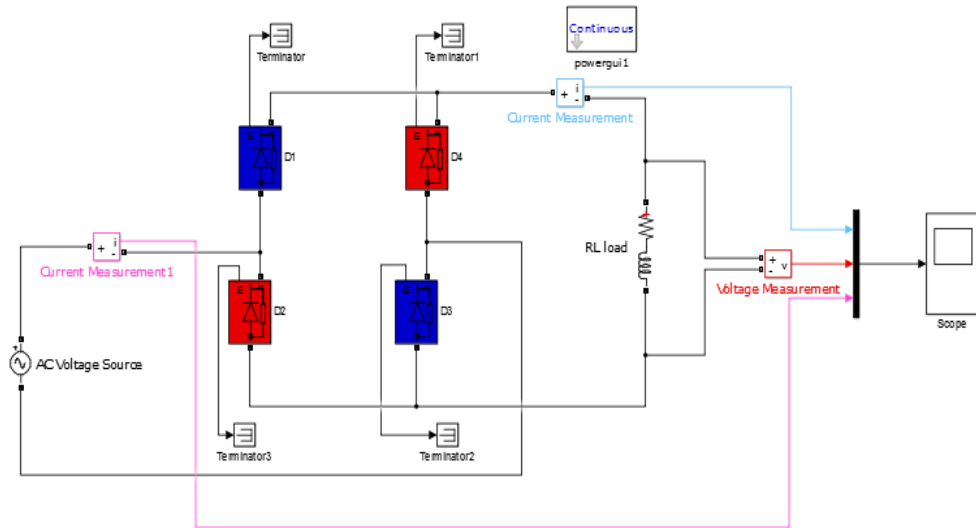


Figure 2.3: MATLAB/Simulink implementation circuit diagram of an uncontrolled single phase full wave bridge rectifier supplying RL-load.

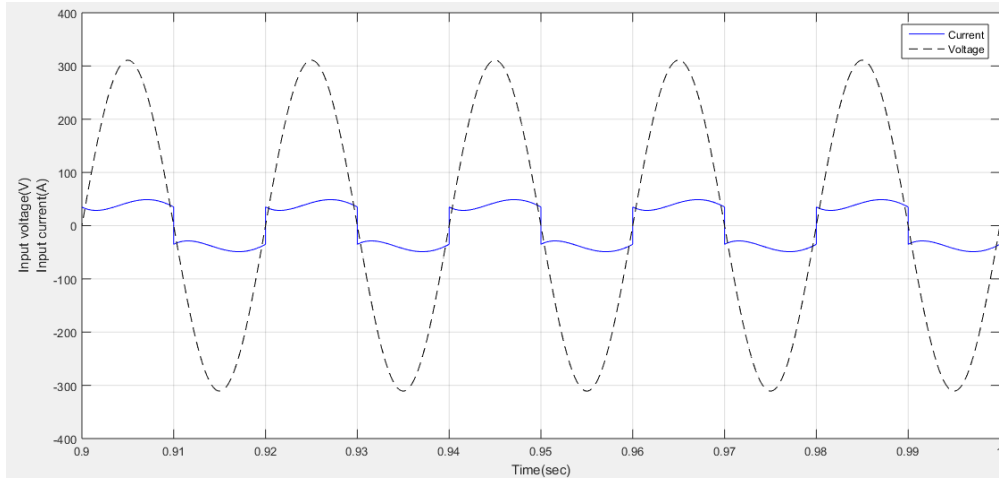


Figure 2.4: Input voltage and input current waveform for uncontrolled single phase full wave bridge rectifier with RL- load.

It is clear that the input current waveform has square shape with distortion. The input voltage is sinusoidal, while the input current becomes out phase due to distortions. Presence of an inductive element in the load makes the current to un-follow the voltage waveform depending upon the value of both load resistance and inductance which results in a distorted wave form of current drawn from the mains, and produces a large spectrum of harmonic signals that may interfere with other equipment. Finally, this result makes conventional AC rectification a very inefficient process.

Table 2.2: Frequency spectrum of the input current.

Harmonic order	1 st	3 rd	5 th	7 th	9 th	11 th	13 th	15 th	17 th	19 th
Frequency [Hz]	50	150	250	350	450	550	650	750	850	950
Input current [A]	52.4	14.30	8.73	6.21	4.78	3.84	3.19	2.69	2.31	1.99

The THD was 39.5%. The highest harmonics were the 3rd, the 5th and the 7th which represent 27.28%, 16.65% and 11.84% (resp.) of the fundamentals.

It is clear from the tabulated results that:

- Lower harmonic odd orders have the higher magnitudes.
 - The magnitude of current harmonics decreases as harmonic order increases.
 - The third harmonic has the largest magnitude of all other harmonics.
- A third harmonic may cause phase imbalances or single phase loads when it is present in the system [19].

The frequency spectrum for the uncontrolled single phase full wave bridge rectifier with R-L load is presented in Fig.(2.5).

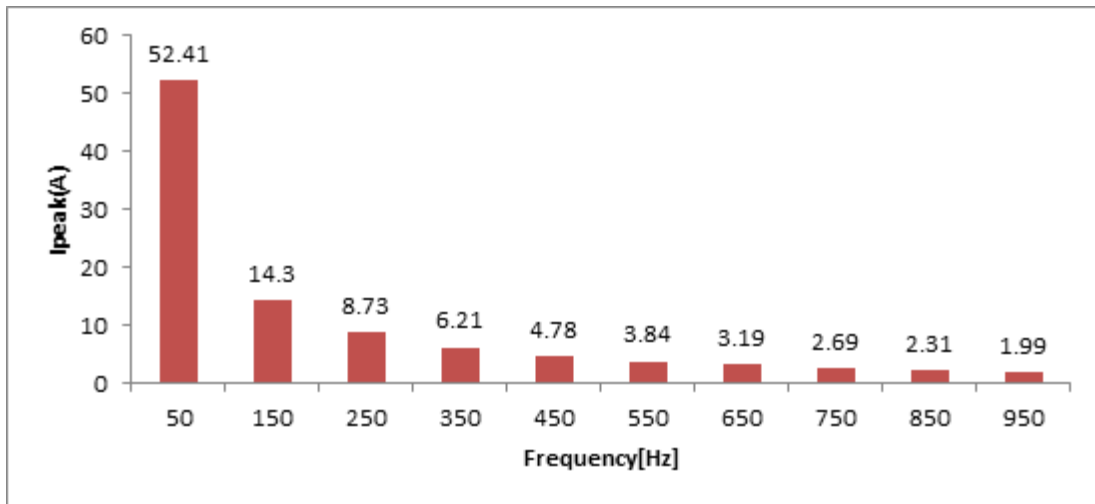


Figure 2.5: Harmonic input current spectrum for the uncontrolled single phase full wave bridge rectifier with RL- load.

2.5.3 Performance parameters

Table 2.3 summarizes the main performance parameters for the uncontrolled single phase full wave bridge rectifier with RL ($R = 5 \Omega$

and $L = 19 \text{ mH}$) load that are needed to compare the performances among different rectifier circuits.

Table 2.3: The complete parameters of uncontrolled single phase full wave bridge rectifier with RL-load.

Parameter Name	Parameter Symbol	Result
Output voltage [V]	V_{rms}	220
Fundamental R.M.S current [A]	I_{rms1}	37.06
Input current [A]	I_{rms}	39.85
Load angle	ϕ	-10.2°
Average output voltage [V]	V_{dc}	196.3
Average output current [A]	I_{dc}	38.83
Input AC power [kW]	P_{in}	8.767
Output DC power [kW]	P_{out}	7.622
Efficiency %	η	86.9
Form Factor	FF	1.12
Crest Factor	CF	1.41
Ripple Factor	RF	0.506
Transformer Utilization Factor	TUF	0.869
Total Harmonic Distortion %	THD	39.5
Power Factor	PF	0.915
Displacement Factor	DF	0.935

Sample calculation is also presented in Appendix B (with all the relevant expressions that are used to find the required parameters)

The following points are disadvantages of uncontrolled single phase full wave rectifiers:

- Total harmonic distortion is 39.5% which is very high and needs to be reduced.
- Efficiency is 86.9 % which is very poor and should be improved.
- Input current is in the form of square wave containing current harmonics of varying amplitude which is highly undesirable.

- There is no control on the conduction time of the diodes.
- The output voltage is uncontrolled.
- These converters usually have a low power factor of 0.915.
- Crest factor and ripple factor almost have lower value.

It should be mentioned that what the researcher has illustrated so far in this section has not been thoroughly discussed in details because it's considered a part to get initial understanding for the next section which is the main concern of this thesis.

2.6 Controlled Full Wave Bridge Rectifiers

While the use of uncontrolled rectifier circuits remains prominent; for some applications, more control and efficiency is more important. This can be accomplished through the use of a controlled rectifier circuit in which thyristors are connected in a full bridge configuration allowing the adjustment of the average output voltage. With control circuitry these devices can be operated with a controllable firing angle (α) that can vary the average and R.M.S of output voltage. Devices that use this technology include Uninterruptable Power Supplies (UPS), low power DC motor drives, as well as cycloconverter [20].

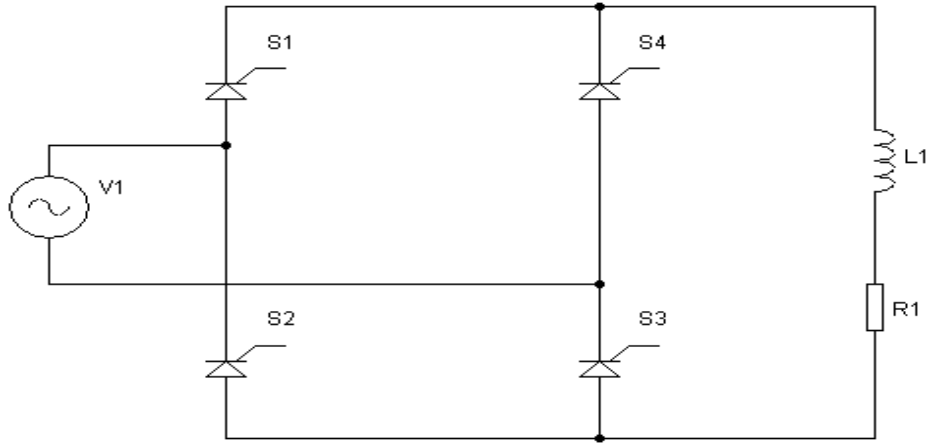


Figure 2.6: Simplified schematic of single phase full wave controlled rectifier with RL -Load.

Fig.(2.6) shows a single-phase full wave controlled rectifier with a highly inductive load because of that the load current continuity is assured. Thyristors S_1 and S_3 are forward-biased during the positive half cycle of supply voltage. When these two thyristors are fired simultaneously at $\omega t = \alpha$, the load is connected to the supply via thyristors S_1 and S_3 . Thyristors S_1 and S_3 will continue to conduct beyond $\omega t = \pi$ as a sequence of the presence of an inductive load. During the negative half cycle, thyristors S_2 and S_4 are forward-biased at $\omega t = \pi + \alpha$, these thyristors are fired into conduction causing thyristors S_1 and S_3 to be reverse-biased and turned off due to line commutation [21].

2.6.1 RL-load, continuous current

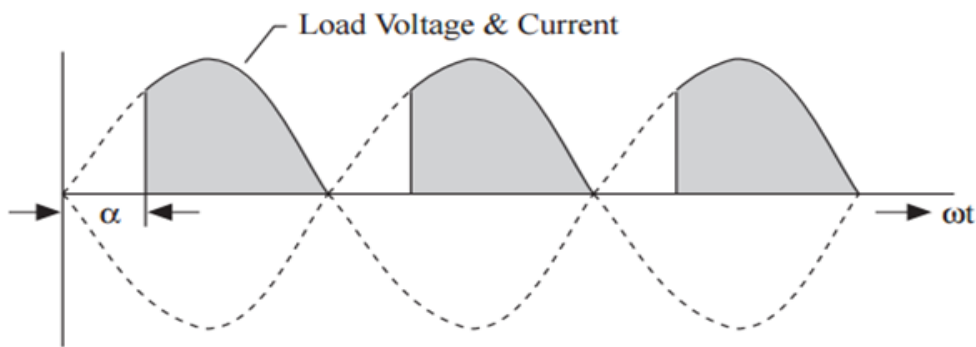
Load current for a controlled full-wave rectifier with RL load can be either continuous or discontinuous and these two cases should be analyzed separately.

With the inductor acting as a source, the load contains an inductor and the SCRs continue to conduct. When the current through an inductor falls, the voltage crossing it, changes sign that is compared with the sign that occurs when its current is rising and its voltage is such that the inductor delivers power to the load resistor feeding back some power to the AC source under certain conditions and keeping the SCRs in conduction forward-biased [21].

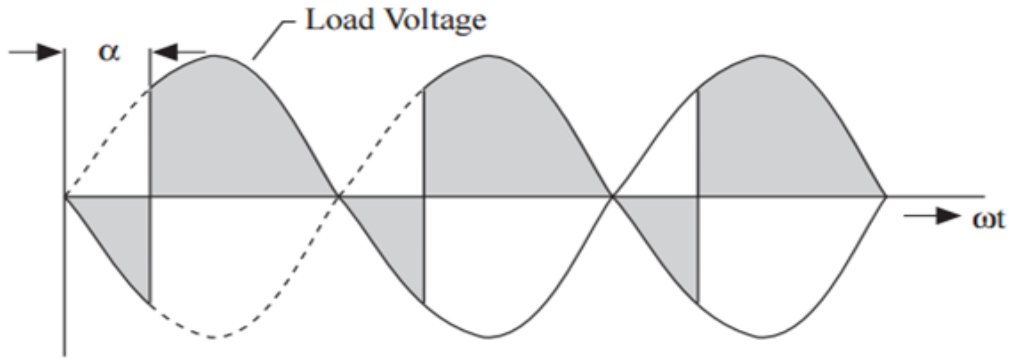
To check whether the load current is continuous or discontinuous, one can use the condition:

$$\alpha \leq \tan^{-1} \left(\frac{\omega L}{R} \right)$$

When the condition is not accomplished, the conduction through the load becomes zero and discontinuous assuming that the inductive load is sufficiently large to keep the load current continuous as shown in Fig.(2.7 ,b) [21].



(a)



(b)

Figure 2.7: Output voltage waveform (a) for resistive load (b) for resistive inductive load (with continuous current conduction) [12].

The simulation of the rectifier is implemented for different conditions. The values of the inductor and resistor are worked out for required load angle. The summary of topology features is presented in Table 2.4.

Table 2.4: Simulation specifications of controlled single phase full wave bridge rectifier with RL-load.

Parameter Name	Symbol	Value
Input voltage (V)	V supply	220 (R.M.S)
Load resistance (Ω)	R	5
Load inductance (mH)	L	19
Supply frequency (Hz)	f	50
Load angle	ϕ	50°
Firing angle	α	30°

2.6.2 System simulation

Fig.(2.8) shows single phase controlled rectifier with series of resistive-inductive load is tested out by using MATLAB /SIMULINK software for different cases. The inductor is adjusted on suitable values in order to make appropriate load angle. This study focuses mainly on the THD of

the input current for different filter configurations with more discussion regarding fixed load finally being presented later in chapter (4).

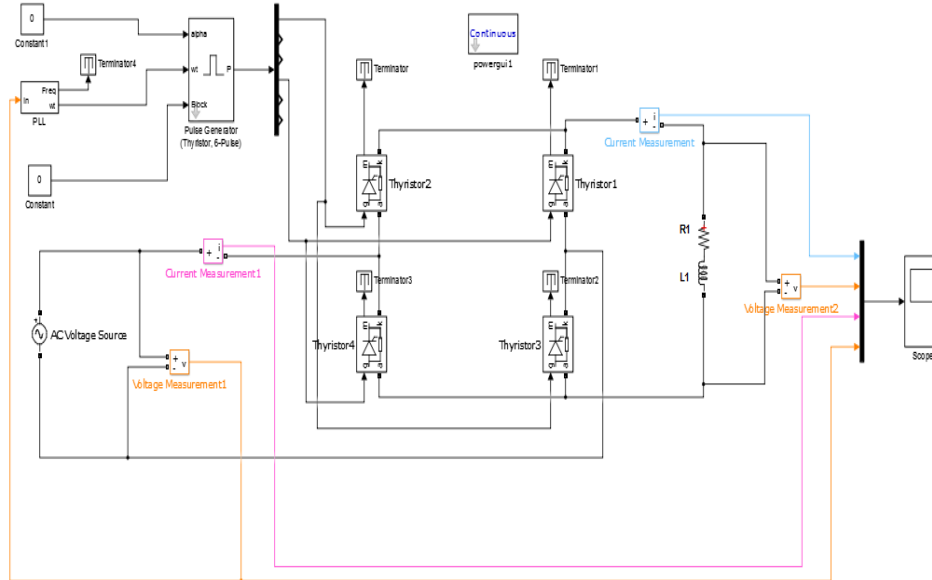


Figure 2.8: MATLAB/Simulink implementation circuit diagram of controlled single phase full wave bridge rectifier supplying RL-load.

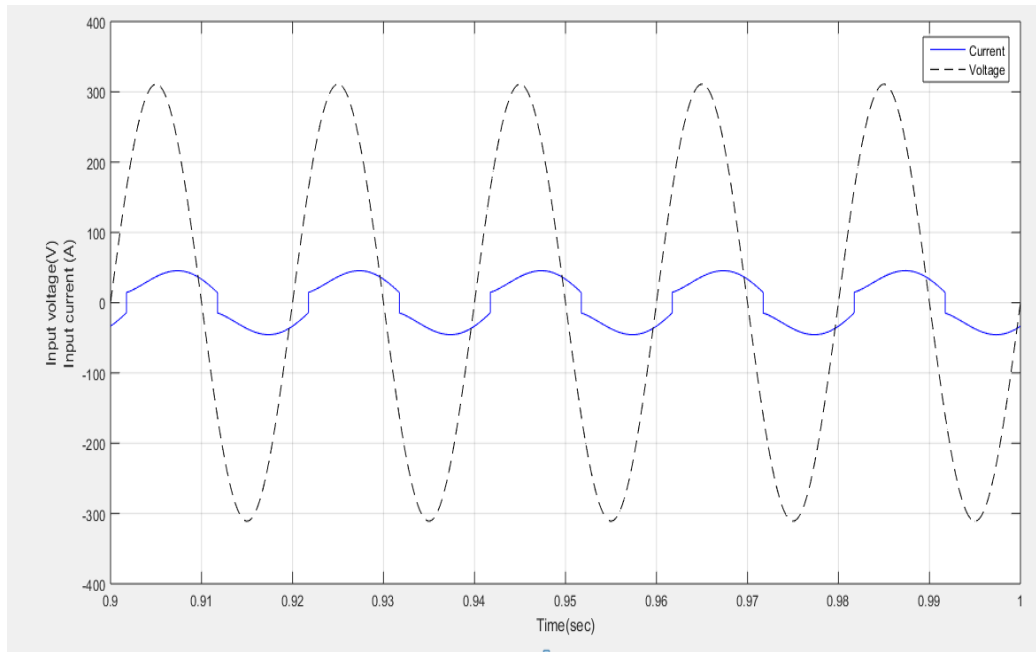


Figure 2.9: Input voltage and input current waveform for controlled single phase full wave bridge rectifier with RL-load at $\alpha=30^\circ$.

Fig.(2.9) shows the behavior of input voltage and current delivered by the source. The same results were mentioned under ‘uncontrolled rectifier (see section 2.5) but without the presence of a firing angle that affects the input current behavior.

The harmonics generated by controlled rectifier on the AC side may be calculated in the same way we did with uncontrolled rectifiers; depending on pulse number. It’s clear that the table (see Table 2.5) can be extended even more.

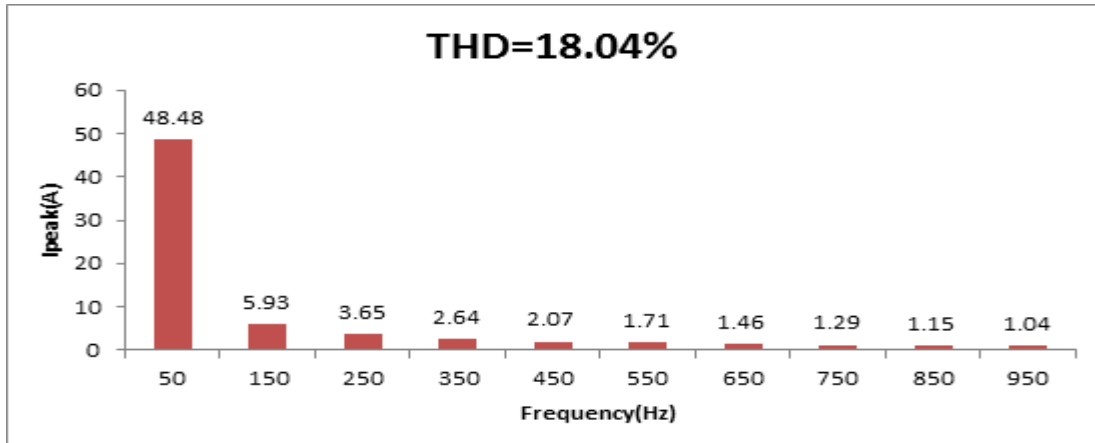
Table 2.5 below shows the amplitude of each harmonic current and compares the harmonic current spectrum caused by different firing angle without filter.

Table 2.5: Frequency spectrum of the input current.

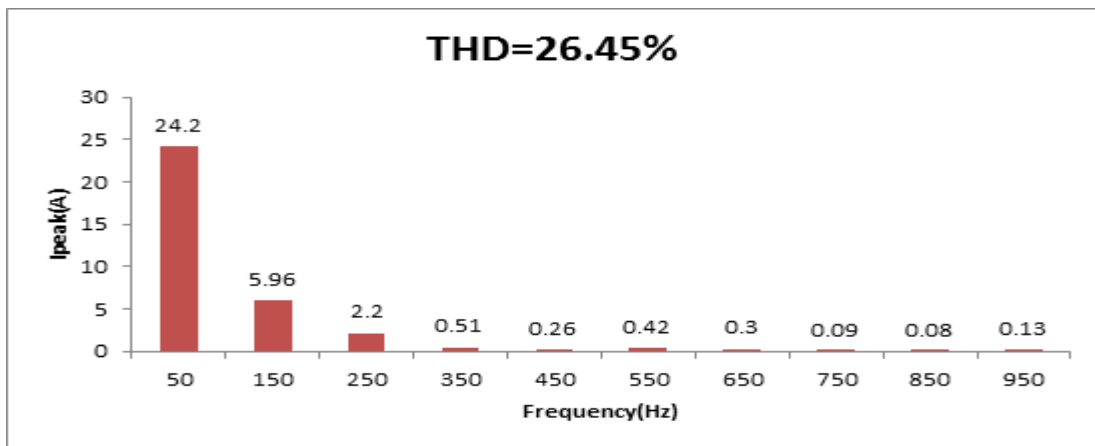
Harmonic order	1 st	3 th	5 th	7 th	9 th	11 th	13 th	15 th	17 th	19 th
Frequency [Hz]	50	150	250	350	450	550	650	750	850	950
I ($\alpha=30^\circ$) [A]	48.48	5.93	3.65	2.64	2.07	1.71	1.46	1.29	1.15	1.04
I ($\alpha=90^\circ$) [A]	24.2	5.96	2.2	0.51	0.26	0.42	0.3	0.09	0.08	0.13
I ($\alpha=120^\circ$) [A]	11.52	5.96	0.56	1	0.1	0.38	0.09	0.19	0.08	0.05

At $\alpha=30^\circ$, THD was 18.04%. The highest harmonics were the 3rd, 5th and the 7th which represent 12.23%, 7.52% and 5.44% (resp.) of the fundamental component. It represents low values compared with uncontrolled rectifiers, but still needs to be decreased.

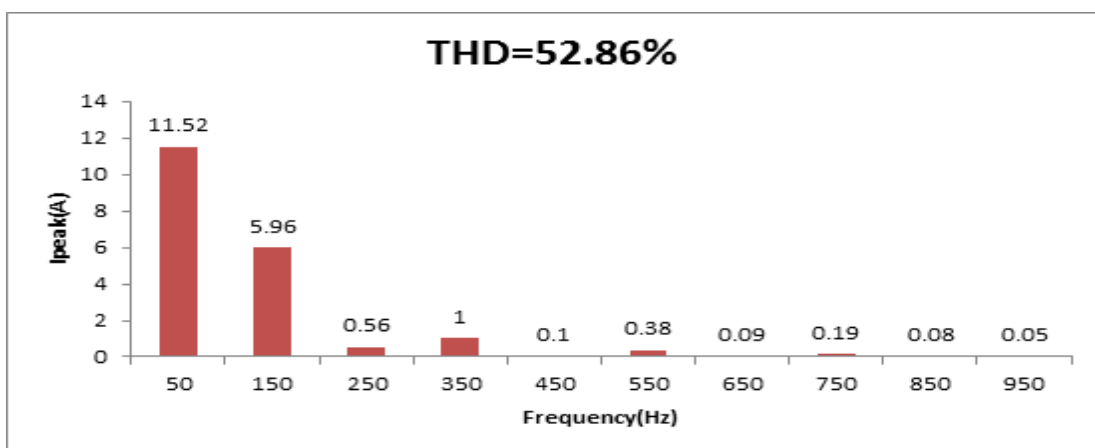
The frequency spectrum of the input current with various firing angle for controlled single phase full wave bridge rectifier with RL-load is illustrated in Fig.(2.10).



(a)



(b)



(c)

Figure 2.10: Frequency spectrum of input current spectrum for controlled single phase full wave bridge rectifier with RL-load (a) at $\alpha=30^\circ$ (b) at $\alpha=90^\circ$ (c) at $\alpha=120^\circ$.

The three spectrums in Fig.(2.10) show that the current of the fundamental wave at (50 Hz) and the corresponding power factor decreases as the firing angle increases while the THD increases as illustrated in Fig. (2.11).

The total harmonic distortion of the current for unfiltered rectifier circuits in Fig. (2.10, a) was measured to 18.04% which is unacceptable for critical applications. The increasing of the firing angle (α) leads to the increase of THD because it's associated with the increment of switching time delay of the thyristors. Consequently, this results in increasing the distortion current in contrast with the sinusoidal form.

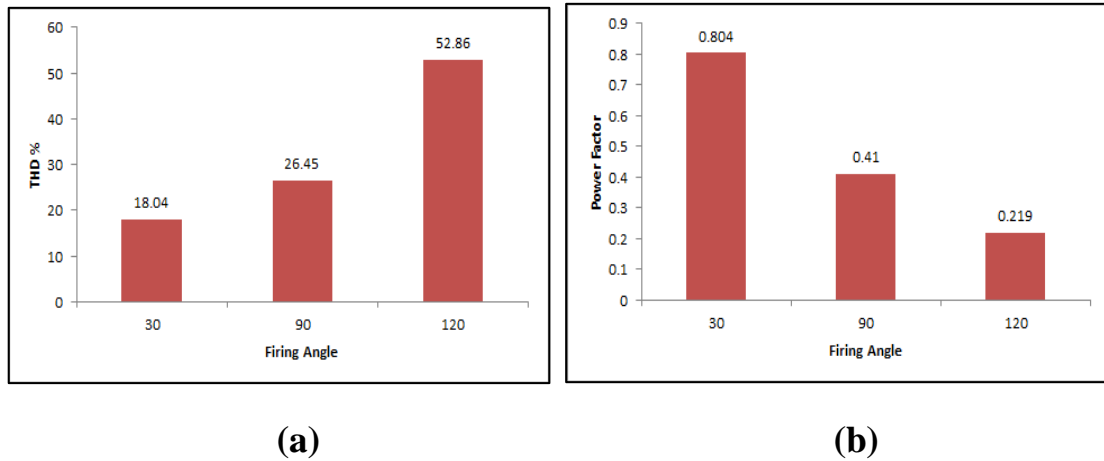


Figure 2.11 : (a) THD of input current (b) power factor for controlled single phase full wave bridge rectifiers with RL- load at $\alpha=30^\circ$, 90° and 120° .

As one can understand from Fig.(2.11), values of THD presented are high and the related PF values are low, while the design of an efficient rectifier requires achieving lower THD and higher PF.

2.6.3 Determination of the circuit parameters

The typical spectrum content of such rectifiers contains only odd harmonics. The sum of odd harmonic currents from $n=1$ up to $n=49$ can be used to calculate the total value of the phase current:

$$I_{prms} = \sqrt{\left(\frac{I_{p1}}{\sqrt{2}}\right)^2 + \left(\frac{I_{p3}}{\sqrt{2}}\right)^2 + \left(\frac{I_{p5}}{\sqrt{2}}\right)^2 + \left(\frac{I_{p7}}{\sqrt{2}}\right)^2 + \dots + \left(\frac{I_{p49}}{\sqrt{2}}\right)^2} \quad (2.3)$$

According to equ.(2.3) at firing angle $=30^\circ$, the value of the input current (I_{rms}) is amounting to 34.83A

$$I_{prms} = \left[\begin{aligned} &\left(\frac{48.48}{\sqrt{2}}\right)^2 + \left(\frac{5.93}{\sqrt{2}}\right)^2 + \left(\frac{3.65}{\sqrt{2}}\right)^2 + \left(\frac{2.64}{\sqrt{2}}\right)^2 + \left(\frac{2.07}{\sqrt{2}}\right)^2 + \left(\frac{1.71}{\sqrt{2}}\right)^2 + \left(\frac{1.46}{\sqrt{2}}\right)^2 + \\ &\left(\frac{1.29}{\sqrt{2}}\right)^2 + \left(\frac{1.15}{\sqrt{2}}\right)^2 + \left(\frac{1.04}{\sqrt{2}}\right)^2 + \left(\frac{.95}{\sqrt{2}}\right)^2 + \left(\frac{.89}{\sqrt{2}}\right)^2 + \left(\frac{.83}{\sqrt{2}}\right)^2 + \left(\frac{.78}{\sqrt{2}}\right)^2 + \left(\frac{.75}{\sqrt{2}}\right)^2 + \\ &\left(\frac{.71}{\sqrt{2}}\right)^2 + \left(\frac{.68}{\sqrt{2}}\right)^2 + \left(\frac{.67}{\sqrt{2}}\right)^2 + \left(\frac{.65}{\sqrt{2}}\right)^2 + \left(\frac{.63}{\sqrt{2}}\right)^2 + \left(\frac{.62}{\sqrt{2}}\right)^2 + \left(\frac{.61}{\sqrt{2}}\right)^2 + \left(\frac{.6}{\sqrt{2}}\right)^2 + \\ &\left(\frac{.59}{\sqrt{2}}\right)^2 + \left(\frac{.59}{\sqrt{2}}\right)^2 \end{aligned} \right]^{1/2}$$

$$= 34.83A$$

THD is a very well-known way of determining and measuring the amount of distortion present on a waveform. For the case of distortion on the input current waveform, THD is defined as:

$$THD = \sqrt{\frac{I_{rms}^2 - I_{1rms}^2}{I_{1rms}^2}} \quad (2.4)$$

$$THD = \sqrt{\left(\frac{I_{rms}}{I_{1rms}}\right)^2 - 1} \quad (2.5)$$

According to equ.(2.3), the value is $I_{prms} = 34.83A$ and referring to Fig.(2.13), $I_{1rms} = 34.28 A$. By applying equ. (2.5), THD is:

$$THD = \sqrt{\left(\frac{34.83}{34.28}\right)^2} - 1 = 17.98\%$$

Things are more complicated because of the non-sinusoidal nature of the current wave form. Therefore, it is not an easy task to determine the phase shift between the current and the voltage waveform [22]. In order to calculate the input power factor value, it requires working out of the displacement factor $\cos(\varphi)$. This is achieved by utilizing the FFT analysis tool, the power factor is defined as follows:

$$PF = \frac{P}{S} = K_{\varphi} K_d \quad (2.6)$$

Where,

P: real power.

S: apparent power.

$$K_d = \frac{I_{1rms}}{I_{rms}} \quad (2.7)$$

K_{φ} : displacement factor is equal $\cos(\varphi_1)$.

φ_1 : the phase angle between the 1st harmonic of the current and the voltage.

I_{rms} : total current.

I_{1rms} : current at fundamental frequency.

K_d and k_{φ} are both factors between 0 and 1.

The power factor is calculated using the above expressions in equ.(2.6).

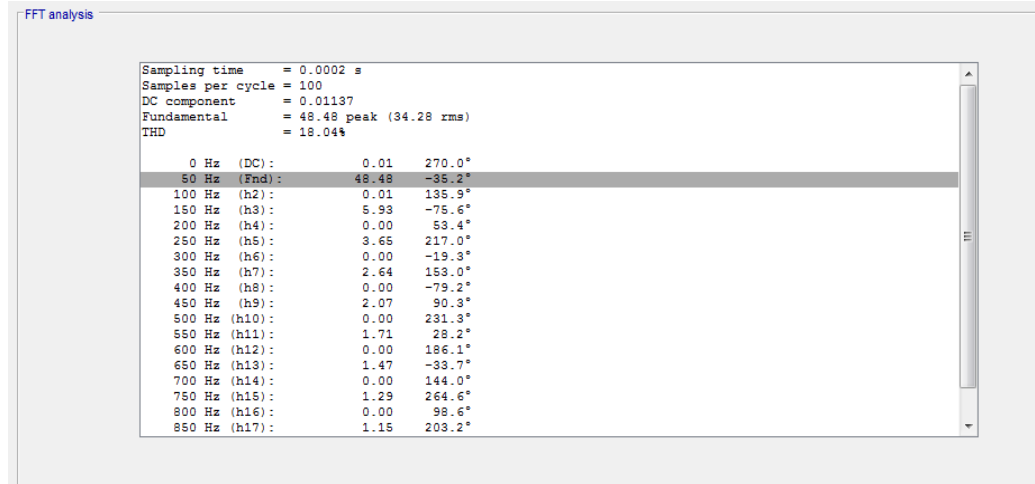


Figure 2.12: FFT analysis of the input current for controlled single phase full wave rectifier with RL-load at $\alpha=30^\circ$.

From Fig. (2.12), one can figure out that the phase angle between the 1st harmonic of the current and the voltage is -35.2° .

Substituting this value in the equ. (2.7):

$$PF = \frac{34.28}{34.83} * \cos(-35.2) = 0.804$$

This significant result shows that the power factor for controlled rectifiers depends on the firing angle α [23] .

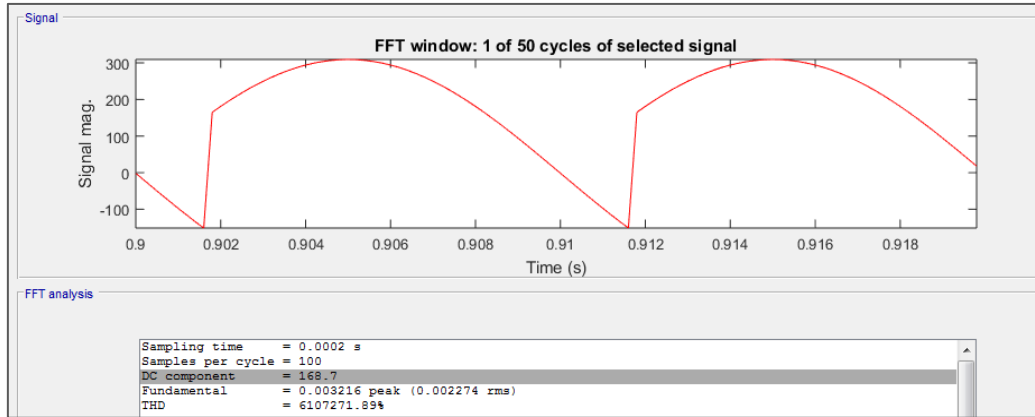


Figure 2.13: Output voltage waveform for controlled single phase full wave bridge rectifier with RL-load at $\alpha=30^\circ$.

To calculate the average output voltage of a single phase full wave converter for continuous current conduction, one should use:

$$V_{dc} = \frac{2V_m \cos \alpha}{\pi} \quad (2.8)$$

Where,

V_m : is the peak value of the input voltage.

α : is the firing angle.

At $\alpha=30^\circ$ and input voltage =311V peak, the output voltage of a single-phase bridge circuit is:

$$V_{dc} = \frac{2 * 311 * \cos 30}{\pi} = 171.46 \text{ V.}$$

The simulated output voltage (DC component) obtained from FFT analysis is closer to the theoretical value obtained from the equ.(2.8).

Average output current (load current) is defined in the following equation as:

$$I_{dc} = \frac{V_{dc}}{R_L} \quad (2.9)$$

$$I_{dc} = \frac{171.46}{5} = 34.292 \text{ A}$$

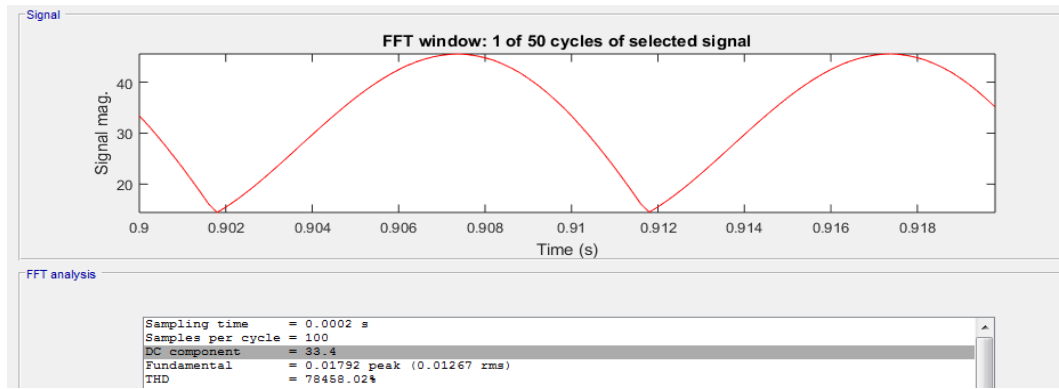


Figure 2.14: Output current waveform for controlled single phase full wave bridge rectifier with RL-load at $\alpha=30^\circ$.

Output current can be found from FFT tool in MATLAB/SIMULINK $I_{dc}=33.4$ A. Simulation results relating to output current show that the source current on AC side is dependent on the load current. Although the current on DC side of the rectifier is positive as shown in Fig.(2.14) above, the current on AC side is bidirectional.

Efficiency (η) is another important parameter used to describe the quality of rectification; it represents the ratio of output power of the rectifier to the input power. The ratio (η) is also known as efficiency which is expressed by:

$$\eta = \frac{P_{dc}}{P_{ac}} * 100\% \quad (2.10)$$

Where,

$$P_{dc} = V_{dc} * I_{dc} \quad (2.11)$$

$$= 168.7 * 33.4 = 5634.58 \text{ W}$$

$$P_{ac} = V_{rms} * I_{rms} \quad (2.12)$$

$$= 220 * 34.83 = 7662.6 \text{ W}$$

$$\eta = \frac{5634.58}{7662.6} * 100\% = 73.53\%$$

It's worth mentioning that controlled rectifiers have lower efficiency than uncontrolled rectifiers.

2.6.4 Representation in decibel form (dB)

Representing the relative amplitudes of the input current, which is tabulated in Table 2.5, can also be done through graphing the current or power for each harmonic. In cases of power representation and because the power is proportional to the square of the amplitude for each harmonic, these numbers often get quite small for the higher harmonics. However, in cases of current representation, harmonic current amplitude is indirectly proportional to the order numbers. As numbers order increases extremely high, the amplitude of the current will be too small for the aforementioned reasons. The current or power are often expressed as a decibel [24], [25].

Decibel is an interval between two frequencies with ratio of 10, e.g. between ω_0 and $10\omega_0$, or between 10 and 100 Hz.

$$\begin{aligned}\frac{a}{dB} &= 10\log_{10} \frac{p_2}{p_1} = 10\log_{10} \frac{V_2^2/R_2}{V_1^2/R_1} \\ &= 10\log_{10} \left(\frac{V_2}{V_1} \right)^2 + 10\log_{10} \frac{R_1}{R_2} \\ &= 20\log_{10} \frac{V_2}{V_1} - 10\log_{10} \frac{R_2}{R_1}\end{aligned}$$

Instead, if $P_2 = I_2^2 R_2$ and $R_1 = R_2$, we obtain

$$\frac{a}{dB} = 20\log_{10} \frac{I_2}{I_1} \quad (2.13)$$

Where,

a: is the magnitude of harmonic current in dB.

I_{mn} : is the peak value of the component of harmonic current.

I_m : is the peak value of the fundamental current wave ($n=1$)

It is important to note from the equation that $10\log_{10}$ is used for power, while $20\log_{10}$ is used for voltage or current.

The harmonic current spectrum can be displayed as a bar graph.

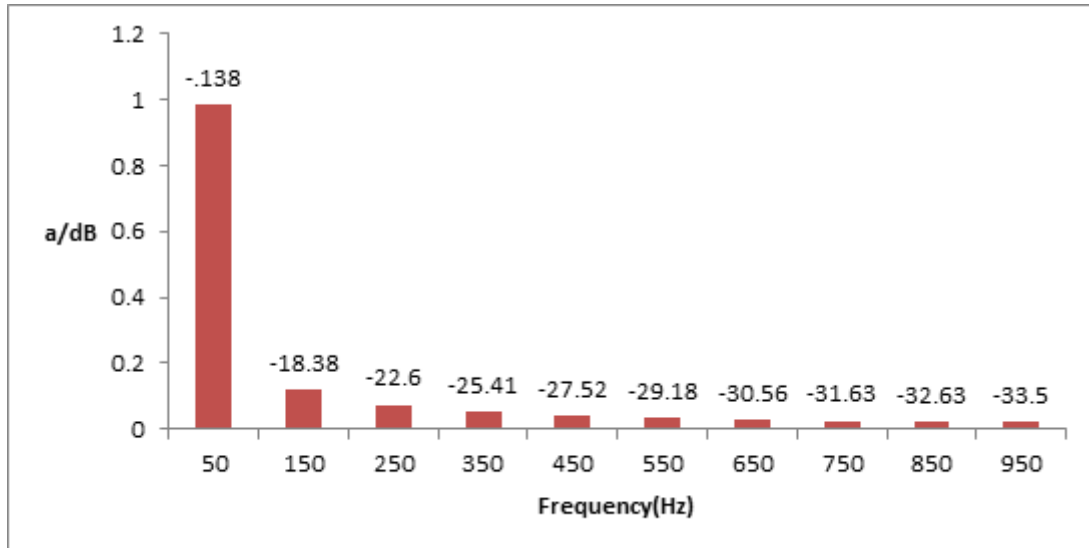


Figure 2.15: Frequency spectrum of input current in dB for controlled single phase full wave bridge rectifier with RL- load at $\alpha=30^\circ$.

As presented, the conventional AC rectification process is accompanied by rich harmonics, which pollute the power system and interfere with other electric equipment, leading to the following:

- High input current fluctuation.
- Low efficiency.
- Poor power factor at AC mains source.
- High losses.
- High harmonics content and undesirable component called ripple, which creates unwanted effects in the system if the ripple exceeds the allowable value.

Thus, filtering is necessary to minimize the problems of power quality, in general, and current harmonics, in particular. Filters are the solution to

solve such problems. Various types of passive filters technique and strategies are used in this study and will also be discussed for meeting standards [2].

Chapter Three

Background and Literature Review

Theoretical Background

This chapter gives a detailed documentation of the theories applied in the project.

3.1 Power Quality

Electric Power Quality (EPQ) can be defined as “keeping the near sinusoidal waveform of the power distribution bus voltages and currents at rated magnitude and frequency”. Another definition of (EPQ) is “Any power problem manifested in voltage, current or frequency deviation that can cause a failure or mal-operation of consumer’s equipment”.

Electric Power Quality is often used to express the quality of voltage, current, power supply and the reliability of service, etc. [27].

As a result of the increased demand of the non-linear loads, the power electronic equipments got so popular. The electric power systems using these equipments have a main disadvantage which is harmonics [28]. The use of rectifiers in these systems produce DC power is considered as main source of these harmonics in the utility [16]. The main troubles caused by harmonics are: voltage sags and swells, transients, under voltage and over voltage, frequency variations, outright interruptions and low power quality for sensitive electronic equipment such as computers

[28]. The above-mentioned problems of harmonics can be reduced or mitigated by the use of power filters [9].

3.2 Nonlinear Loads

A nonlinear load can be defined as an electrical load that draws current discontinuously or which impedance varies throughout the cycle of the input AC voltage waveform [7].

In the linear loads the current and voltage are assumed to be proportional. The presence of harmonic current in waveforms and fundamental currents causes distortion in these waveforms, change them to non-sinusoidal, and that how non-linear load are created [29].

Some examples of nonlinear loads are:

1. Thyristors-controlled reactors (TCRs).
2. Static VAR compensators (SVCs).
3. Silicon-controlled rectifier (SCR) heating.
4. Induction heating.
5. Arc welding [28].

When a non-sinusoidal current drawn by a nonlinear power load passes through the different kind of impedences, it will produce a voltage harmonics in the power system which will affect the power system components mainly the sensitive ones [30]. As its expected 60% of the

load on utility system will be non-linear in the following 10 years (and this expansion will include residential sector and household appliances) [28]. The main and a real challenge that will face any power quality is the harmonic mitigation for electric utilities around the world, where the competition, supply quality, security and reliability are the essentials for any economic survival [31].

3.3 Basic Harmonic Concepts

Harmonics are defined as a mathematical way of describing distortion of the voltage or the current wave form. As a term, harmonics are defined as “a component of waveform that occurs at an integer multiple of the fundamental frequency” [18]. For example for a fundamental of 50 Hz, the third harmonic would be 150 Hz and the fifth harmonic would be 250 Hz and so on [32].

Large numbers of electric equipment that have nonlinear operating characteristics when used in the power distribution circuits will produce nonlinear voltage and current. The best analysis of periodic non-linearity is done using the Fourier transform, and that’s why the nonlinear current and voltages are generally referred to as harmonics [15].

Harmonics arise as currents. As these currents flows through the impedances, the harmonic voltages are produced in the system, and increased through the installation. It is important to know that the current distortion measurements are suffixed with ‘I’ while voltage distortion figures with ‘V’. It is important to know that the harmonic spectrum as

the effects depend on the harmonic order. Simple total harmonic distortion (THD_I , THD_V) measurements are of little use for diagnostic purposes [32].

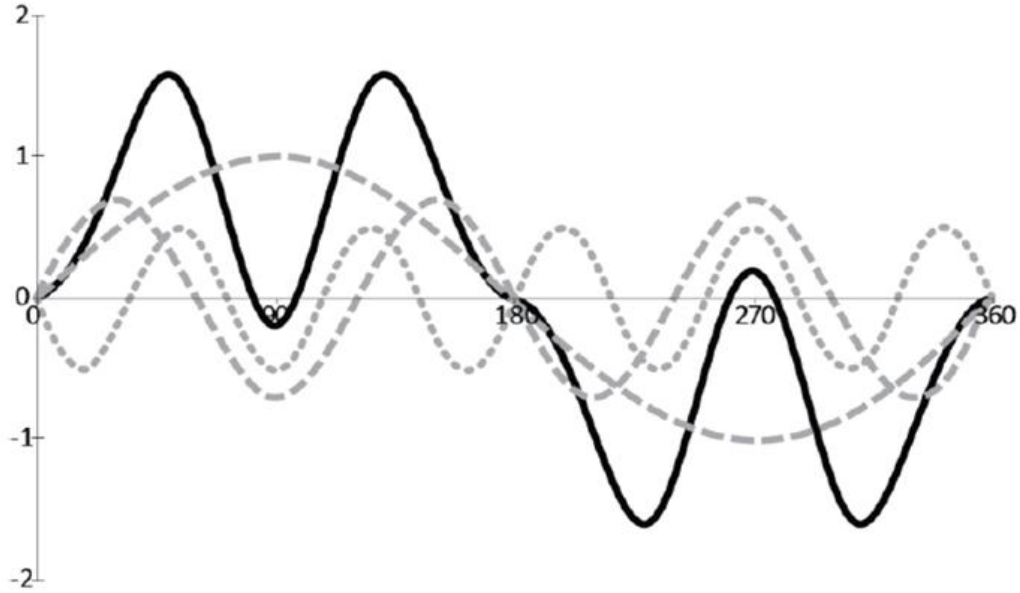


Figure 3.1: Distorted composite current waveform [32].

3.3.1 Types of harmonics

1- Integer Harmonics: Harmonic with frequencies equals to integer multiple of fundamental frequency. These are further classified into two main categories; Odd harmonics, and Even harmonics. These two categories are further discussed below.

A. Odd Harmonics: Harmonic with frequencies equal to Odd integer multiple of the fundamental frequency. These harmonics can be expressed as :

$$i_n = I_n \sin(2\pi nft)$$

Where,

$$n = 3, 5, 7, 9, \text{ etc.}$$

I_n : The amplitude of the harmonic component of order n .

B. Even Harmonics: Harmonic with frequencies equal to even integer multiple of the fundamental frequency. These harmonics can be expressed as:

$$i_n = I_n \sin (2\pi nft)$$

Where,

$$n = 2, 4, 6, 8, \text{ etc.}$$

I_n : The amplitude of the harmonic component of order n .

2- Sub Harmonics: The second type of harmonics, which have frequencies of lower value than the fundamental frequency value. These harmonics can be expressed as:

$$i_n = I_n \sin (2\pi nft)$$

Where,

$$n < 1; \text{ e.g. } 0.2, 0.6, 0.7, 0.9, \dots \text{ etc.}$$

I_n : The amplitude of the harmonic component of order n .

3- Inter Harmonics: The third type of harmonics which have frequencies of higher values than fundamental frequencies values, these harmonics can be expressed as:

$$i_n = I_n \sin (2\pi nft)$$

Where,

$n > 1$ but not integer; e.g.: 1.3, 1.9, 2.8 . . . etc.

I_n : The amplitude of the harmonic component of order n [27].

3.3.2 Causes and sources of harmonics

3.3.2.1 Causes

Harmonic currents are generated from the switching behavior of rectifier using semiconductor switching devices. This rectifier is considered as a harmonic current source or a model where the interaction between the AC source network and the converter DC system is taken into consideration.

As shown in Fig.(3.2), Even harmonics flow through the load where Odd ones flow through the supply source. Harmonics that are fed into the supply system and propagate the power system can be either increased or reduced [20], [33].

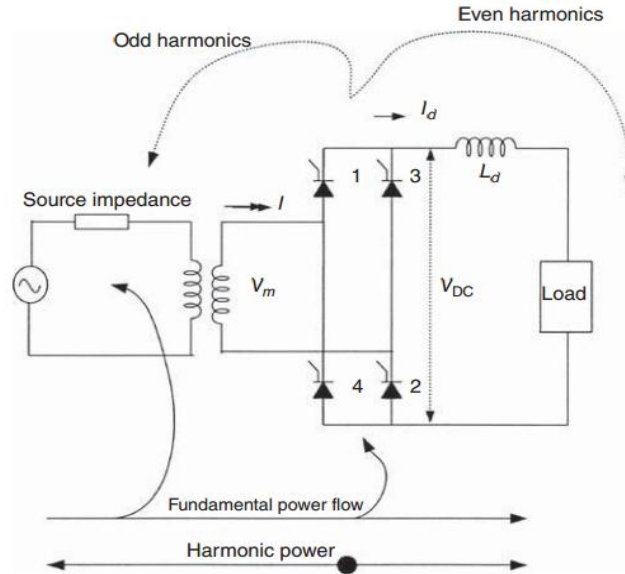


Figure 3.2:Single phase two- pulse controlled rectifier as a source of harmonic generation and harmonic power flow [28].

As mentioned previously, the harmonic voltage distortion is generated by the interaction of the harmonic current emissions from a variety of the sources and the power system impedance. These harmonic emissions arise from all types of non-linear load which include: large industrial loads connected at transmission or distribution levels, smaller commercial and residential distribution system customer loads, distributed generation installations, the power system and traditional generation equipment. It should be mentioned that the most significant harmonic contributors in the presence of these current emissions are the system electronic loads which include the following:

- i. Switch mode power supplies (SMPS), present in computers, televisions, microprocessors.

- ii. Rectifiers, present in DC motor drives, regulated power supplies, battery chargers.
- iii. Inverters, present in variable speed ac drives and now a days in Indian homes.
- iv. Static VAR compensators.
- v. Cycloconverters.
- vi. High voltage DC transmission converters.

The real challenge that faces the designers and specifiers is to use the proper mitigation technique to reduce the levels of harmonics emission resulted from the source mentioned above.

Proper mitigation techniques will ensure the safety and resilience of installation and also meet the harmonic limits [32], [34].

3.3.2.2 Sources

The main sources of the harmonics in electric power systems can be categorized as:

- a) Magnetization nonlinearities of transformer.
- b) Rotating machines.
- c) Arcing devices.
- d) Semi-conductor based power supply.

- e) Inverter fed AC drives.
- f) Thyristors controlled reactors.
- g) Phase controllers.
- h) AC regulators [27].

3.3.3 Types of harmonic sources

A. Current-Source Nonlinear Loads (CSNLs)

As shown in Fig.(3.3,a), the sufficient DC inductance in the thyristors rectifier (which is considered as a common and typical source of harmonic current) produces DC current. The switching operation through this rectifier will generate harmonics that will cause a current wave form distortion as shown in Fig.(3.4). Because the harmonic current contents and characteristics are less dependent on the AC side, this nonlinear load behaves like a current source. And that's why it is called a current-source nonlinear load and represented as a current source as shown in Fig.(3.3,b). Similarly, a diode rectifier with a sufficient DC inductance and a highly inductive load with SCR AC power control, etc., is also considered as current-source nonlinear load.

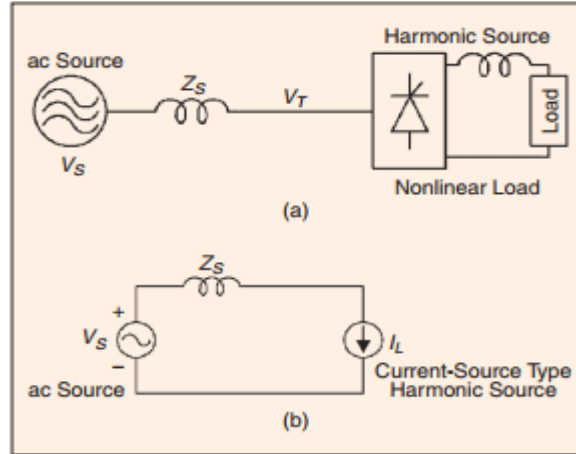


Figure 3.3: Typical current-source nonlinear load (a) thyristors rectifier for dc drives, heater drives, etc. (b) per-phase equivalent circuit of thyristors rectifier [35].

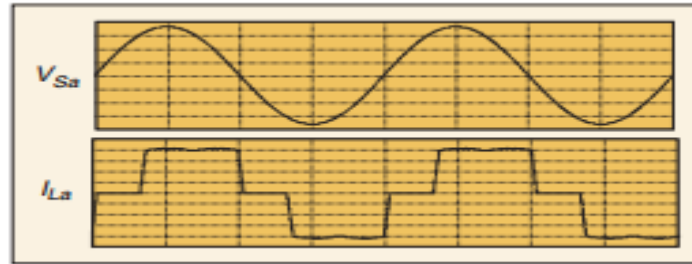


Figure 3.4: Typical voltage and current waveforms of thyristors rectifier, source voltage V_{Sa} and line current I_{La} [35].

B. Voltage-Source Nonlinear Loads (VSNLs)

The voltage at the rectifier input terminal is less dependent on the AC impedance, and despite the high current distortion. Its harmonic amplitude is greatly affected by the AC side impedance and source voltage unbalance. Therefore, diode rectifiers behave like a voltage source rather than a current source.

Fig.(3.5,a) shows the typical current and voltage waveforms while Fig.(3.5,b) shows the equivalent circuit of the diode rectifier system

where it is represented as a harmonic voltage source (or voltage source nonlinear load).

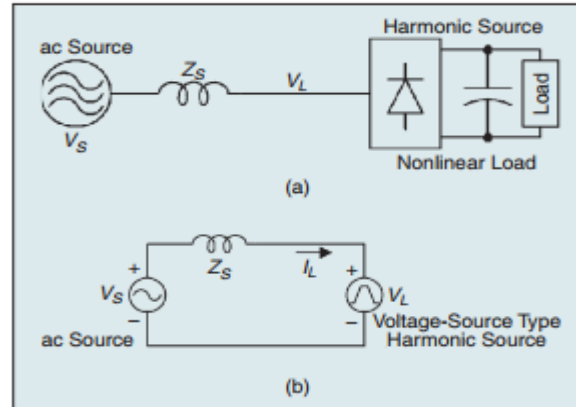


Figure 3.5: Typical voltage-source nonlinear load (a) diode rectifier for ac drives, electronic equipment, etc. (b) per phase equivalent circuit of diode rectifier[35].

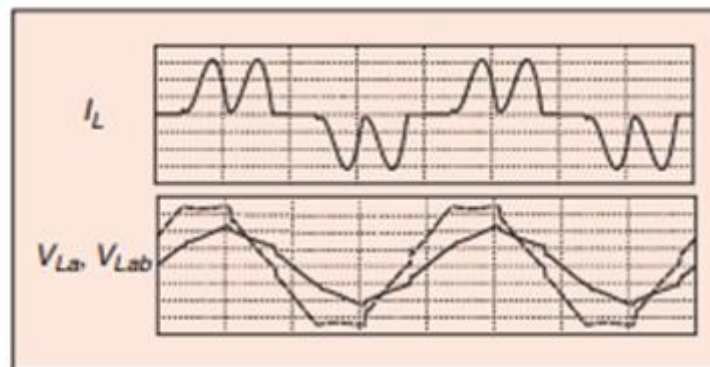


Figure 3.6: Typical current and voltage waveforms of diode rectifier, line current I_L , line-to-neutral voltage V_{La} , and line-to-line voltage V_{Lab} at rectifier input[35].

3.3.4 How harmonics are generated

In a simple circuit (circuit that contains linear elements resistance, inductance and capacitance), the current that flows in such circuit is proportional to the applied voltage at certain frequency. So as the voltage applied is a sinusoidal, the flowing current will also be sinusoidal, as shown in Fig.(3.7) which illustrates the load-line that

represents the relationship between the applied voltage (lower right quadrant) and the resulting load current (top left quadrant) [32].

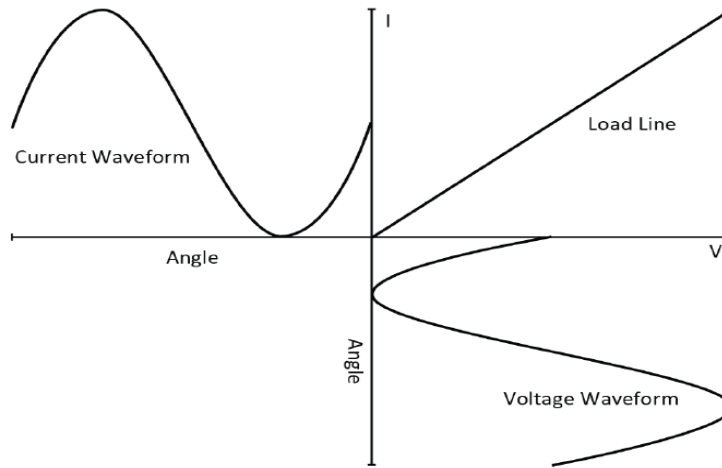


Figure 3.7: Current waveform in a linear load.

The non-sinusoidal currents results when the current flowing through the load is nonlinear with respect to the applied voltage.

The load-line shown in Fig.(3.8) shows the case where a reactive element is added to the circuit. This reactive element will cause a phase shift between the voltage and current waveforms, reduce the power factor, but will also keep the circuit linear.

The load in such situations (illustrated in Fig.(3.8)) is a simple full wave rectifier and capacitor such as the input stage of a typical switched mode power supply. The shape of the load line which will be more complex than illustrated in Fig.(3.8) which shows that the supply voltage should exceed the voltage stored on reservoir capacitor(close to the peak of the voltage sine wave).

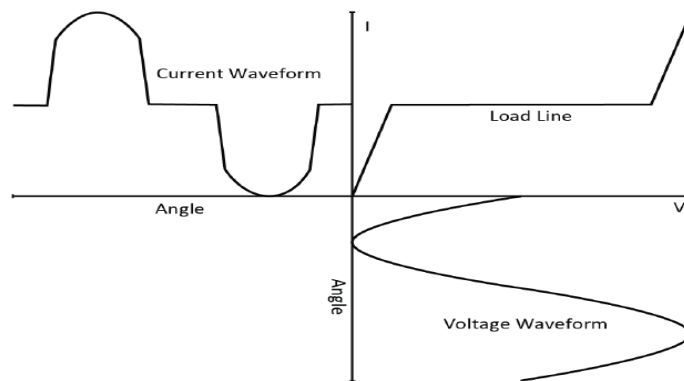


Figure 3.8: Current waveform in non-linear load.

The difference between the cyclical waveform and symmetrical waveform such is that the distorted current wave form in cyclical one can be deconstructed into a sinusoid at the fundamental frequency plus a number of sinusoids at Even and Odd frequencies, while in symmetrical one, the positive and negative half cycles are of same shape and magnitude, all Even order harmonics have a magnitude of zero. These types of harmonics are not common since the half wave rectification is not widely used.

The circuit shown in Fig.(3.9) represents a simulation to a circuit of non-linear load. This simulation can be done by connecting a linear load in parallel with a number of current sources that each one of these sources representing harmonic frequencies. As the fundamental current converted by the load to harmonic current flows through source impedance and all the parallel paths, a harmonic voltage is generated across the supply impedance [32].

It should be mentioned that when the harmonics are suspected or their absence should be verified, the current is the element that should be measured.

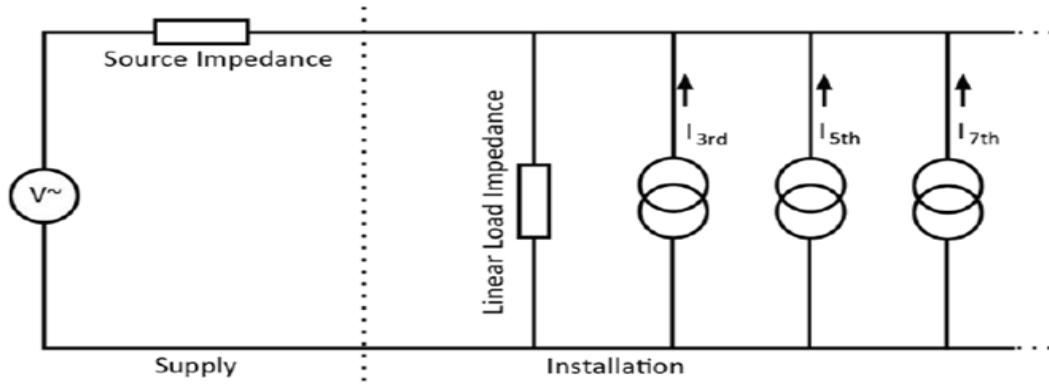


Figure 3.9: Equivalent circuit of a non-linear load [32] .

The reason why the voltage generators is not considered as a harmonic generator is that the magnitude of the voltage is proportional to the source impedance and that will lead the generator to be a current source, and since the source impedances are very low , the harmonic voltage distortion resulted from a harmonic current will be also very low.

This will indicate that there is no harmonic problem while in fact large harmonic currents present, this assures what was mentioned above that the current is the element that should be measured when harmonic problem appears [32].

3.3.5 Harmonic mitigation measures

In order to limit the harmonic currents and associated voltage distortion within the limits, the majority of nonlinear loads associated with bulk power need addition of mitigation equipment. Harmonic mitigation measures are required to achieve the following tasks:

1. Meeting local harmonic emission limits.
2. Reducing overloading of, e.g., cables and transformers.
3. Improving resilience of equipment by reducing voltage waveform distortion [36].

3.3.6 Harmonics impacts on power system components

Harmonics cause distortions of the voltage and current waveforms, which have adverse effects on electrical equipment [28]. However, harmonics have bad effects on application and operation of the electrical power system components. In fact, these harmonics can derated these components such as transformer, reactor, capacitors, cables, switchgear, relays, motor, generators and electronic equipment [15].

3.3.7 Harmonic limit standards

To judge the severity of harmonic distortion, various standards have been established for harmonic voltage distortions that can affect the operation of other devices connected to the same power grid. One of these standards is IEEE 519 by the American Institute of Electrical and

Electronic Engineers. The limit used in this standard is the percentage of total harmonic voltage distortion. This limit is different depending on the type of building and the sensitivity of electrical equipment that may be used in each one of these buildings. As shown in Table 3.1, the limitation is strict for the building where sensitive electronic equipment may be used [37].

Table 3.1: IEEE 519 standards for total harmonic voltage distortion.

Application Class	THD (%)
Sensitive Applications • Airports/Hospitals • Telecommunication Facilities	3%
General Applications • Office Buildings/Schools	5%
Dedicated Systems • Factories	10%

When measuring THD%, it should be equal or less than 5% as measured at any point of common coupling (PCC), in addition that any individual harmonic voltage distortion should not exceed 3% of the fundamental. Higher level of harmonic distortion can be allowable as the equipment is operating safely at such high levels. It should be mentioned that this method is not practical especially in systems where industrial loads are supplied from a common power point. In a power system, all operating modes should be considered for harmonic limits. If certain operating modes last for only a small fraction of time but produce higher harmonic distortion, it may not be necessary to provide additional harmonic mitigation techniques for that short duration [36].

3.3.8 Total harmonic distortion

THD can be defined as “a measure of the effective value of the harmonic components of a distorted waveform and sometimes considered as the potential heating value of the harmonics relative to the fundamental” and it can be used for both voltage and current measurement. It is an indicator for:

1. How much extra heat will be recognized when a distorted voltage is applied across a resistive load.
2. Additional losses caused by the current flowing through a conductor.

The limitation of using this index is that it is not an accurate indicator of the voltage stress within a capacitor because that is related to the peak value of the voltage waveform but not to its heating value [27].

3.3.9 Harmonics and system power factor

Power Factor (PF) is defined as “the measure of real power (P) with respect to apparent power (S), for any electrical load”. Actually it conveys the relationship between the input voltage and current waveform for any electrical load.

3.3.9.1 Power factor in systems with only linear loads

For pure and clean sinusoidal waveforms (for pure sine wave for both current and voltage), power factor presents the value of the cosine angle between the current and voltage where the phase shifts between them

equals zero. The value of P.F will vary between 0 and 1. P.F can be either:

1. Lagging: which refers to inductive load where the current lags the voltage.
2. Leading: which refer to capacitive load where the current leads the voltage [38].

3.3.9.2 Power factor in power System with nonlinear loads

The Power Factor with nonlinear loads turns to a term of total power factor that includes two main components:

1. Displacement: is the ratio of active power to the apparent power of fundamental wave.
2. Distortion: is that the part that is with the harmonic voltage and currents [20].

Both components are illustrated in Fig.(3.10, a, b).

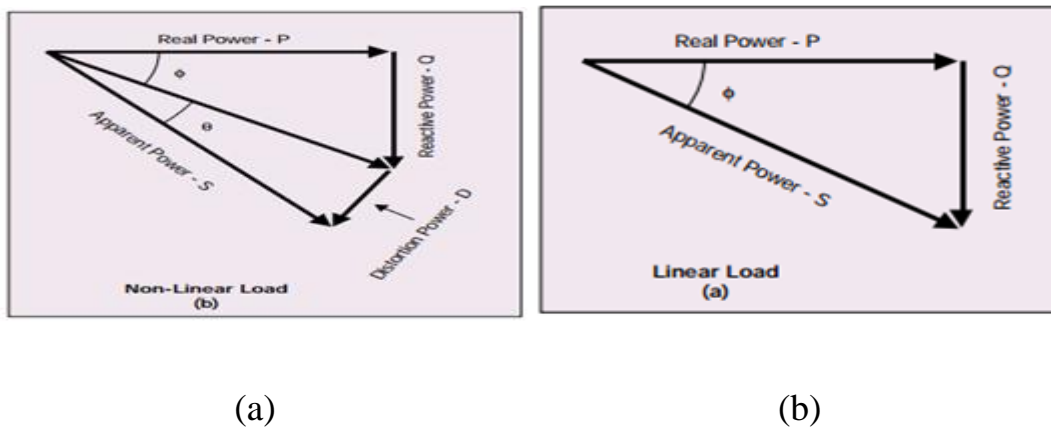


Figure 3.10: Power factor vectors relationship (a) for non-linear load (b) for linear load [23].

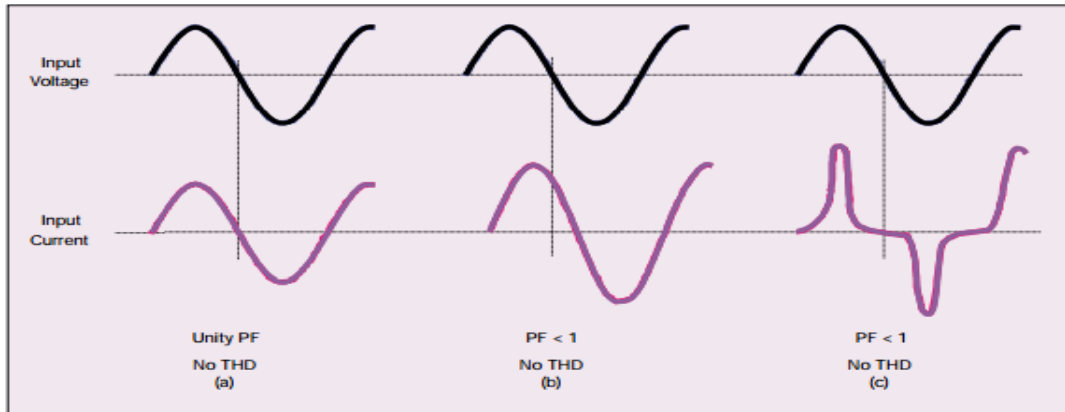


Figure 3.11: AC input voltage vs. current relationships [23] .

Fig.(3.11,a) represents the most familiar situation, which is purely resistive linear load. The input voltage, the PF in this case is unity and the THD is zero since the current waveform is sinusoidal and in-phase with input voltage.

Fig.(3.11,b) represents the case which is only with a linear reactive load where the current waveform is still pure sinusoid, it is phase-shifted from the voltage waveform and it will result in a power factor that is less than unity. Due to the fact that the input current waveform maintains sinusoidal, THD is still zero.

Fig. (3.11, c) describes the behavior of a nonlinear load. In this case, the current waveform is non-sinusoidal, which results in a power factor less than unity and a non-zero THD.

3.4 Power Filter Topologies

One of the components that affect power quality, equipment life and efficiency in any power system is harmonics which can be described as undesirable components in the sinusoidal waveform of the AC power supply. It is necessary to monitor the harmonics in any power system. If the harmonics are present, they can be rectified by using suitable methods such as filters [39].

The five techniques that can be used to reduce harmonics and at the same time can fulfill the requirements created by the current harmonic standards [40].

To design harmonic filters, it should be taken into consideration that

- Filters are used to reduce AC system currents and voltages to the allowed level.
- Filters are used to prevent the convertor system from absorbing reactive power [41].

3.5 Harmonic Filter

Since the harmonic filters are mainly the set of passive(R, L, C) and/or active (transistors, op-amps) components that are used to select or reject a band of frequencies, their main purpose is to purify any undesirable frequencies created by nonlinear characteristics of some electronic devices or signals picked up by the surrounding medium.

Other functions for filters are:

- Overcome the problems of harmonics by keeping them at the allowed limits.
- Filter can be tuned to create a low impedance path or ‘trap’ to a harmonic by setting the circuit to resonant frequency (f_r) where the response is at its maximum. The circuit is then said to be in state of resonance.

Power filters are classified as the following:

1. Passive filters.
2. Active filters.
3. Hybrid filters.

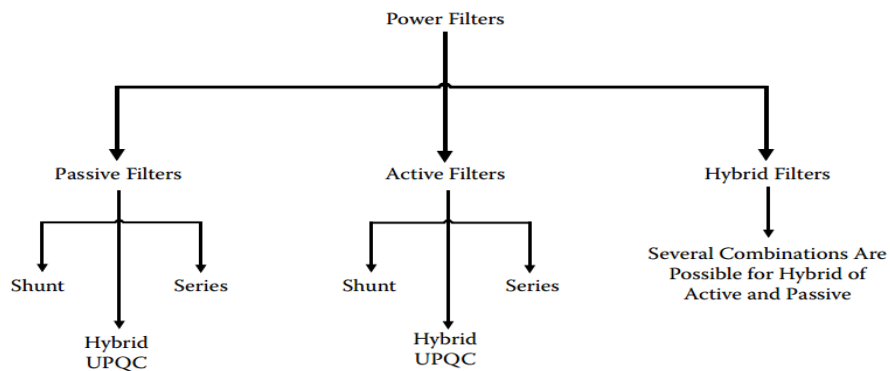


Figure 3.12:Classifications of power filters [9] .

Passive filters are the main concern in this study.

3.5.1 Passive filter

In order to shunt the harmonic currents off the line or to block their flow between parts of the system by setting the elements at a selected resonant frequency where the response is at its maximum, passive filters are used as the simplest way to do this. These filters of R, L and C elements connected in different combinations to gain desired suppression of harmonics. Another advantage of using these filters is to provide reactive power consumption and improve power quality of the system [42], [43].

However, the main disadvantage of these filters:

1. The potential of interacting in adverse way with the power system, so its performance will depend mainly on the system source impedance.
2. To eliminate a particular harmonic frequency 20 filters can be used, this indicates that the number of passive filters increases as the number of harmonics in the system.

Passive filter can be classified depending on their topology, connection, and the number of phases. The topology classification can be shunt, series and hybrid and further sub classified as tuned and damped to act as low-pass and high-pass for shunt filters or to act as low-block and high block for series filters. PPFs may be connected in shunt, series or (a combination of both) used for compensating different types of nonlinear loads [44].

In the design, it must be taken into consideration that the passive filters attract harmonics from other sources. Taking series filter as an example, those filter are usually connected in parallel with the nonlinear load and offer very low impedance to the harmonic frequencies that need to be mitigated. For example, for mitigating, 5th and 7th harmonic distortion, one set of filters would be needed to mitigate 5th Harmonics, and another set of filters would be needed to mitigate 7th harmonics. At series resonance, the filters impedance in the circuit is left only with the resistive impedance since the inductive reactance and capacitive reactance cancel each other.

In conclusion the performance of passive filters will be affected by the change of sources and load impedances [32].

3.5.1.1 Passive shunt filters

Passive filters are used to provide a low impedance path for harmonic currents so that they flow in the filter and not the supply Fig.(3.13). The filter may be designed for a single harmonic or for a broad band depending on requirements.

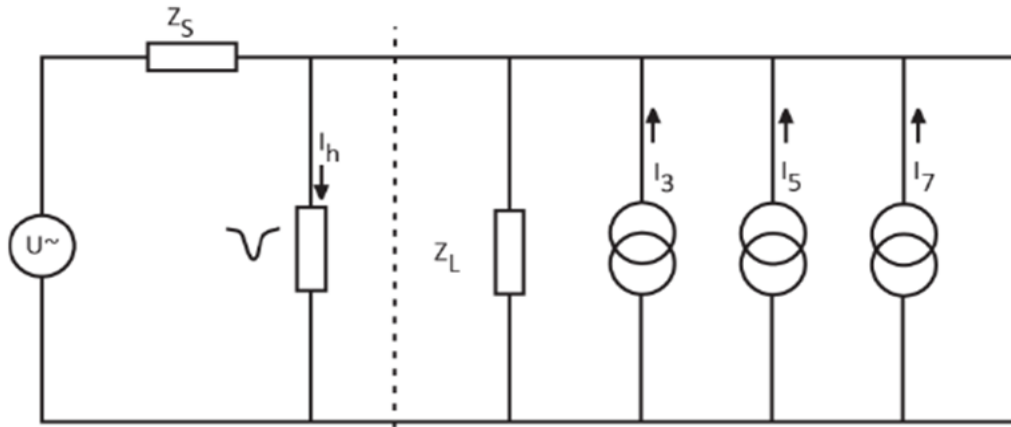


Figure 3.13: Passive harmonic shunt filter [32].

For increasing the series impedance at harmonic frequencies and to reduce the proportion of current that flows back into the supply, more complicated filters are designed and used, as shown in Fig.(3.14).

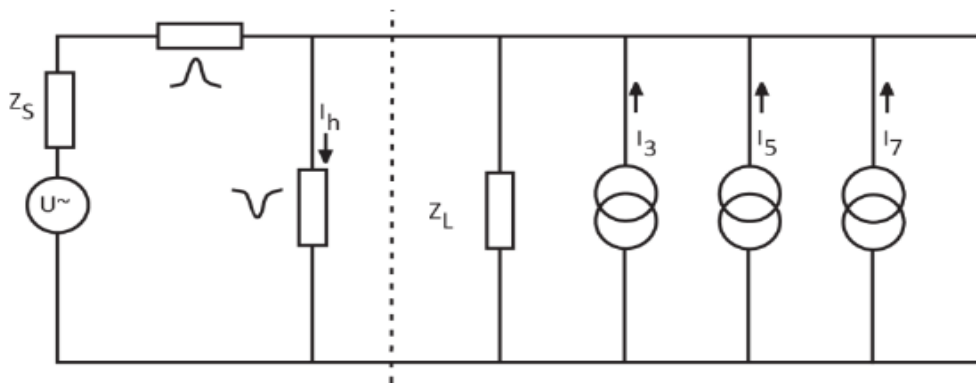


Figure 3.14: Passive series and shunt filters [32].

Shunt filters reduce the harmonic current flowing back in to the supply, but do not reduce (and may increase) the effect of harmonic current in neutrals and on transformers. Usually, shunt filters are designed to control a few lower order harmonics and are integrated with the power factor correction equipment.

Shunt filters are usually used in power systems to suppress harmonics. They are not preferable to use in the single installation because of the problems they create, also in power systems they have many problems that depends on their characteristics that can be determined using the impedance ratio of the source and shunt passive filter. It should be mentioned that the SPF shows lower impedance than the source at specific tuned frequency to reduce the harmonic currents flowing into the source. The main problems can be summarized as follows:

1. The performance of the shunt passive filter is affected by the source impedance, which can't be determined accurately and its value depends on the system configuration strongly.
2. The shunt passive filter fall down in series resonance with the source impedance since it acts as a current sink to the harmonic voltage included in the source voltage.
3. Harmonic amplifying phenomenon may occur in the case when a parallel resonance or anti resonance created between the source impedance and SPF at specific frequency [45].

3.5.1.2 Passive series filters

The passive series filter can be defined as a group of simple series band stop filters either in the phase or in the neutral, while the passive shunt filters can only provide a controlled path for harmonics , the passive series filter blocks harmonic currents. On the other side, a high

harmonic voltage drop appears across the supply on the load side creating a high distortion in supply's voltage. This distortion can highly affect some items of equipment, some items of the equipment are relatively insensitive to this distortion but others are very sensitive. Therefore, this type of filters is not generally recommended and should be applied carefully [32].

3.6 Passive Filters Configuration

3.6.1 Low-pass filters

A low-pass filter is a circuit offers an easy passage to low-frequency signals and difficult passage to high-frequency signals. The basic two types of low pass filters that can offer passage mentioned above are:

1. Inductive low-pass filter.
2. Capacitive low-pass filter.

The two types mentioned above are shown in Fig.(3.15)

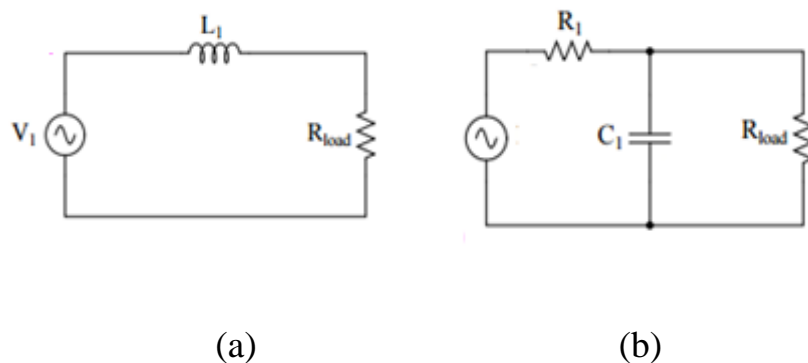


Figure 3.15 : (a) Inductive low-pass filter (b) capacitive low-pass filter.

As the frequency increases, two trends appear in the circuit and lead to high drop of the voltage across series resistor (R_1):

1. The increment of inductor's impedance in series that tends to block high-frequency signals from reaching to the load.
2. The depression of capacitor's impedance in parallel with the load resistance tends to short out high-frequency signals [43].

3.6.2 High-pass filters

A high-pass filter works in the opposite of a low-pass filter; it offers an easy passage of a high-frequency signal and difficult passage to a low-frequency signal.

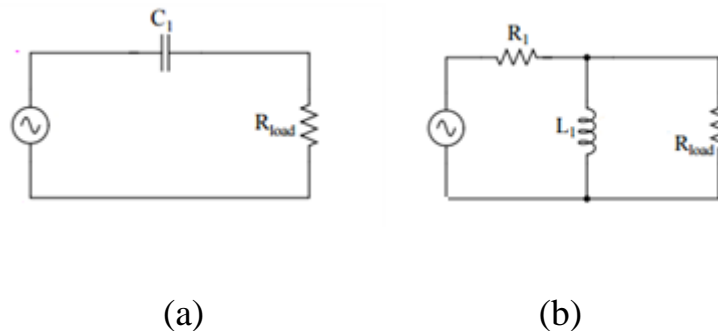


Figure 3.16 : (a) Capacitive high-pass filter (b) inductive high-pass filter.

As the frequency decrease, two trends appear in the circuit and lead to high drop of the voltage across series resistor (R_1):

1. The increment of capacitor's impedance in series that tends to block low-frequency signals from reaching to the load.

2. The depression of impedance in parallel tends to short out low-frequency signals from reaching to the load.

3.6.3 Band-pass filters

The band pass filter can be described as a circuit that combines the properties of low-pass and high-pass into a single filter. The result is called a band-pass filter. This type of filters is usually used to do the needed filtering of particular band, spread or frequency from a wider range of mixed signals.

Creating a band pass filter from a low-pass and high-pass filter can be illustrated using block diagrams.

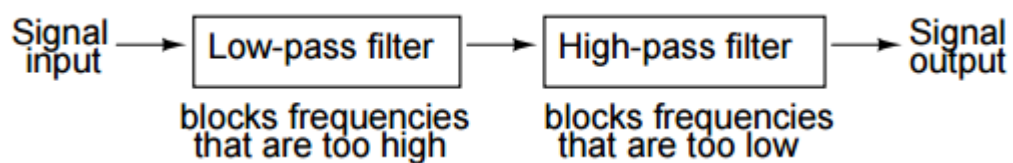


Figure 3.17:System level block diagram of a band-pass filter.

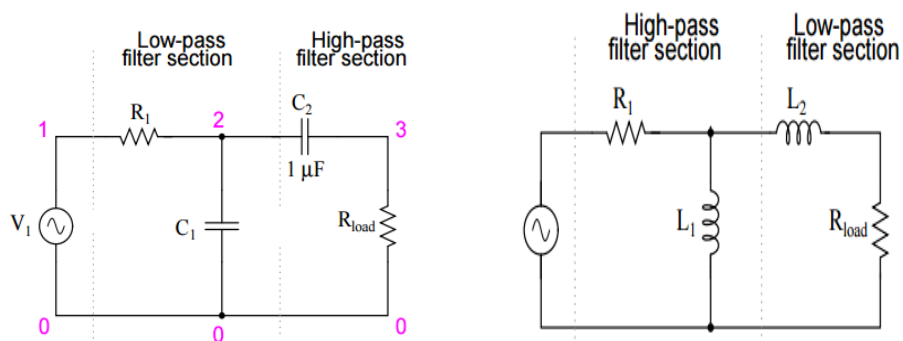


Figure 3.18:System level block diagram of a band-pass filter.

3.6.4 Band-stop filters

The band –stop filter can be described also as a circuit that made out of both a low-pass and a high-pass filter. The difference between this type of filters and the band pass filters is the way of connecting filters, here the filter are connected in parallel not in series, as shown in (Fig.(3.19))

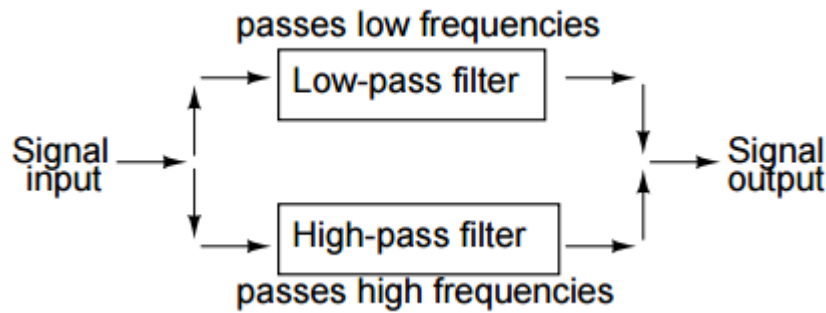


Figure 3.19: System level block diagram of a band-stop filter.

Fig.(3.20) shows the way of connection in details. The components of low-pass filter are R_1 , R_2 , and C_1 and they are connected in T-configuration. The components of high-pass filter are C_2 , C_3 , and R_3 and they are connected in T-configuration as well. This arrangement is known as a “Twin-T” filter.

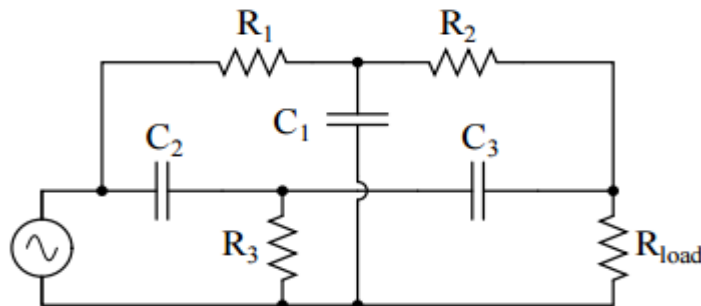


Figure 3.20:“Twin-T” band-stop filter.

Band –stop filters are usually used to pass all frequencies above and below a particular range set by the component value, therefore, this type of the filters is also known as band-elimination, band-reject, or notch filters [43] .

3.7 Selection of Power Filters

Power filters can be selected based on the following factors:

- Nature of load (voltage fed, current fed, or both of them).
- Pattern of supply system (single-phase and three-phase three-wire, three-phase four-wire).
- Type of loads (fixed, variable, fluctuating).
- Compensation required in current (harmonics).
- Compensation required level (THD, individual harmonic reduction meeting specific standard, etc.).
- Environmental factors (ambient temperature, altitude, pollution, humidity, etc.).
- Cost, size, weight.
- Efficiency.
- Reliability [9].

The summary of results of previous research which are related to input passive filter techniques with single-phase uncontrolled rectifier systems are introduced in next section.

3.8 Passive Filter for Different Circuits

3.8.1 Rectifier with resistive load

In most power electronic applications, rectifier is used to convert AC sine wave voltage to DC voltage. Using rectifier with diode is considered as inexpensive way to convert AC to DC in an uncontrolled manner. Conventional AC/DC single phase rectifier with resistive load is considered to be ideal case.

In this case study, the assumptions are: the main source 220 R.M.S/50Hz, with resistive load which is designed for 0.3 kW as shown in Fig.(3.21)

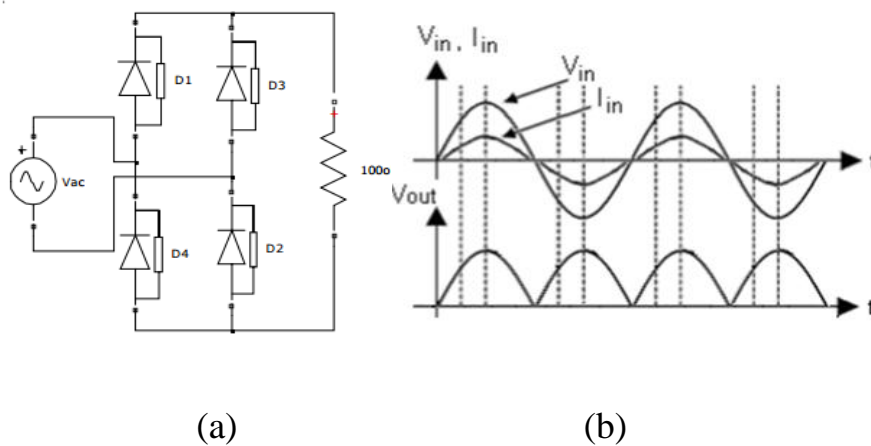


Figure 3.21 : (a) Single phase rectifier (b) input and output waveforms.

In the circuit shown in Fig.(3.21 ,a) when the pure resistive is connected as load, the input current will follow the wave form of input voltage as shown in Fig.(3.10,b) it should be mentioned that the power factor will be unity because of the high ripple of output voltage which can be minimized by using a capacitor added at DC side [46].

3.8.2 Rectifier with capacitive filter in the output side

The rectifier can be created by connecting a large capacitor as a filter on the DC side. It is used to produce DC output voltage pure from ripple as possible. The main disadvantage is the high current distorted current drawn from utility due to the high peak input current produced by charging the capacitor during the peak input voltage [47].

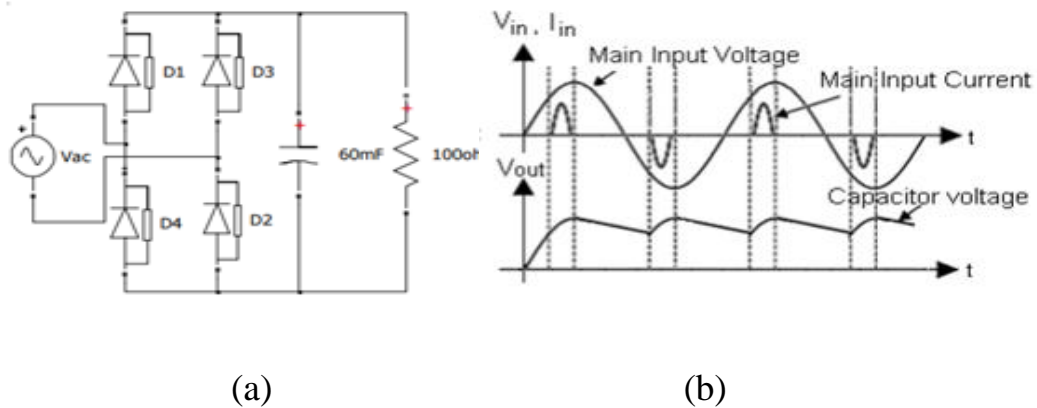
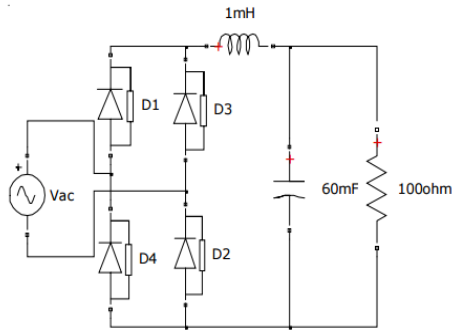


Figure 3.22 : (a) Single phase full wave bridge rectifier (b) input and output waveforms.

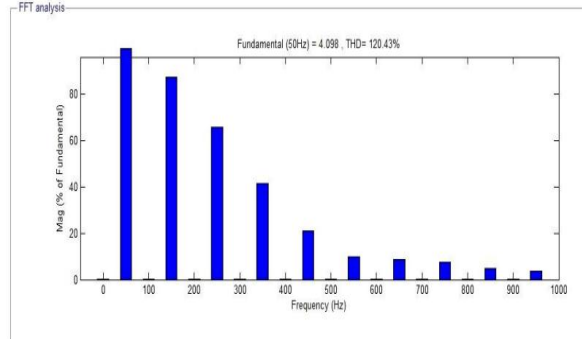
3.8.3 Rectifier with LC- filter in the output side

As shown in the previous section, using capacitor had drawn a heavy, inrush current. The advantage of adding an inductor is to enlarge the conduction angle of current pulse which will reduce the peak of the

current. Also the obtained values of THD will be less than those obtained from the capacitive filter.



(a)

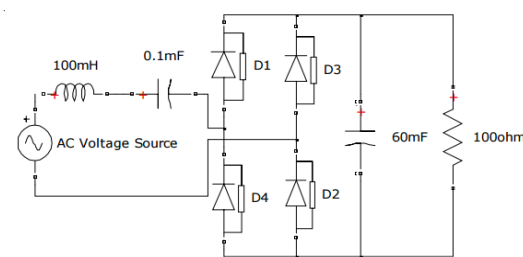


(b)

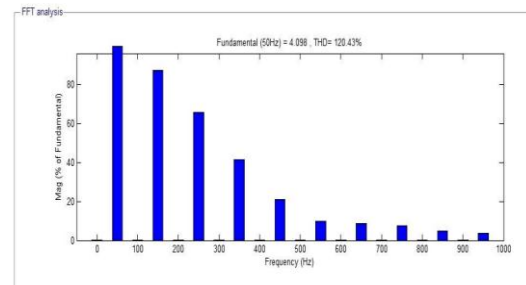
Figure 3.23 : (a) Single phase full wave bridge rectifier with LC- filter in the output side (b) FFT analysis of input current waveform for series resonant filter.

3.8.4 Rectifier with series resonant filter

A series resonant filter is tuned to block any harmonic frequencies. The use of series resonant filter will increase the value of power factor and reduce the value of THD at the same time in order to satisfy the resonance condition. The simulation of this circuit is shown in Fig.(3.24).



(a)



(b)

Figure 3.24: (a) Single phase full wave bridge rectifier with series resonant filter (b) FFT analysis of input current waveform for series resonant filter.

3.8.5 Rectifier with parallel resonant filter

Parallel LC-filter is tuned to resonate a particular harmonic frequency.

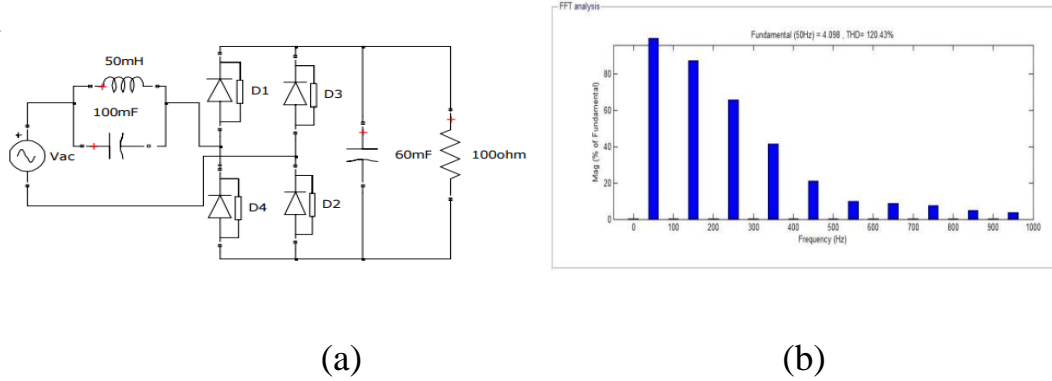


Figure 3.25:(a) Single phase full wave bridge rectifier with parallel resonant filter (b) FFT analysis of input current waveform for parallel resonant filter.

From the line current spectrum for these configuration, it can be noticed that the waveform contains lower frequency orders 3rd, 5th, 7th, 9th that will have higher current harmonics and will be closer to the fundamental one.

Table 3.2: Comparison of the results obtained from the analyzed circuits [46].

Circuit Type	Displacement Factor	Distortion Factor	PF	THD%
Resistive load	0.9999	1	0.9999	0.52
Capacitive filter in the output side	0.9997	0.2185	0.2184	446.48
LC -filter in the output side	0.972	0.6388	0.6209	120.43
Series resonant LC-filter in the input side	0.9174	0.9594	0.8801	29.41
Parallel resonant LC- filter in the input side	0.8147	0.9296	0.7574	39.62

Table 3.2 shows that for a resistive load there is almost no distortion in the input current with THD value of 0.52%. In order to eliminate the output voltage ripple a capacitor is added. The addition of a capacitive filter at the output increases the distortion in the input current to a value of 446.48% which is highly undesirable. For LC- filter in the output side the THD value becomes 120.43% and PF equals 0.6209 which means that when the LC-filters was added in the output side, it decreased THD value and increased PF value in comparison with the previous one when capacitive filters was used. Other passive filters increase the value of the power factor at the input and reduce the distortion as shown when the series resonant LC- filter is connected in the input side. It reduces the value of THD to 29.41% and increases PF value to 0.8801. This means that adding LC-series resonant filter, reduces THD but increases PF .Finally, when a parallel resonant LC-filter is connected at the input side, it increases the THD value to 39.62% but decreases the PF value to 0.7574. After this comparison the best configuration according to the results is the series resonant LC-filter connected in the input side.

3.8.6 Rectifier with improved passive wave shaping filter

To overcome the disadvantage of the high values of total harmonic distortion associated with the parallel resonant LC- filter and to improve the power factor, a capacitor C_b is connected in parallel between the parallel resonant tank and the rectifier bridge as shown in Fig. (3.26). This capacitor could compensate the reactive power and absorb the

distortion power. This method is called as improved passive wave shaping method. The capacitor C_b in this case can filter out the high harmonics, to have better filter feature and to improve the input power factor. For a designed L_r and C_r values, C_b is selected so that the input power factor, at rated output power reaches its peak value. In improved method, the single phase rectifier is designed for 5 kW load from 220V R.M.S with 5% output voltage ripple and its frequency is 50 Hz. The power factor value is found to be 0.9852 and the THD is decreased to 14.9% [48]. The advantages of the improved method:

1. Lower input current total harmonic distortion due to the significant filter feature of capacitor C_b
2. Higher input power factor.
3. Increased efficiency of the rectifier [48].

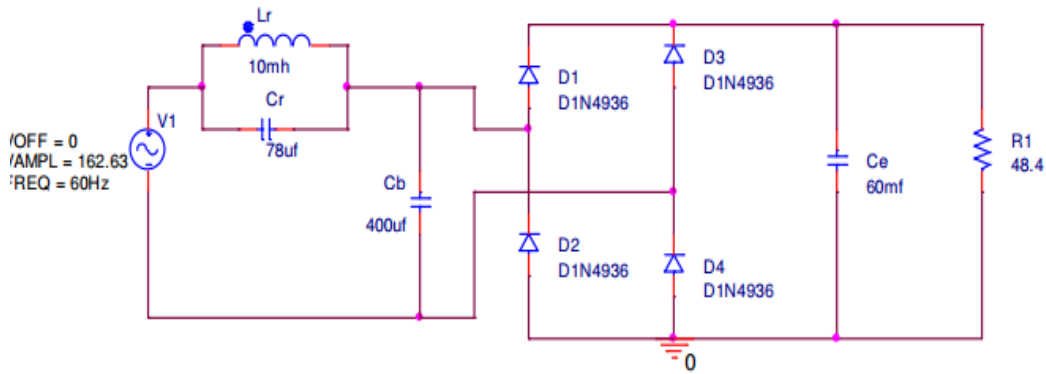


Figure 3.26: Single phase full wave bridge diode rectifier using improved passive wave shaping method [48] .

The range of the C_b values is from 100 μF - 10 mF. These values are selected so that the input power factor at a rated output power reaches its peak value. The THD and PF values are calculated for different values of C_b by simulating the circuit for each value of C_b .

Table 3.3: Calculated power factor values of different values of capacitance C_b .

C_b	THD%	Power Factor (PF)
100 μF	8.312	0.6405
200 μF	4.7675	0.8533
300 μF	3.55	0.9575
400 μF	2.62	0.9960
500 μF	2.071	0.9956
1 mF	0.99	0.807
5 mF	0.1437	0.59116
10 mF	2.614	0.5578

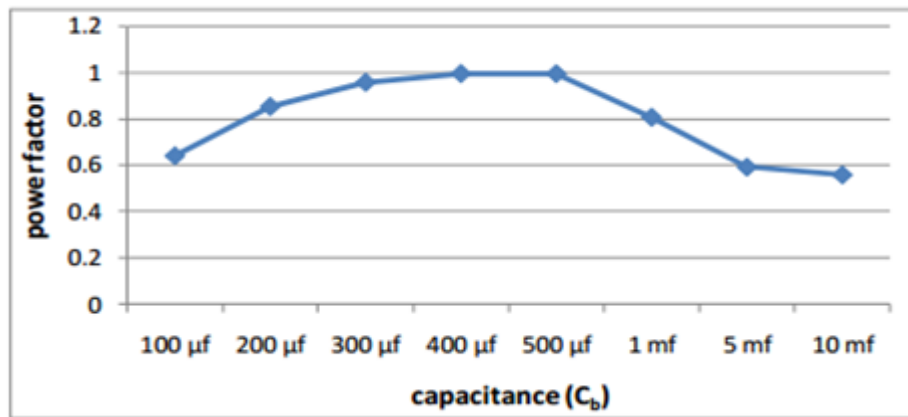


Figure 3.27: Variation of power factor with respect to capacitance C_b .

This method can be the most effective method to reduce the value of THD that it may reach a value of 2% and improve PF value to reach 0.996. This can be achieved by selecting the appropriate shunt filter C_b . C_b values are chosen in the range from (100 μF - 10 mF) so that the input

power factor at rated output power reaches its peak value. In this method, PF value is closer to 1 and THD value is closer to 0 [48].

3.8.7 Rectifier with AC side inductor

This method is performed by adding an inductor connected at the AC-side of the diode bridge and in series with the line voltage as shown in Fig.(3.17).

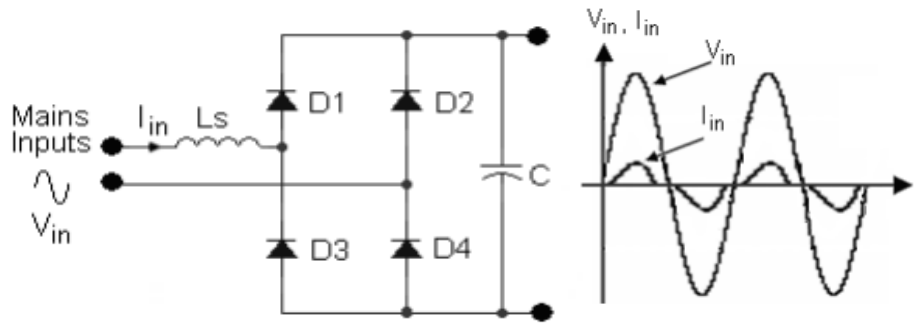


Figure 3.28: Rectifier with AC-side inductor and inputs waveforms [11] .

In this circuit the shape of line current can be improved, but, the maximum power factor that can be obtained is 0.76.

3.8.8 Rectifier with shunt LC- filter

Single phase analysis is used to design the input filter. The equivalent circuit for each phase of the input filter is shown in Fig.(3.29). $I_{s,n}$, is the source current composed of n harmonics and $I_{i,n}$ is the n^{th} harmonic current generated by the rectifier circuit. L and C are the per-phase filter inductance and capacitance of the three-phase circuit. By using current division analysis the source current $I_{s,n}$ is given in equ. (3.1).

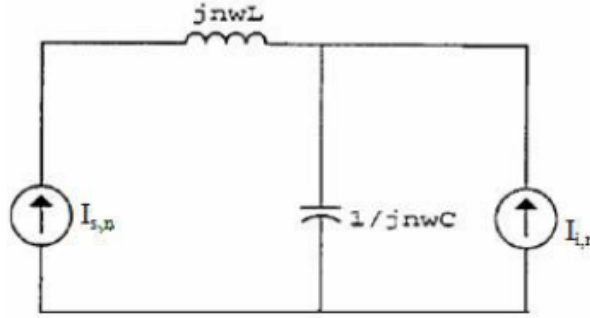


Figure 3.29: Input filter circuit per phase [11].

$$LC = \frac{1}{(n\omega)^2} \left[\frac{I_{s,n}}{I_{i,n}} + 1 \right] \quad (3.1)$$

Where,

ω : angular velocity (314 rad).

n^{th} : harmonic frequency.

By analyzing the frequency spectrum, the dominant harmonics occurs at $n = 440$, the source current is 10.2 A while the 50 Hz fundamental component of the source is approximately at 22 A. The dominant harmonic component must be declined to the 3% of the source fundamental. Hence, $I_{i,n} = 0.66\text{A}$. The input filter component values are then calculated using equ. (3.3).

$$LC = \frac{1}{(440 \cdot 314)^2} \left[\frac{10.2}{.66} + 1 \right]$$

Assuming $L = 66\mu\text{H}$, C is found to be $13\mu\text{F}$

Another method is to design different LC-filter combinations like parallel LC-filter, series LC-filter, shunt LC-filter and parallel and shunt LC-filter to reduce harmonic distortion and correct the power factor in full wave rectifier circuit. This circuit is connected to R load, load specifications are taken to be 100W, 4A and 24V from a regulated power supply [49].

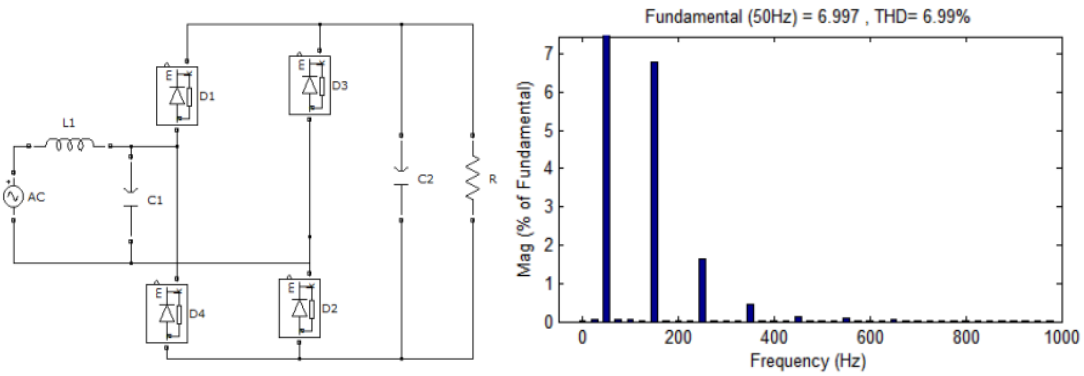


Figure 3.30:Simulation circuits and current harmonics spectrum of shunt LC- filter [49].

The simulated results for different filter parameters are shown in Table 3.4

Table 3.4: Simulated results for shunt LC- filter.

L(mH)	C(μ F)	PF	V _o (V)	I _{rms} (A)	THD%
14.3	220	0.9915	23.13	4.96	6.99
15.5	254.59	0.9966	25.29	4.5	6.95
16.7	266.244	0.9972	25.77	4.68	6.10
17	250.71	0.9966	25.13	4.45	6.35

The Analysis of designing different LC-filter combinations is presented in Table 3.5.

Table 3.5: Simulated comparative results.

Configuration	Power Factor	THD%
Without filter	0.66	105.7
Parallel-LC	0.9827	17.79
Series-LC	0.99	7.011
Shunt-LC	0.997	6.11
Parallel and shunt filter	0.9998	3.45

In conclusion, the proposed configuration of shunt LC and parallel and shunt combination filter can achieve the best results. Harmonic values are still within the harmonic limits and the output voltage is maintained constant for all the values.

3.8.9 Rectifier with LCL- third order low pass filter

L and C can be determined based on the following criteria:

- Filter should provide higher reactance to reduce the flowing of harmonic current. The lowering of harmonic current should be compared to L-filter which offers low reactance for harmonic current bypassing.

It is clear that the THD % is reduced in the T-filter over L-filter topology but still above allowable limit ($< 5\%$), while the phase difference between input voltage and input current in T-filter is reduced to half compared to phase difference in L-filter which leads to double the value of power factor in T-filter [49].

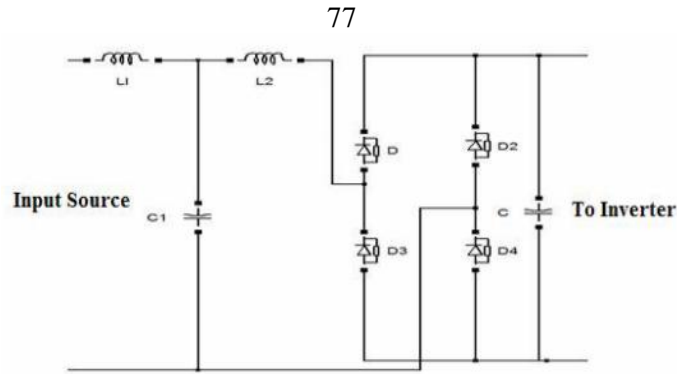


Figure 3.31:T-Filter with rectifier circuit [11].

Table 3.6: Components and specifications used in T-Filter.

T-Filter	
Components	Specification
L_1	66 μ H
L_2	66 μ H
C_1	33 μ F

- The THD is reduced by 7.89% using L-filter and 8.69% using T-filter.
- The PF is improved to 0.5878 L-filter and 0.9135 using T- filter.
- Phase difference between input voltage and input current is reduced from 54° using L-filter to 24° using T- filter.

3.8.10 Rectifier with harmonic trap filter

Another possibility is to use a harmonic trap filter. The harmonic trap consists of a series resonant network, connected in parallel to the AC source and tuned at a harmonic that must be attenuated for example, the filter shown in Fig.(3.32) has two harmonic traps, which are tuned at the 3rd and 5th harmonic respectively [47].

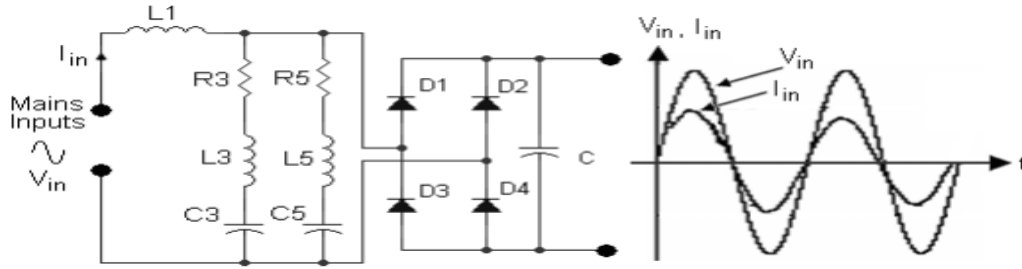


Figure 3.32: Rectifier with harmonic trap filter and inputs waveforms.

Some of the advantages of this circuit are minimizing frequency losses, providing low impedance to tuned frequency and improving the shape of line current. However, the maximum power factor that can be obtained is 0.95. This resonant circuit is very sensitive to line frequency and it can import harmonics from other nonlinear loads. The voltage regulation is also low [47]. The purpose is to achieve minimum value of THD% and maximum value of PF and close as possible to the theoretical values, which are zero for THD % and one for PF, practically it is not possible to achieve this purpose in single phase diode rectifier circuit.

Chapter Four

Results and Analysis

This chapter illustrates the seven different passive filter topologies for low power output, with 220V/50 Hz AC input. This chapter also clarifies the results from the MATLAB/Simulink and by using FFT tools.

The seven different topologies are:

1. Single phase controlled rectifier with L-filter
2. Single phase controlled rectifier with series input resonance -filter.
3. Single phase controlled rectifier circuit with parallel input resonant-filter.
4. Single phase controlled rectifier circuit with parallel LC-filter in series with inductor L-filter.
5. Single phase controlled rectifier circuit with second order high pass-filter.
6. Single phase controlled rectifier circuit with third order high pass T-filter.
7. Single phase controlled rectifier circuit with third order high pass π -filter.

All methods are compared in terms of THD, power factor and other important parameter.

4.1 L-Filter- First Order

When the current passing through an inductor, it begins to fall, the inductor maintains the current to continue by acting as a source. The L-filter is usually used to reduce the input current's ripple and harmonics by changing the inductor current slowly as it can't be changed suddenly [22].

The current passing through the AC line reactors produces electrical losses which were not considered in the original design of the rectifier, and that leads to a voltage drop across the AC line reactor which reduces the voltage of the load. This means the power delivered by the power supply will decrease, and as the output power is restricted with rating current of load, the power delivered by the power supply will not be able to the drop voltage at load. Many problems occur due to the voltage losses, such as minimizing the rectifier efficiency and increasing the generated heat which must be dissipated [37]. The easiest methods used in the design ,is inserting an inductor (L_2) at the AC-side of controlled rectifier, in series with the main voltage source in order to improve the power factor, and to reduce the THD of the input line current, so as to improve the line-current waveform via delaying the current which is prevented to grow up quickly. The following section is dedicated for analyzing the operation of this circuit.

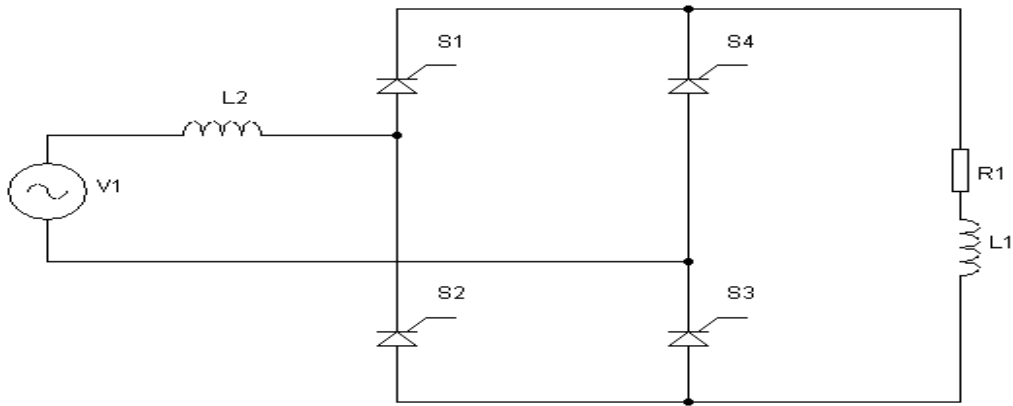


Figure 4.1: Simplified schematic of controlled single phase full wave bridge rectifier with RL-load and input L-filter.

4.1.1 System simulation using L- filter

Use MATLAB/SIMULINK to simulate the circuit presented in Fig.(4.2)

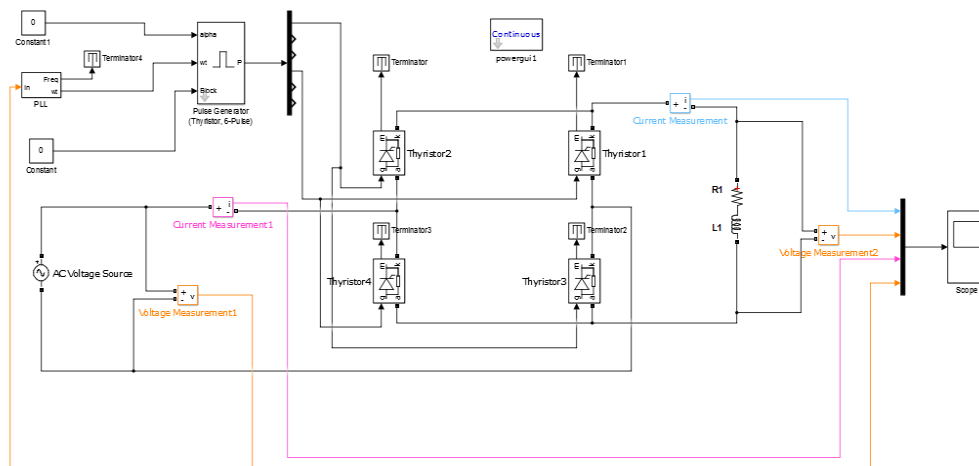


Figure 4.2: MATLAB/Simulink implementation circuit diagram of controlled single phase full wave bridge rectifier with RL-load and input L-filter.

The analyzed results in this section include different values of inductor (10-500) mH. The rectifier circuit parameters are shown in the Table 4.1.

Table 4.1: Simulation specifications of controlled single phase full wave bridge rectifier with L-filter.

Parameter Name	Symbol	Value
Input voltage (V)	V_Supply	220 (R.M.S)
Load resistance (Ω)	R_1	5
Load inductance (mH)	L_1	19
Input filter inductance (mH)	L_2	60
Supply Frequency (Hz)	f	50
Load angle	ϕ	50°
Firing angle	α	30°

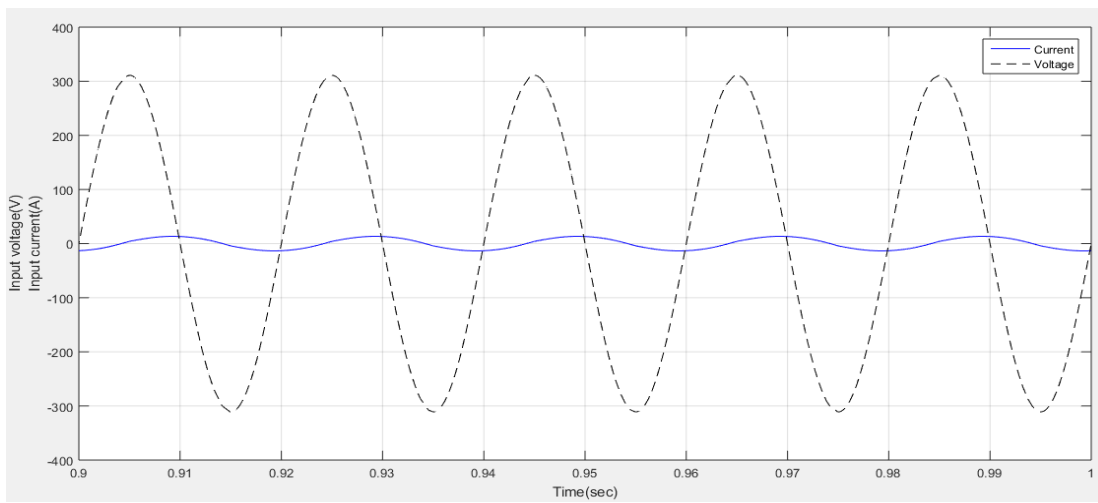


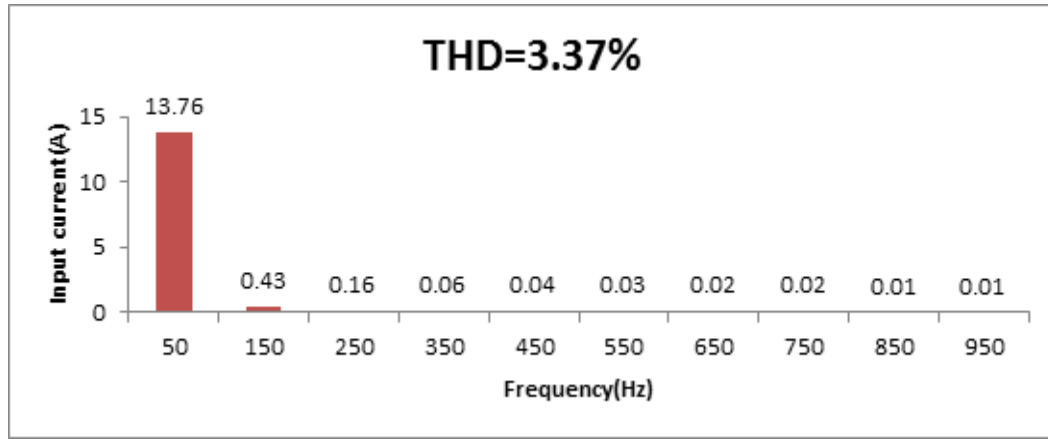
Figure 4.3: Input voltage and input current waveform for controlled single phase full wave bridge rectifier with RL-load and input L-filter at $\alpha=30^\circ$.

Fig.(4.3) shows the comparison between simulated input voltage and input current. The input voltage of the rectifier is assumed to be pure sinusoidal on the AC side, while the input drawn current is changing from square waveform after the insert L-filter and appears as symmetrical sine wave, the simulated response shows that the phase difference between voltage and current waveform is large. Hence, the power factor is poor. The writer's aim is to control the grid current and the grid voltage to obtain a zero displacement between them.

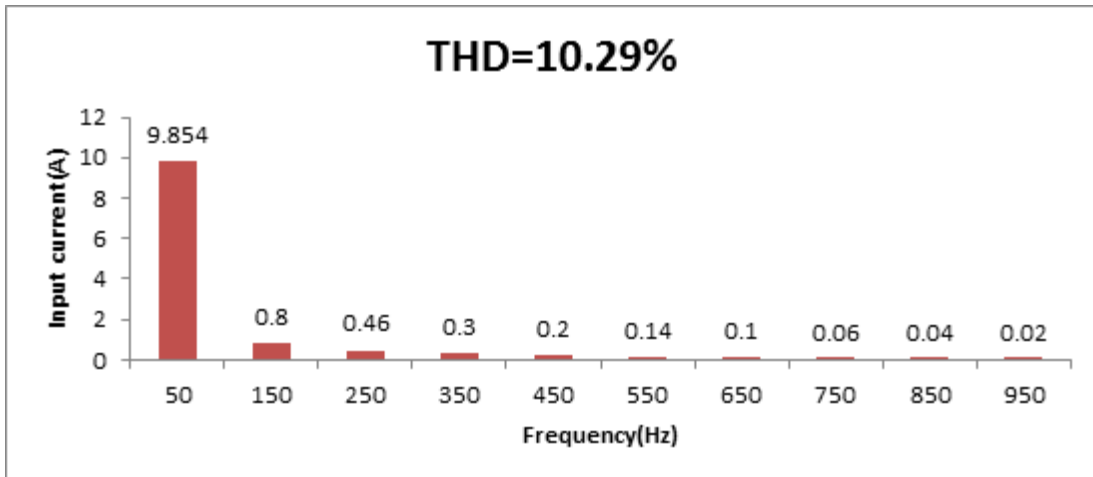
Table 4.2: Frequency spectrum of the input current.

Harmonic order	1 st	3 th	5 th	7 th	9 th	11 th	13 th	15 th	17 th	19 th
Frequency [Hz]	50	150	250	350	450	550	650	750	850	950
$I(\alpha=30^\circ)$ [A]	13.76	0.43	0.16	0.06	0.04	0.03	0.02	0.02	0.01	0.01
$I(\alpha=90^\circ)$ [A]	9.854	0.8	0.46	0.3	0.2	0.14	0.1	0.06	0.04	0.02
$I(\alpha=120^\circ)$ [A]	4.261	1.71	0.23	0.21	0.17	0.01	0.08	0.06	0.01	0.04

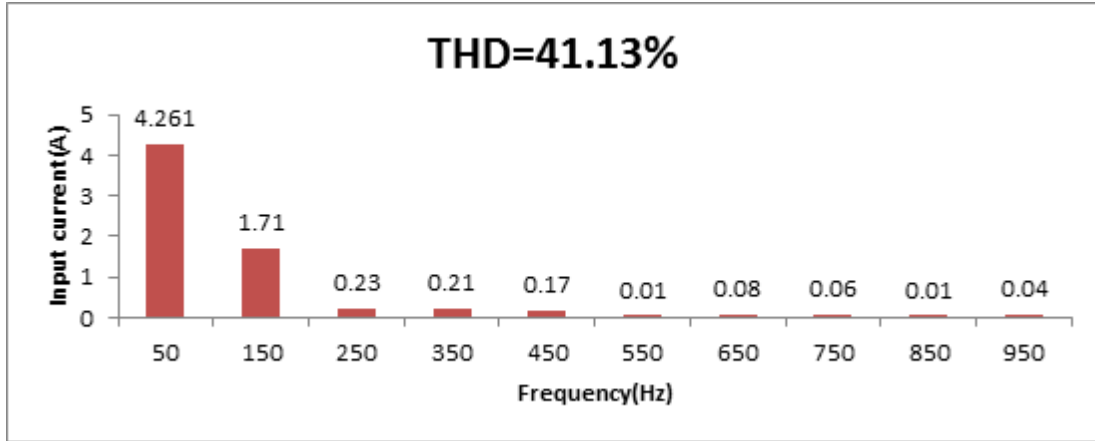
Fig.(4.4) shows the frequency spectrum of the input current with various firing angle for controlled single phase full wave bridge rectifier with L-filter.



(a)



(b)



(c)

Figure 4.4: Frequency spectrum of input current spectrum for controlled single phase full wave bridge rectifier with RL-load and input L-filter (a) at $\alpha=30^\circ$ (b) at $\alpha=90^\circ$ (c) at $\alpha=120^\circ$.

In this case, at $\alpha=30^\circ$, before using the harmonic filter, the amplitude of input current was 48.48 A. The total harmonic distortion for the input waveforms was calculated by using the THD formulas for the current and the results were as follows:

1. THD was 18.04% (before using filter).
2. THD appeared as 3.37% (after using filter).

This result (after using the filter) reaches the most strings IEEE standard, and decreases the THD of the input current generously, which is a great effort. Similarly, the insert of L-filter caused a high reduction of third harmonic from 5.93A to 0.43A. This leads to use a large inductor, but on the other hand a large inductor will make distortion input current waveform while in this point the lower odd order is to increase very little

with rising firing angle, which finally leads to non-sinusoidal waveform with more THD%.

Fig.(4.5) shows the amplitude of each harmonic current and it compares the harmonic current spectrum caused by a controlled rectifier with and without L-filter.

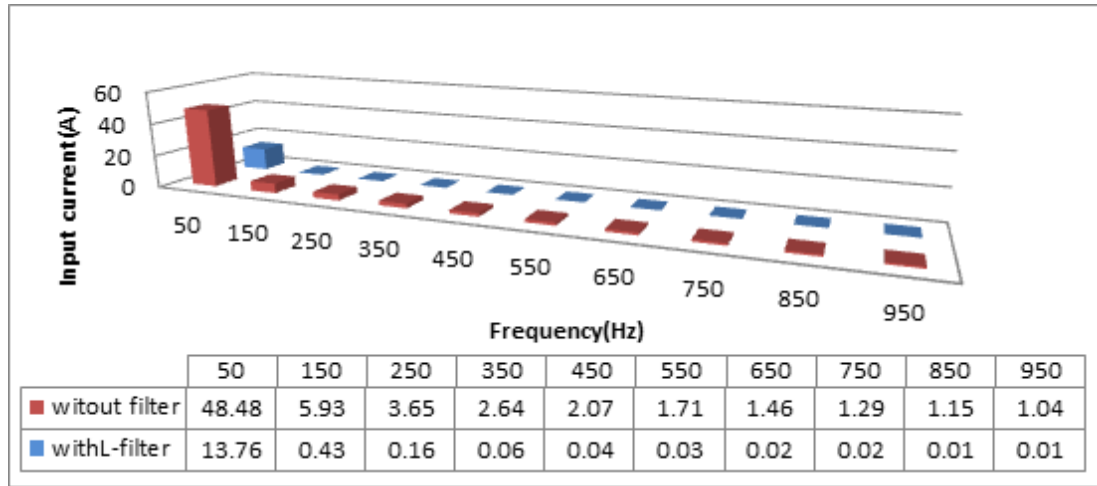
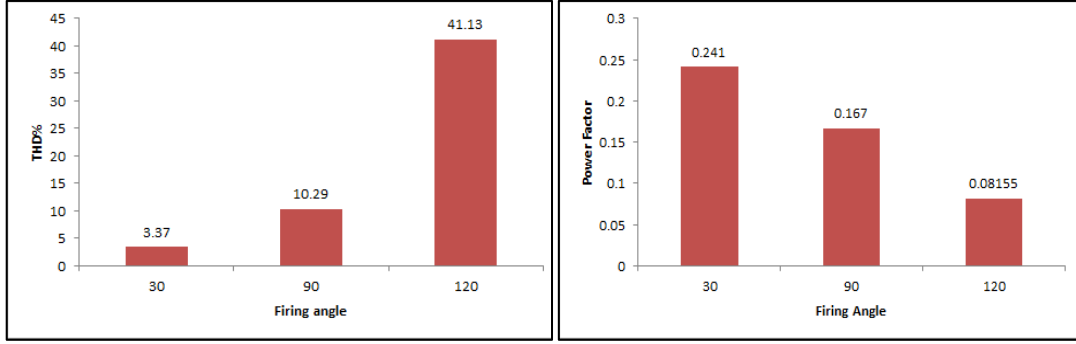


Figure 4.5: Comparison among the harmonic current spectrums for single phase full wave bridge rectifier with RL-load and input L-filter and without it.

Fig.(4.6, a, b) show THD and PF as function of firing angle. After the insertion of L-filter, the input current has been improved. Then, it is obvious that when firing angle starts to increase, the THD increases at same time so the power factor begins to decrease.



(a)

(b)

Figure 4.6: (a) THD of input current (b) power factor for controlled single phase full bridge with RL-load and input L-filter at $\alpha=30^\circ, 90^\circ, 120^\circ$.

4.1.2 Determination of the Circuit Parameters

Using equ. (2.3), we get the following result for the R.M.S value of the input current:

$$I_{\text{prms}} = \left[\left(\frac{13.75}{\sqrt{2}} \right)^2 + \left(\frac{.43}{\sqrt{2}} \right)^2 + \left(\frac{.16}{\sqrt{2}} \right)^2 + \left(\frac{.05}{\sqrt{2}} \right)^2 + \left(\frac{.04}{\sqrt{2}} \right)^2 + \left(\frac{.03}{\sqrt{2}} \right)^2 + \left(\frac{.02}{\sqrt{2}} \right)^2 + \right. \\ \left. \left(\frac{.01}{\sqrt{2}} \right)^2 + \left(\frac{.01}{\sqrt{2}} \right)^2 + \left(\frac{.01}{\sqrt{2}} \right)^2 + \left(\frac{.01}{\sqrt{2}} \right)^2 + \left(\frac{.01}{\sqrt{2}} \right)^2 + \left(\frac{.01}{\sqrt{2}} \right)^2 + \left(\frac{.01}{\sqrt{2}} \right)^2 + \left(\frac{.01}{\sqrt{2}} \right)^2 + \right. \\ \left. \left(\frac{.01}{\sqrt{2}} \right)^2 + \left(\frac{0}{\sqrt{2}} \right)^2 + \left(\frac{0}{\sqrt{2}} \right)^2 + \left(\frac{0}{\sqrt{2}} \right)^2 + \left(\frac{.01}{\sqrt{2}} \right)^2 + \left(\frac{0}{\sqrt{2}} \right)^2 + \left(\frac{0}{\sqrt{2}} \right)^2 + \left(\frac{0}{\sqrt{2}} \right)^2 + \right. \\ \left. \left(\frac{0}{\sqrt{2}} \right)^2 + \left(\frac{0}{\sqrt{2}} \right)^2 \right]^{\frac{1}{2}}$$

$$= 9.728\text{A}$$

From equ.(2.5), we obtain THD :

$$\text{THD} = \sqrt{\left(\frac{9.728}{9.722} \right)^2 - 1} = 3.51\%$$

There is slight difference between the result estimated previously and the result estimated by FFT analysis.

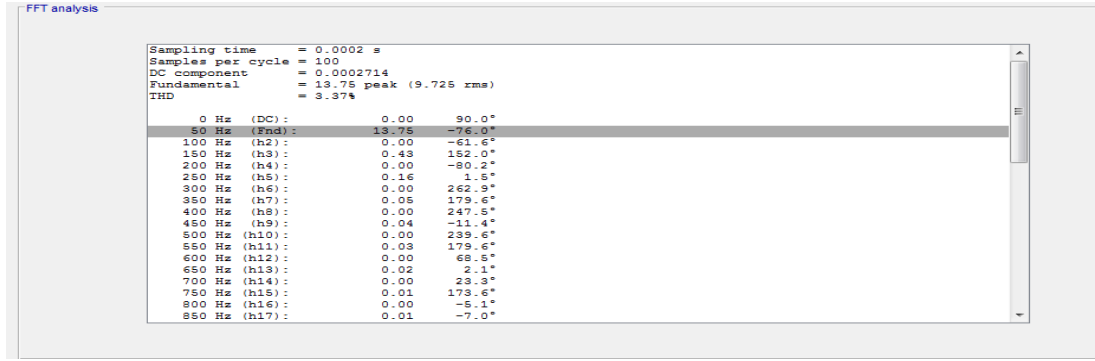


Figure 4.7: FFT analysis results of the input current for controlled single phase full wave bridge rectifier with RL-load and input L-filter at $\alpha=30^\circ$.

For this topology, from the above simulation results, we get the following results:

$$I_{\text{prms}} = \frac{I_{\text{peak}}}{\sqrt{2}}$$

$$= \frac{13.757}{\sqrt{2}} = 9.728\text{A}$$

$$X_L = \omega * L \quad (4.1)$$

$$= 2 * \pi * f * L = 2 * \pi * 50 * .06 = 18.84\Omega$$

$$Q_L = I^2 * X_L \quad (4.2)$$

$$= (9.728)^2 * 18.84 = 1.780 \text{ kVAr}$$

From equ.(2.6), the power factor is:

$$\text{PF} = \frac{9.722}{9.728} * \cos(-76) = 0.241$$

The power factor is found to be 0.804 when using rectifier without filter. And it is 0.241 when using series L-filter which would be unacceptable for critical applications. Poor power factor results from excessive phase

shift between both input current and voltage waveforms, especially in the case where the firing angle is large.

For more clarification concerning $\alpha = 30^\circ$, the input displacement $(\phi)_{v,i}$ between the waveform of input current and input voltage = -76° . For $\alpha = 90^\circ$ the displacement angle $(\phi)_{v,i}$ increases to -80.3° and for $\alpha = 120^\circ$ the displacement angle $(\phi)_{v,i}$ becomes -85° .

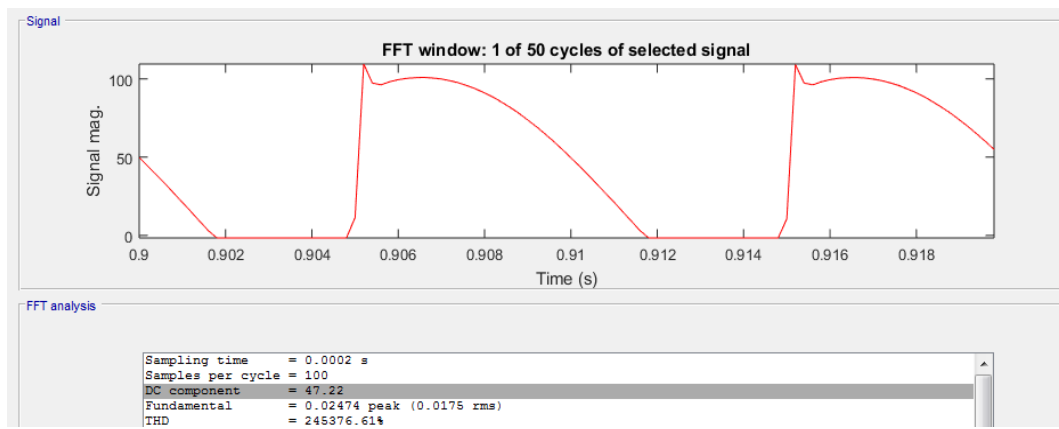


Figure 4.8: Output voltage waveform for controlled single phase full wave bridge rectifier with RL-load and input L-filter at $\alpha = 30^\circ$.

From FFT tool in "MATLAB/SIMULINK" we can obtain the average output voltage of single phase full-wave rectifier, after adding L-filter $V_{dc} = 47.22V$, for the same circuit without filter. Output voltage was 168.7V. In general, this is a great decreasing in the output voltage, due to the large voltage drop across inductor.

Applying the equ. (2.8), the average output voltage is:

$$V_{dc}(\text{before}) = \frac{2 \cdot 311 \cdot \cos 30}{\pi} = 171.46 V$$

The voltage drop voltage across this L-filter is given by:

$$\Delta V = I * X_L \quad (4.3)$$

Where,

ΔV : is drop voltage across the inductor.

X_L : is the reactance of inductor.

I : R.M.S current flowing through inductor.

Substituting X_L in the equ. (4.3) to obtain ΔV :

$$\Delta V = I * j(2 * \pi * f) * L$$

$$= 9.728 \angle -76^\circ * (2 * \pi * 50) * .06 \angle 90^\circ = 183.38 \angle 14^\circ \text{ V}$$

$$V_{in}(\text{new}) = \left(\sqrt{2} * 220 \angle 0^\circ - \sqrt{2} * 183.38 \angle 14^\circ \right) = 86.37 \angle -46.57^\circ \text{ V}$$

$$V_{dc}(\text{after}) = \frac{2 * 86.37 * \cos 30}{\pi} = 47.61 \text{ V}$$

The simulated output voltage (DC component) obtained from FFT analysis tools in Fig.(4.8) is 47.22V and it is close to the theoretical value obtained from the equation (47.61V).

Applying equ. (2.9), the average output current is:

$$I_{dc} = \frac{47.22}{5} = 9.444 \text{ A}$$

The simulated value was 9.513 A as shown in Fig.(4.9), both values are close to each other.

It is noticed that the output current of the conventional rectifier in Fig.(4.9) was 34.292A, after using L-filter, it was calculated to be 9.444A and this happens due to the enormous reduction in DC output voltage.

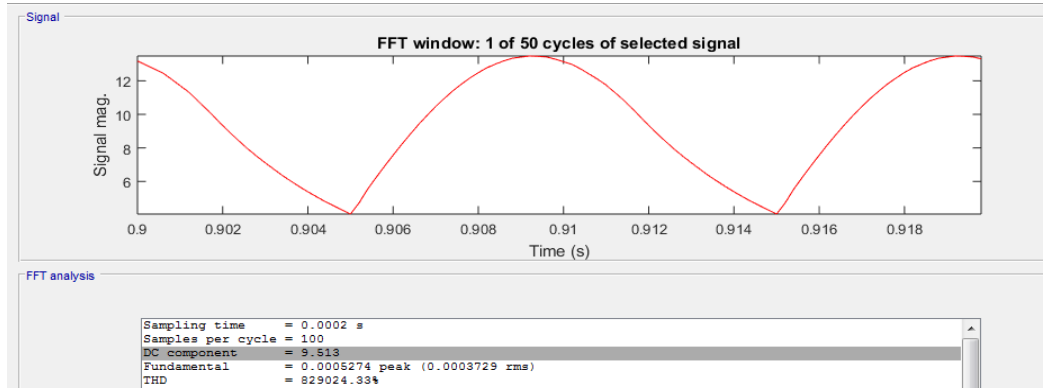


Figure 4.9: Output current waveform for controlled single phase full wave bridge rectifier with RL-load and input L-filter at $\alpha=30^\circ$.

4.1.3 Efficiency

As previously mentioned, using equ.(2.11, 2.12 , 2.10) and according to simulated values obtained from MATLAB/SIMULINK:

$$P_{dc} = 47.22 \times 9.513 = 449.2 \text{ W}$$

$$P_{ac} = 220 \times 9.728 = 2140.16 \text{ W}$$

$$\eta = \frac{449.20}{2140.16} \times 100\% = 20.989\%$$

According to the previous results, it is seen that the input filter topology has lowered the efficiency in comparison with the topology without filter which was 73.53% as calculated in equ.(2.10).

4.1.4 Representation in decibel form (dB)

Fig.(4.10) shows the frequency spectrum in dB for the input current of controlled single phase full wave bridge rectifier with input L-filter at $\alpha=30^\circ$.

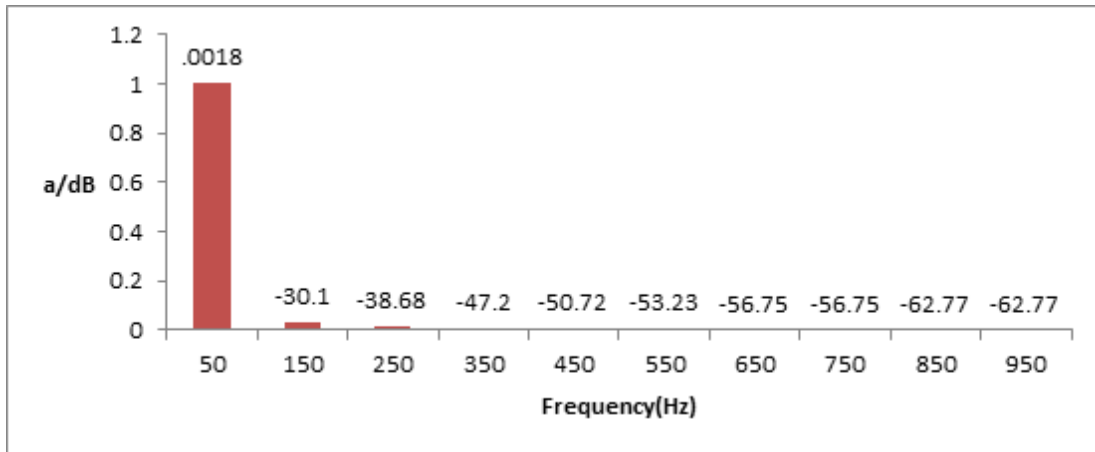
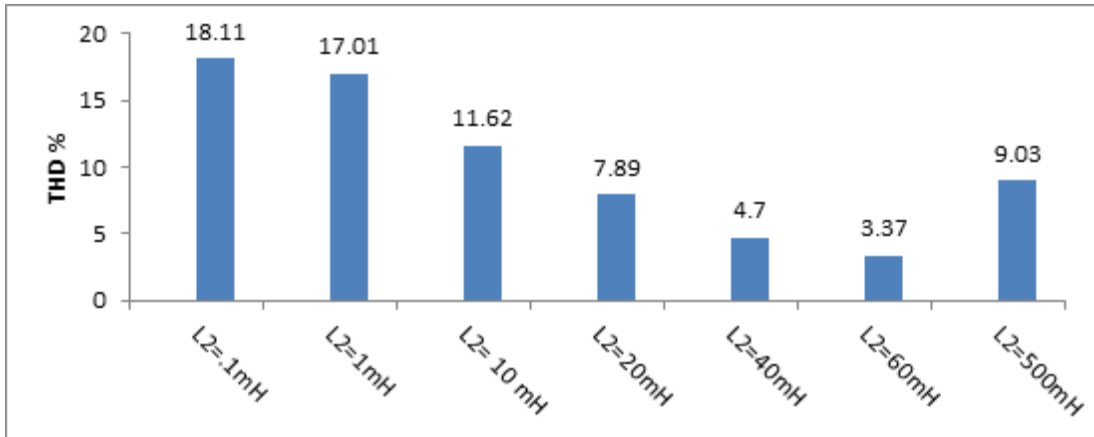


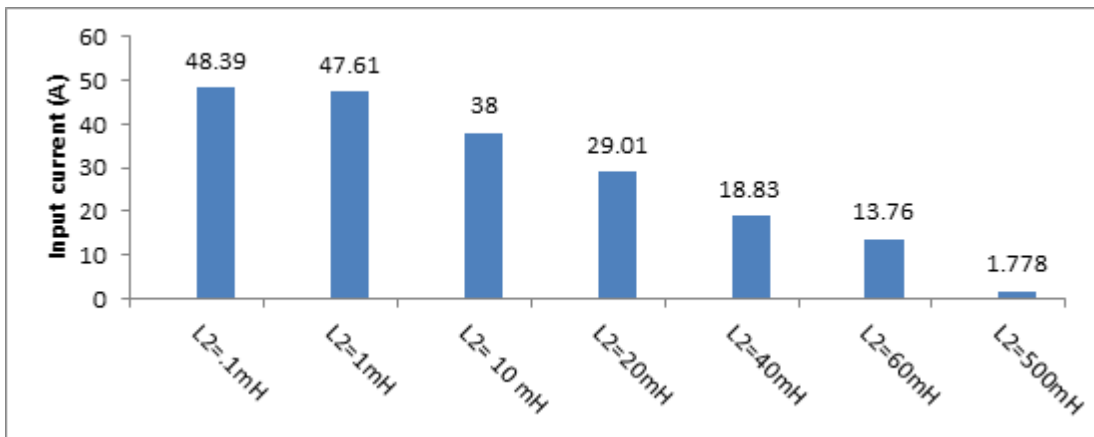
Figure 4.10: Frequency spectrum of input current in dB for controlled single phase full wave bridge rectifier with RL-load and input L- filter at $\alpha=30^\circ$.

Fig.(4.11) clarifies simulation results for many values of L-filter on the THD of the input current , the input current and the output voltage of the single phase full wave bridge rectifier at $\alpha=30^\circ$.

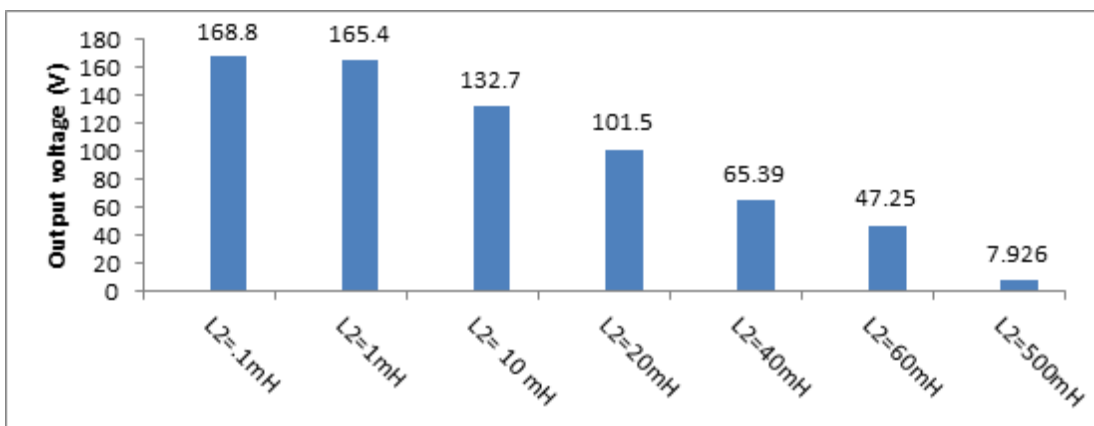
4.1.5 Comparison between the obtained results



(a)



(b)



(c)

Figure 4.11: (a) THD of the input current (b) input current harmonic (c) output voltage for controlled single phase full wave bridge rectifier with RL- load and various input L-filter values at $\alpha=30^\circ$.

Using L- filter is not acceptable for many reasons such as: The great voltage drops occur due to the fast reaction against the change in the current passing through it. Fig.(4.11,a) shows that when the value of the L-filter increases, the THD of the input current decreases. In addition, it creates a problem represented in increasing the input reactance according to equ.(4.1). The input current decreases with increasing the L-filters as shown in Fig.(4.11,b). As the value of L- filter increases, large reactance has negative impact on the output voltage leading to an increase of AC voltage drop. The DC output voltage will be mitigated and it can't be controlled and regulated as shown in Fig.(4.11,c).

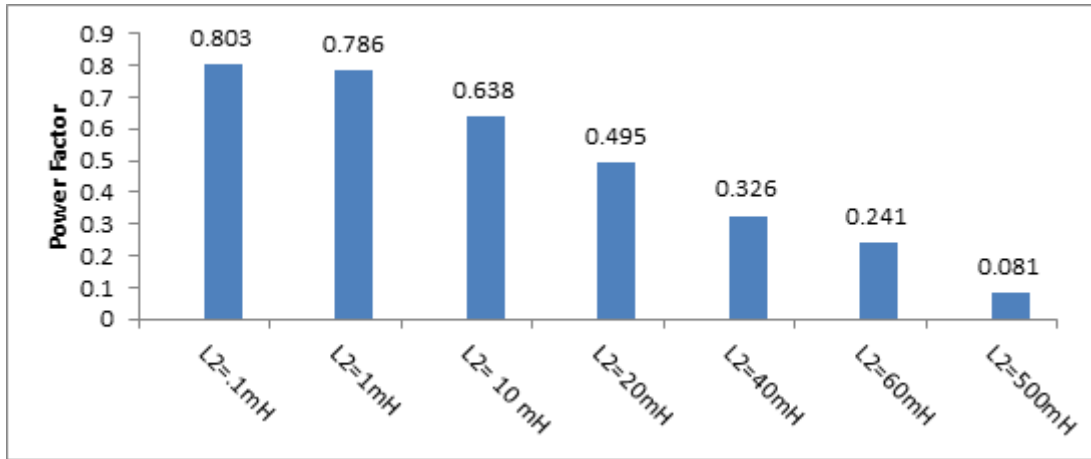


Figure 4.12: Power factor for controlled single phase full wave bridge rectifier with RL-load and various input L-filter values at $\alpha=30^\circ$.

Improvements in power factor can be achieved by electing small values of input inductor filter, which produces small voltage drop, small phase displacement factor, small THD, and large magnitude of input current. Large value, size, weight and cost of L-filter will produce low power factor and high input current distortion.

The characteristics of the input L -filter are:

- Simple because it consists of one element.
- It can improve harmonic current distortion from 70% to 85% at the best condition and these percents are able to be increased if the L-filter value is taken with others into consideration.
- Low cost compared with other configurations since this kind of filter contains a single component. Its value is determined by the amount of the reactive power to be installed as will be described later.
- Reduces current harmonics and eliminate other lower odd harmonics [47].
- Improves the input current wave form but it is still non-sinusoidal and has very high harmonic content especially when using small values of L-filter in micro hennery as shown in Fig.(4.13)

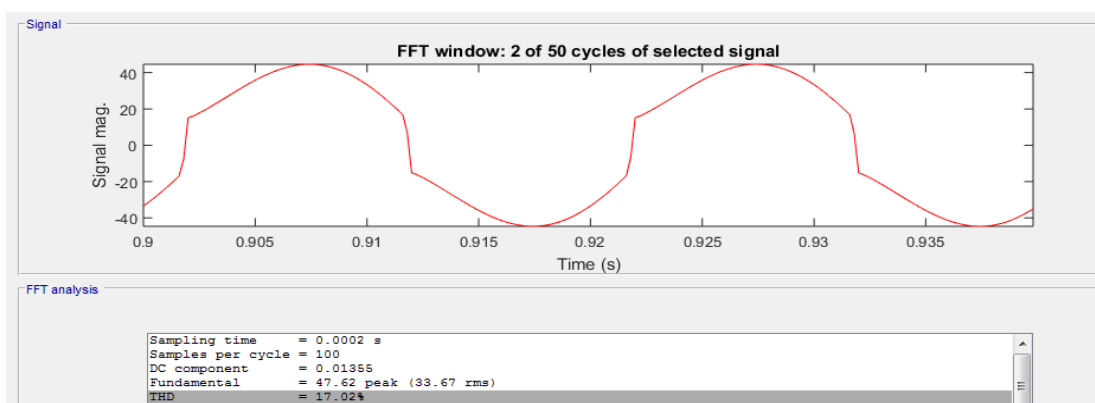


Figure 4.13: Input current waveform for controlled single phase full wave bridge rectifier with RL-load and input L-filter (1mH) at $\alpha=30^\circ$.

- L- filters are very scarcely used, basically due to the weight and bulkiness of inductors. Large inductors may need magnetic shielding to prevent them from picking up or causing electromagnetic interference within the circuit, or with adjacent circuits. However, the mixture of capacitance and inductance in certain circuits may increase unexpected filtering effects.

4.1.6 Filter cost

In controlled rectifier circuit which uses thyristors, there is a link between the output voltage which doesn't come without cost and the ability to control the output voltage as firing angle increase. Thyristors conduction time is relied on the input current. On the contrary, more harmonics will be drawn from the mains as the conduction time of thyristors becomes smaller. In addition, neighboring loads and power system equipment may be affected by voltage and current distortion which will adverse the effect that may come to the distribution transformer which are not rated to deal with large amount of harmonics. This results in the excess of harmonic contents for both at input and output. Therefore, the cost of the equipment will increase approximately twice and also the weight will increase more than standard. The mentioned effects can add up and cost lager issue to the entire power system [21] and this will be our best interest to find ways to minimize such cost if we were designing the single passive controlled rectifier with the input passive filter [16]. Before selecting the passive harmonic

filters, it should be determined the types, the numbers and the capacities of the filter in order to satisfy the requirements of harmonic filtering, reactive power compensation and power factor improvement [50].

4.1.7 Comparison between the costs of the filters

Calculating the relative costs of the components for the passive filters is a complex process, due to the large number of contributory factors which must be taken in consideration [51]. In attempt to estimate comparative cost of the inductor and capacitor for various filter configurations, it has been assumed that at the same power rating, the capacitor cost is half of the inductor cost [52]. This means that the cost of inductive power has been taken as twice of the capacitive power. Using these assumptions is possible to calculate the approximate and comparative costs of all filter configurations described in this study [51].

4.1.8 Reactive power

Most common practice for harmonic mitigation is the installation of passive harmonic filters. The passive filter techniques are very good choice for constant loads and when dealing with low and medium frequency that exhibits the best relationship cost-benefit among all other mitigation techniques. More reliable and simple design is to reduce the amplitude of the low frequency harmonic .All these advantages can be lost if the input filter is not properly designed. An oversized input filter unnecessarily adds cost and volume to the design and compromises system performance [48], [49].

The following table clarifies the values of the inductor and their reactive compensation.

Table 4.3: Examples of calculated reactive power for different values of L-filter.

L_2 [mH]	I_{prms} [A]	X_L [Ω]	Q [kVAr]
0.1	34.22	0.0314	0.0367
1	33.67	0.314	0.3559
10	26.87	3.14	2.267
20	20.51	6.283	2.643
40	13.82	12.566	2.4
60	9.728	18.849	1.78
500	1.258	157.079	0.248

According to the tabulated results, it is found that the reactive power depends on the value of the inductor which determines its current and reactance.

4.2 Series Input Resonance LC- Filter (Band Pass)

When the capacitor in the filter is used, it reduces the voltage ripple while the internal resistor in the capacitor causes loss for that reason the capacitor should be chosen for minimum loss. As long as the input L-filter is used, the input current will begin to decline which will lead to poor power factor. As a result, using other configurations will be more efficient.

In this section, using MATLAB/SIMULINK the controlled single phase full wave bridge rectifier has been simulated with passive filter in its simplest form, which is a series resonance LC-filter (band pass). It is inserted between the AC source and the input of the controlled rectifier

with RL-load. In order to compensate for the harmonic currents created by nonlinear equipment, to prevent the return of these currents back to the source and to obtain a pure sinusoidal form of the input current. Neither inductance nor capacitance of the input LC-filter must be chosen arbitrarily. The inductor should be chosen first [53].

To obtain the best compromise between size, cost and performance the inductance should be chosen between 10 mH to 500 mH. This filter is used to reduce THD, to improve the power factor, to increase the reliability and the efficiency of the grid. X_L must be equal to X_C , and to provide small impedance path for harmonic current at resonance.

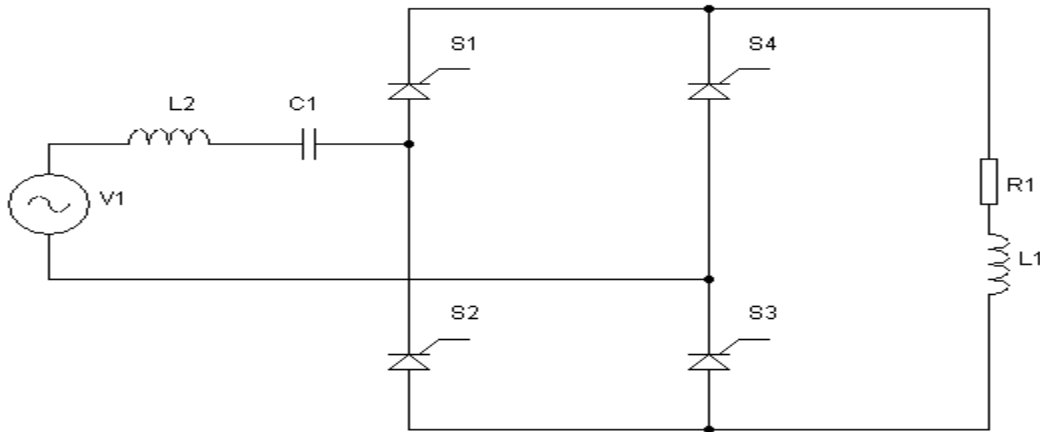


Figure 4.14: Simplified schematic of controlled single phase full wave bridge rectifier with RL- load and series input resonance filter.

4.2.1 System simulation using series input resonance filter.

MATLAB/SIMULINK is used to simulate the circuit for various values of series input resonance filter.

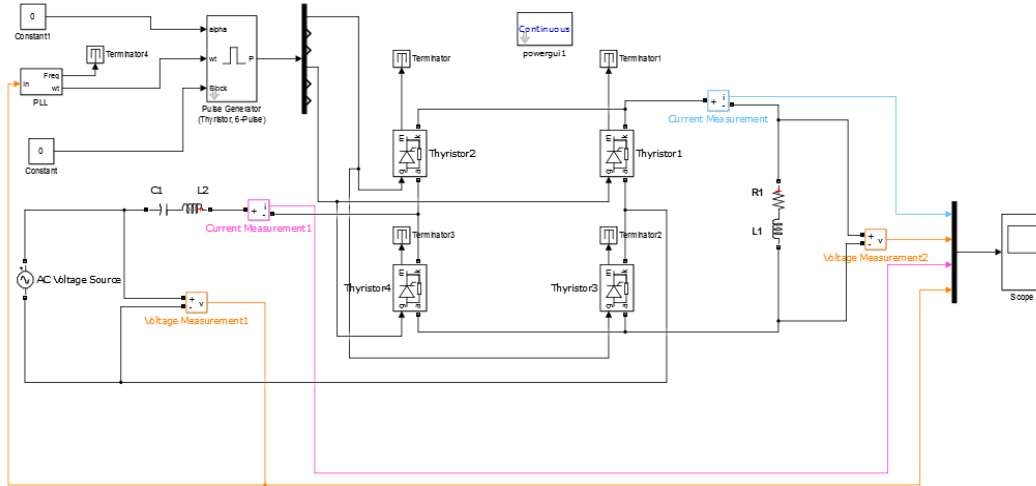


Figure 4.15: MATLAB/Simulink implementation circuit diagram of controlled single phase full wave bridge rectifier with RL- load and series input resonance filter.

Since there is no mathematical formula available to design a series of capacitor-inductor filter, the value of the inductor and the capacitor are chosen arbitrarily but both of them must meet the resonant frequency condition. This filter is used to reduce the magnitude of harmonic current and the harmonic voltage distortion. The filter maintains large input current, and keeps a small drop voltage. In addition, it blocks DC current component of large value.

C_1 and L_2 are chosen so that the resonance condition is secured, where ω is obtained as follows:

$$\omega_r = \frac{1}{\sqrt{L_2 C_1}} \quad (4.4)$$

Substitute $\omega_r = 2 * \pi * f_r$,

$$f_r = \frac{1}{2\pi\sqrt{L_2 C_1}} \quad (4.5)$$

Where,

f_r = Resonance frequency, Hz.

L_2 = Filter inductance, Henrys.

C_1 = Filter capacitance, Farads.

At resonance, the series LC-filter represents minimum impedance to pass a signal and blocks the rest of signals of other frequencies.

Table 4.4: Simulation specifications of controlled single phase full wave rectifier with series input resonance filter.

Parameter Name	Symbol	Value
Input voltage (V)	V supply	220 (R.M.S)
Load resistance (Ω)	R_1	5
Load inductance (mH)	L_1	19
Line inductor filter (mH)	L_2	60
Capacitor (μ F)	C_1	168.8
Supply frequency (Hz)	f	50
Load angle	ϕ	50°
Firing angle	α	30°

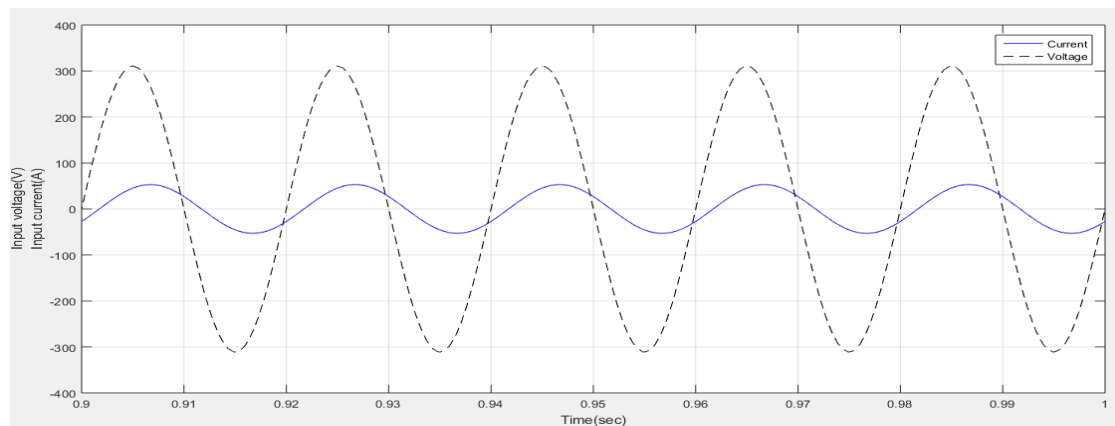


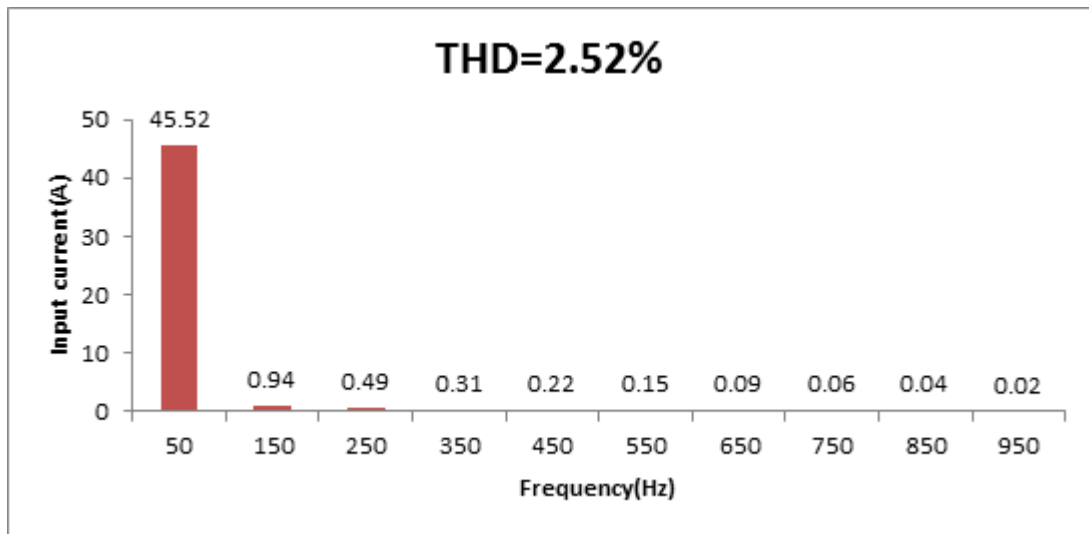
Figure 4.16: Input voltage and input current waveform for controlled single phase full wave bridge rectifier with RL-load and series input resonance filter at $\alpha=30^\circ$.

The mentioned LC-filter performs ideally at resonance frequency since its impedance becomes zero and the filter appears completely as a resistance. It allows a sinusoidal input current to be achieved, but with a phase shift with respect to the source voltage.

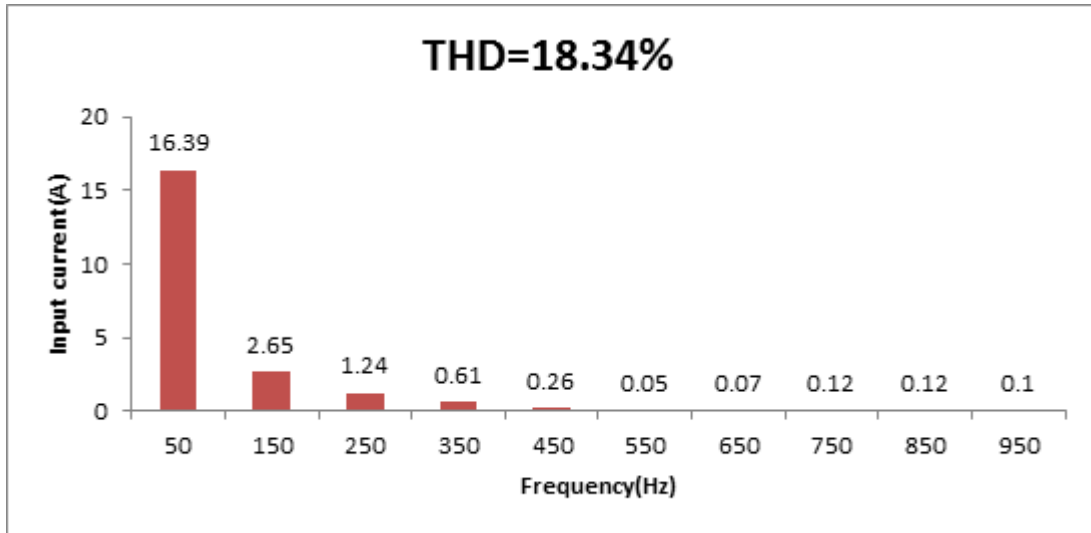
Table 4.5: Frequency spectrum of the input current.

Harmonic order	1 st	3 th	5 th	7 th	9 th	11 th	13 th	15 th	17 th	19 th
Frequency [Hz]	50	150	250	350	450	550	650	750	850	950
$I(\alpha=30^\circ)$ [A]	45.52	.94	.49	.31	.22	.15	.09	.06	.04	.02
$I(\alpha=90^\circ)$ [A]	16.39	2.65	1.24	.61	.26	.05	.07	0.12	.12	.1
$I(\alpha=120^\circ)$ [A]	5.55	2.32	.19	0.33	0.19	.04	.12	.05	.05	.06

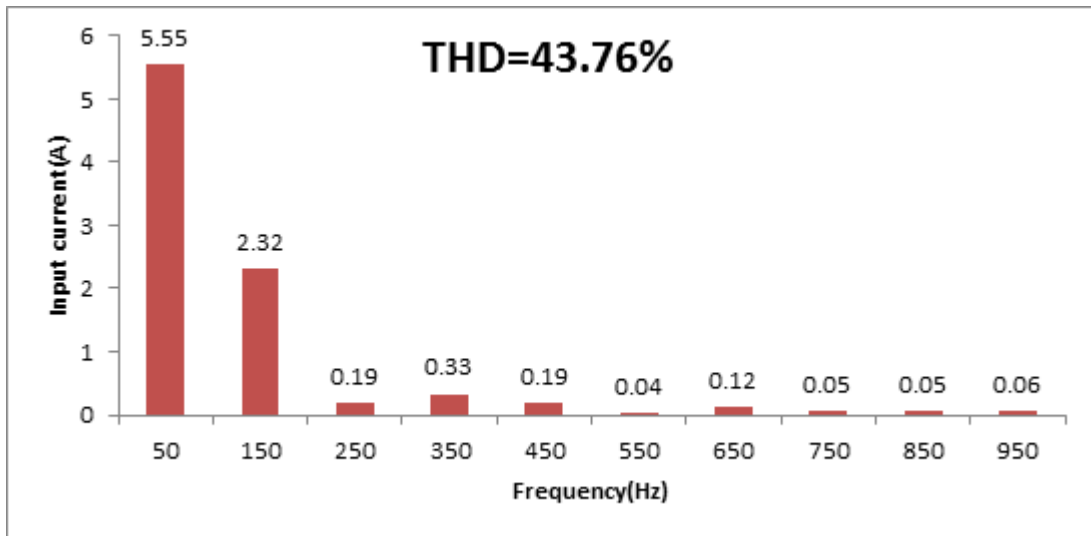
Fig.4.17 shows the frequency spectrum of the input current with various firing angle for controlled single phase full wave bridge rectifier with series input resonance filter.



(a)



(b)



(c)

Figure 4.17: Frequency spectrum of input current for controlled single phase full wave bridge rectifier with RL-load and series input resonance filter (a) at $\alpha=30^\circ$ (b) at $\alpha=90^\circ$ (c) at $\alpha=120^\circ$.

Fig.(4.17) illustrates the current waveform and its harmonic analysis. FFT analysis results show that the most significant harmonic components in the input current are mainly 3rd, 5th and 7th harmonics. After the compensation through the LC- filter, the 3rd harmonic is largely

reduced. Another result is that input current becomes pure sinusoidal as in Fig.(4.16). The THD becomes 2.52% which is less than the national standard level of 5%. In addition, the input current becomes higher than its value at L-filter.

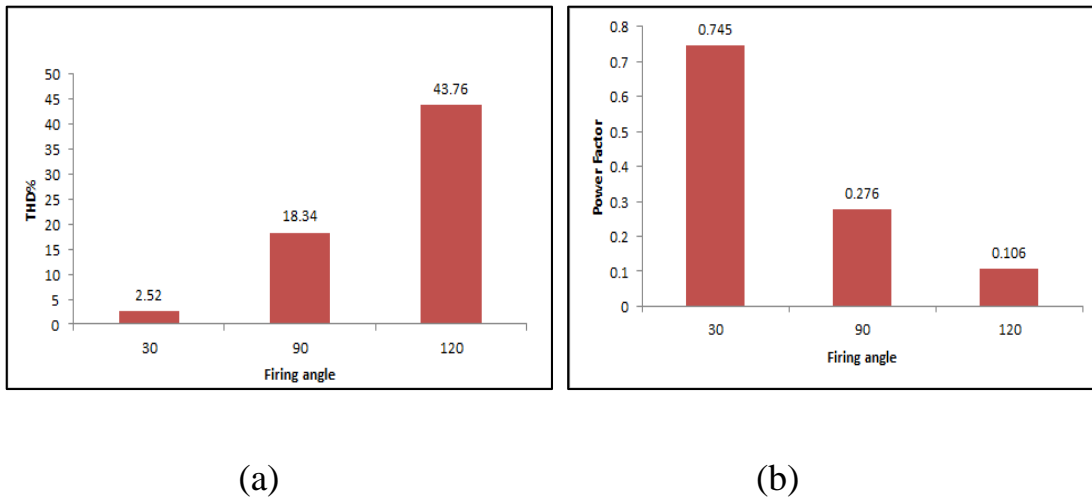


Figure 4.18: (a) THD of input current (b) power factor for controlled single phase full wave bridge rectifier with RL-load and series input resonance filter at $\alpha=30^\circ, 90^\circ, 120^\circ$.

When the firing angle increases, the input current decreases. Both THD of input current and displacement angle increase that leads to decrease the power factor as shown in Fig.(4.18,a, b).

4.2.2 Determination of the circuit parameters

From equ.(2.3), the R.M.S value of the input current is:

$$I_{\text{prms}} = \left[\left(\frac{45.51}{\sqrt{2}} \right)^2 + \left(\frac{.93}{\sqrt{2}} \right)^2 + \left(\frac{.49}{\sqrt{2}} \right)^2 + \left(\frac{.31}{\sqrt{2}} \right)^2 + \left(\frac{.22}{\sqrt{2}} \right)^2 + \left(\frac{.16}{\sqrt{2}} \right)^2 + \left(\frac{.1}{\sqrt{2}} \right)^2 + \right. \\ \left. \left(\frac{.06}{\sqrt{2}} \right)^2 + \left(\frac{.04}{\sqrt{2}} \right)^2 + \left(\frac{.02}{\sqrt{2}} \right)^2 + \left(\frac{.01}{\sqrt{2}} \right)^2 + \left(\frac{.02}{\sqrt{2}} \right)^2 + \left(\frac{.03}{\sqrt{2}} \right)^2 + \left(\frac{.03}{\sqrt{2}} \right)^2 + \left(\frac{.02}{\sqrt{2}} \right)^2 + \right. \\ \left. \left(\frac{.02}{\sqrt{2}} \right)^2 + \left(\frac{.01}{\sqrt{2}} \right)^2 + \left(\frac{.01}{\sqrt{2}} \right)^2 + \left(\frac{.01}{\sqrt{2}} \right)^2 + \left(\frac{.01}{\sqrt{2}} \right)^2 + \left(\frac{.01}{\sqrt{2}} \right)^2 + \left(\frac{.02}{\sqrt{2}} \right)^2 + \left(\frac{.02}{\sqrt{2}} \right)^2 + \right. \\ \left. \left(\frac{.01}{\sqrt{2}} \right)^2 + \left(\frac{.01}{\sqrt{2}} \right)^2 \right]^{1/2}$$

$$= 32.19\text{A}$$

From equ. (2.5), the THD is:

$$\text{THD} = \sqrt{\left(\frac{32.19}{32.18} \right)^2 - 1} = 2.49 \%$$

From the simulated result, THD = 2.51% as shown in Fig.(4.19).

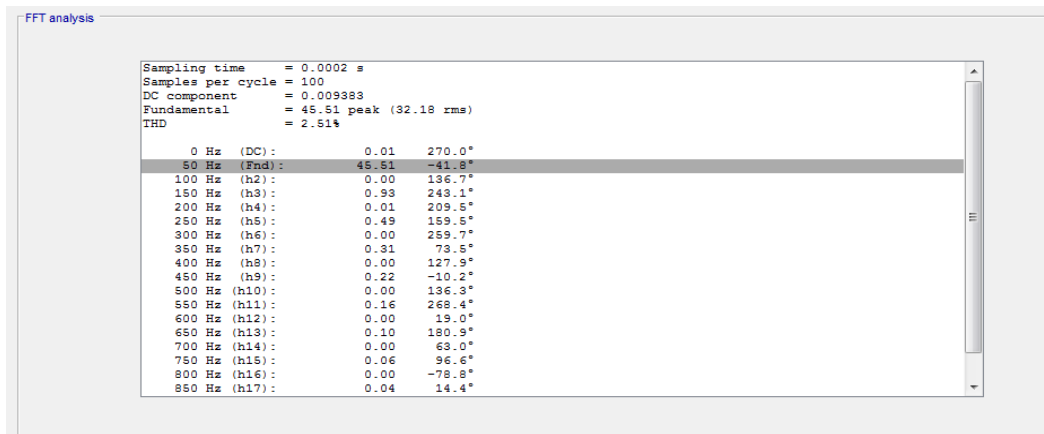


Figure 4.19: FFT analysis results of the input current for controlled single phase full wave bridge rectifier with series input resonance filter at $\alpha=30^\circ$.

From Fig.(4.19), it is clear that phase shift between input voltage and current is highly reduced compared with the L-filter where the phase shift amounts to -76° .

From calculated results and FFT analysis shown, for $\alpha=30^\circ$, and after connecting the series input resonance filter=60 mH, 168.8 μ F, the following results were obtained

$$I_{\text{prms}} = \frac{45.52}{\sqrt{2}} = 32.19\text{A}$$

Referring to equ. (4.1):

$$X_L = 2 * \pi * f * L_2 = 2 * \pi * 50 * .06 = 18.84 \Omega$$

$$X_{C_1} = \frac{1}{\omega C_1} \quad (4.6)$$

$$= \frac{1}{2 * \pi * f * C_1} = \frac{1}{2 * \pi * 50 * .0001688} = 18.85 \Omega$$

The capacitor's reactance decreases with increasing frequency while the reactance of an inductor is opposite of this. Combining the above capacitor and inductor in series we obtain the reactive power of each component according to equ.(4.2):

$$Q_{L_2} = (32.19)^2 * 18.84 = 19.52 \text{ kVAr}$$

$$Q_{C_1} = I^2 * X_{C_1} \quad (4.7)$$

$$= (32.19)^2 * 18.85 = 19.532 \text{ kVAr}$$

From equ.(2.6), the power factor is:

$$PF = \frac{32.18}{32.19} * \cos(-41.8) = 0.745$$

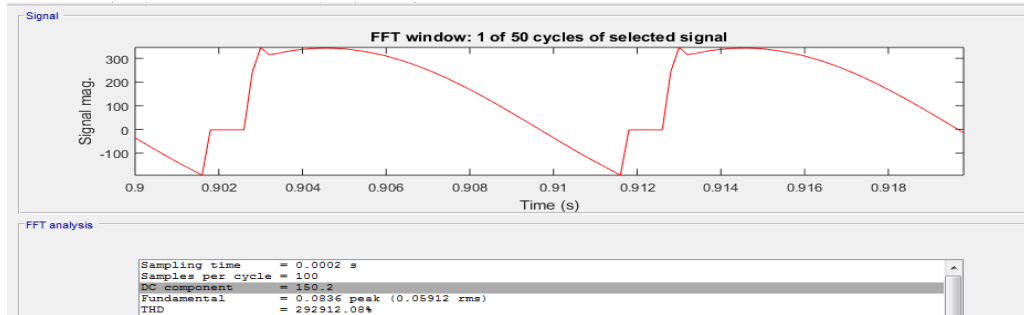


Figure 4.20: Output voltage waveform for controlled single phase full wave bridge rectifier with RL-load and series input resonance filter at $\alpha=30^\circ$.

The FFT window of the output voltage is given in Fig.(4.20) which shows the average output voltage $V_{dc} = 150.2$ V

From equ. (4.3), the voltage drop across series input resonance filter is:

$$\Delta V_{L_2} = I * j(2 * \pi * f) * L_2 = 32.19 \angle -41.8^\circ * (2 * \pi * 50) * .06 \angle 90^\circ$$

$$= 606.76 \angle 48.2^\circ \text{ V}$$

$$\Delta V_{C_1} = I * X_{C_1} \quad (4.8)$$

$$\Delta V_{C_1} = I * \frac{1}{j(2 * \pi * f) * C_1}$$

$$= 32.19 \angle -41.8^\circ * \frac{1}{j(2 * \pi * 50) * .0001688} = 607.01 \angle -131.8^\circ \text{ V}$$

$$\Delta V = \Delta V_{L_2} + \Delta V_{C_1}$$

$$= .249 \angle -48.14^\circ \text{ V}$$

$$V_{in}(\text{new}) = \left(\sqrt{2} * 220 \angle 0^\circ - \sqrt{2} * .249 \angle -48.14^\circ \right) = 310.76 \angle -.04^\circ \text{V}$$

$$V_{dc}(\text{after}) = \frac{2 * 310.76 * \cos 30}{\pi} = 171.4 \text{V}$$

The simulated output voltage is 150.2V, while the theoretical value obtained from the equation is 171.41V. It is noticed that, there is a difference between these two the values due to the deviation of the output voltage from the form of the two half line waves in one cycle.

Applying equ. (2.9), the average output current is:

$$I_{dc} = \frac{150.2}{5} = 30.04 \text{ A}$$

However, the simulated value is 29.73 A as shown in Fig.(4.20).

In this case, it is noticed that the value of the output current is larger than its value at insertion of L-filter where it amounts to 9.513A and results in reduction of the DC output voltage.

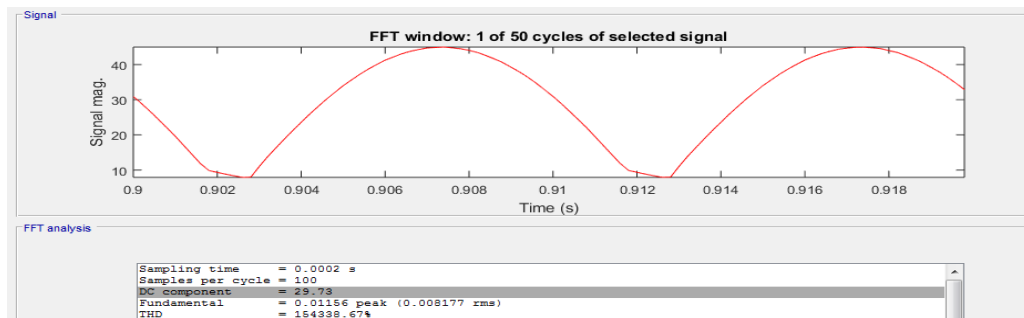


Figure 4.21: Output current waveform for controlled single phase full wave bridge rectifier with RL-load and series input resonance filter at $\alpha=30^\circ$.

4.2.3 Efficiency

From equ.(2.11, 2.12, 2.10) and according to simulation obtained from MATLAB/SIMULINK:

$$P_{dc} = 150.2 * 29.73 = 4465W$$

$$P_{ac} = 220 * 32.19 = 7081W$$

$$\eta = \frac{4465}{7081} * 100\% = 63.05\%$$

From the above results, the series input resonance filter has an efficiency of 63.05% compared to L-filter where the efficiency was 20.98%.

4.2.4 Representation in decibel form (dB)

Fig.(4.22) shows the frequency spectrum in dB for the input current of controlled single phase full wave bridge rectifier with series input resonance filter at $\alpha=30^\circ$.

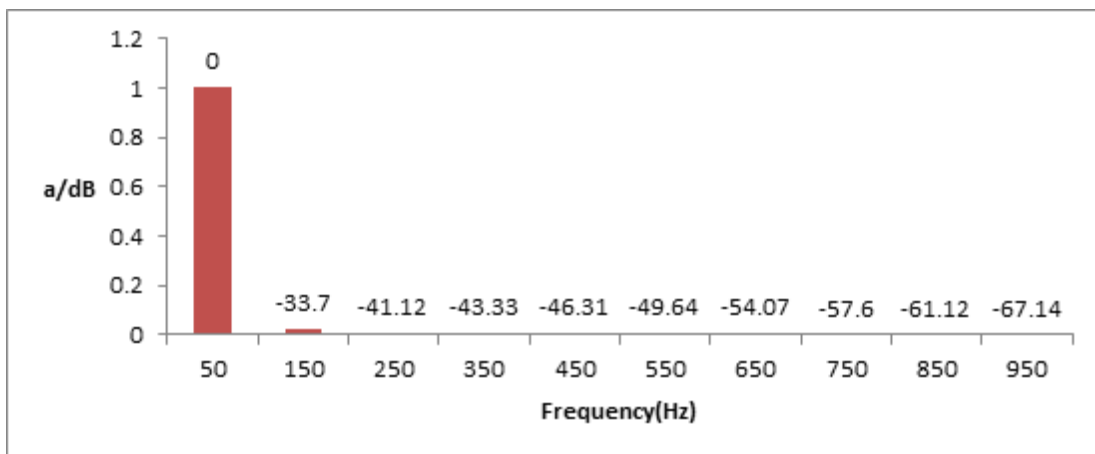
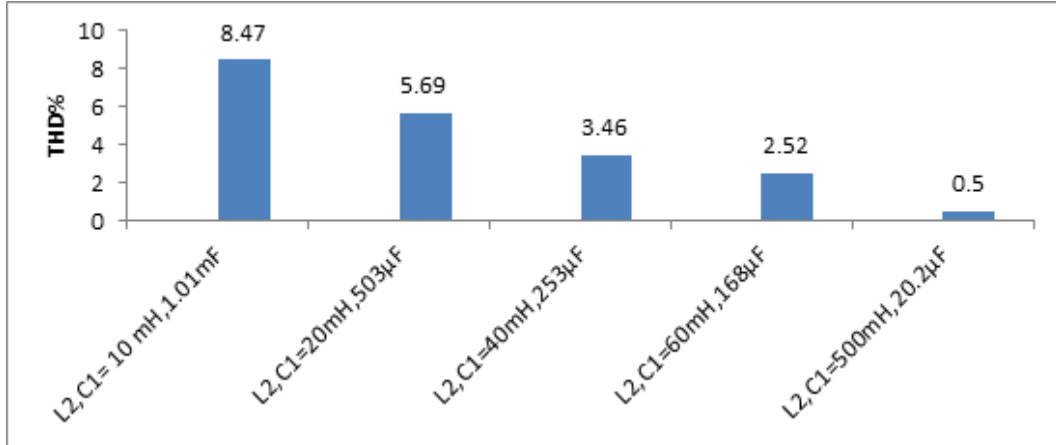
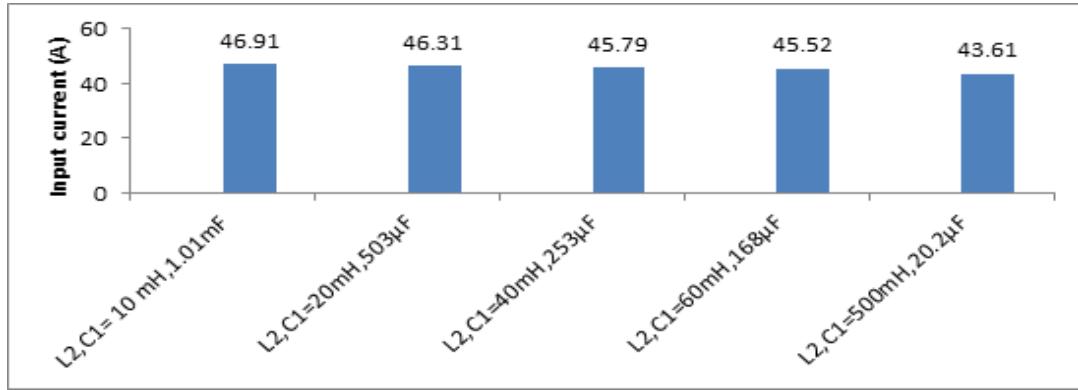


Figure 4.22: Frequency spectrum of input current in dB for controlled single phase full wave bridge rectifier with RL- load and series input resonance filter at $\alpha=30^\circ$.

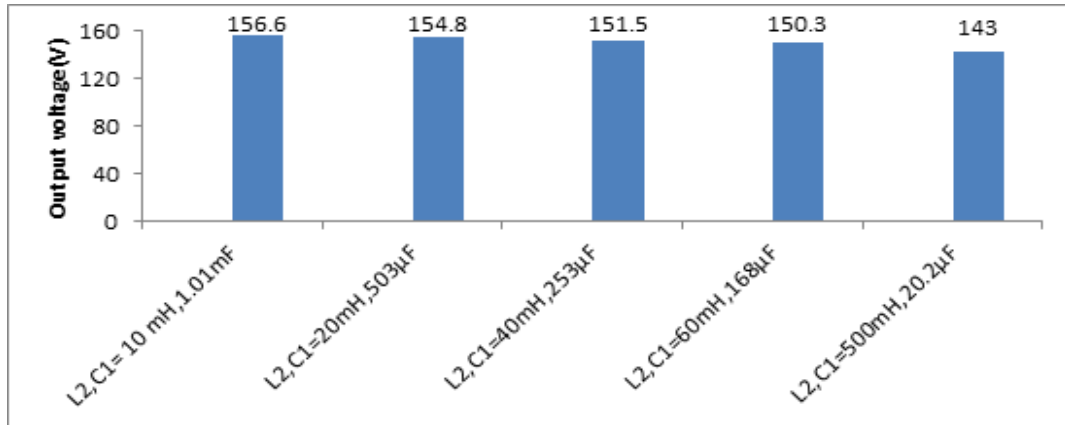
4.2.5 Comparison between the obtained results



(a)



(b)



(c)

Figure 4.23: (a)THD of input current (b) input current (c) output voltage for controlled single phase full wave bridge rectifier with RL-load and various series input resonance filter values at $\alpha=30^\circ$.

From Fig.(4.23 ,a,b), the THD and the input current decrease as the values of the filter increases (resp.), while Fig.(4.23,c) shows that the output voltage keeps almost constant. With respect to power factor it decreases according to Fig.(4.24).

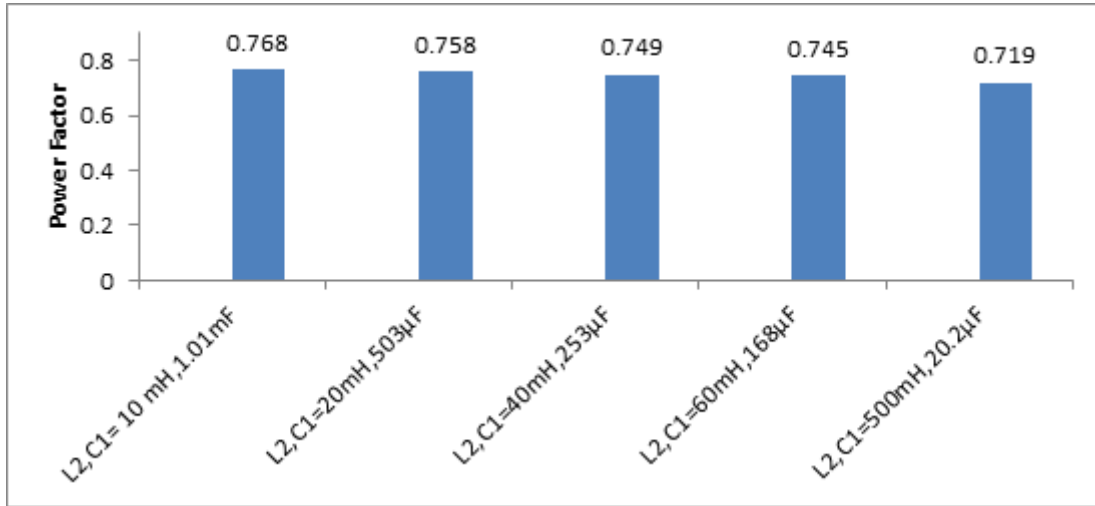


Figure 4.24: Power factor for controlled single phase full wave bridge rectifier with RL-load and various series input resonance filter values at $\alpha=30^\circ$.

4.2.6 Reactive power

For the series LC-input resonance filter, the reactive power can be obtained by summation of the total quantity of reactive power for L and C as indicated in the following table.

Table 4.6: Examples of calculated reactive power for different values of series input resonance filter.

L_2 [mH]	C_1 [μF]	I_{prms} [A]	X_L [Ω]	X_C [Ω]	Q_L [kVAr]	Q_C [kVAr]	Q_{total} [kVAr]
10	1010	33.18	3.14	3.151	3.456	3.468	6.924
20	503	32.74	6.283	6.328	6.734	6.783	13.517
40	253	32.38	12.566	12.581	13.175	13.190	26.365
60	168	32.19	18.849	18.85	19.521	19.532	39.053
500	20.2	30.82	157.079	157.079	149.20	149.20	298.4

4.3 Parallel Input Resonance LC- Filter (Band Stop)

The shape of the input current can be improved by using a combination of low-pass input or output filters. There are also several solutions for improving the shape of the input current that depends on the resonance networks which are used to attenuate harmonics. For example, a band-stop filter of the parallel resonance type, tuned at the line frequency. It is introduced between the AC source and the load. Series input resonance filter topology can give good results in improvement of power factor, but this improvement will not be satisfactory as the THD % will be reduced. So, other topologies will be implied. Parallel input resonance LC- filter can be calculated according to the following formula:

$$Z_n = \frac{nX_L * \frac{X_C}{n}}{jnX_L - \frac{jX_C}{n}} \quad (4.9)$$

Where,

X_L : Reactance of input resonant inductor at fundamental frequency.

X_C : Reactance of input resonant capacitor at fundamental frequency.

n: Order number of harmonic.

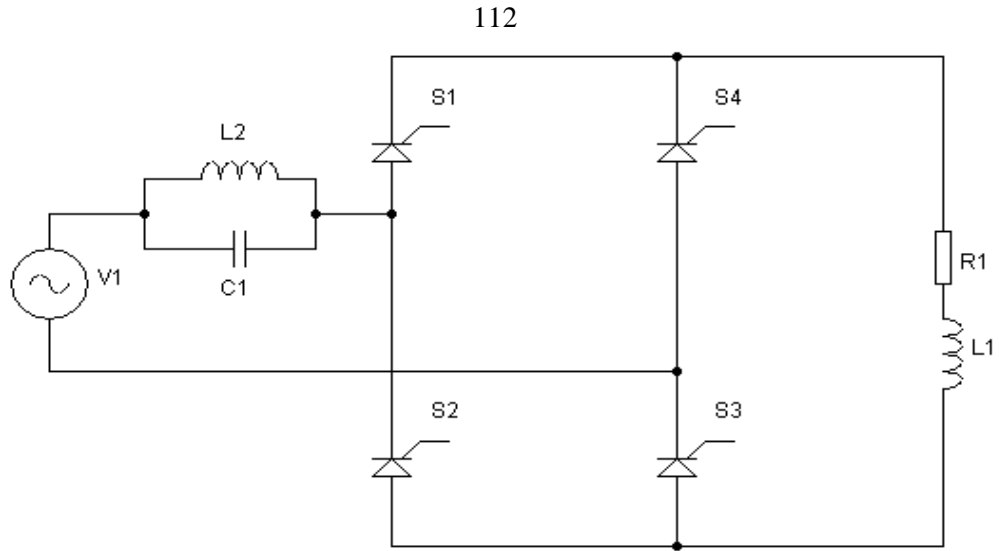


Figure 4.25: Simplified schematic of controlled single phase full wave bridge rectifier with RL-load and parallel input resonance filter.

Based on previous two configurations which have indicated high harmonics at 3rd frequency, we apply equ.(4.10) at $n=3$:

$$3X_{L_2} = \frac{X_{C_1}}{3}$$

$$C_1 = \frac{1}{9 * \omega^2 L_2} \quad (4.10)$$

The parallel LC-filter presents high reactance at resonant frequency, thereby blocking the signal from the load at that frequency. Conversely, it passes signals to the load at any other frequencies.

4.3.1 System simulation using parallel input resonance filter

MATLAB/Simulink is used to simulate the rectifier circuit with the parallel input resonance filter.

Table 4.7: Simulation specifications of controlled single phase full wave rectifier with parallel input resonance filter.

Parameter Name	Symbol	Value
Input voltage (V)	V Supply	220 (R.M.S)
Load resistance (Ω)	R_1	5
Load inductance (mH)	L_1	19
Line inductor filter (mH)	L_2	60
Capacitor (mF)	C_1	1.68
Supply frequency (Hz)	f	50
Load angle	ϕ	50°
Firing angle	α	30°

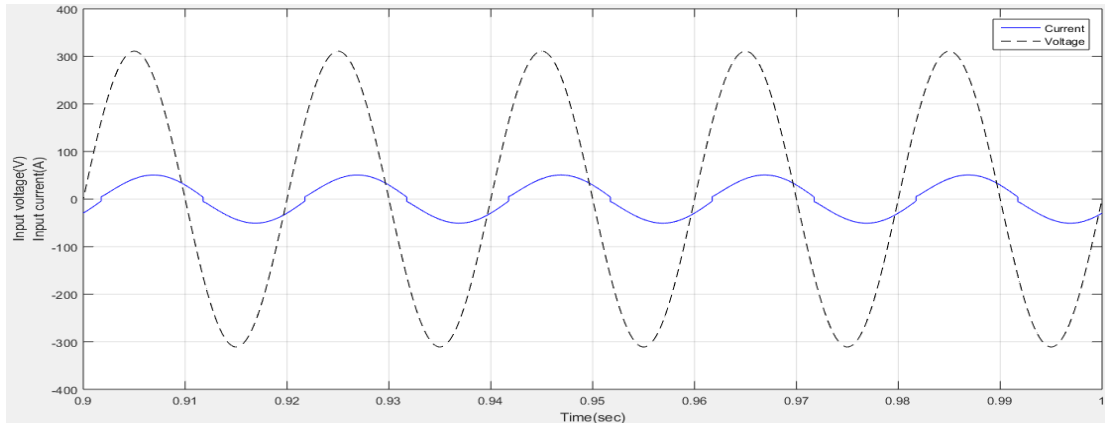


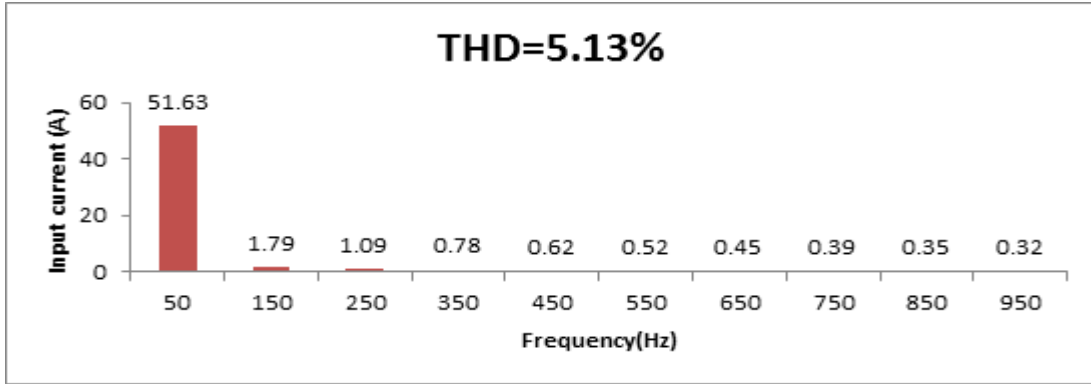
Figure 4.26: Input voltage and input current waveform for controlled single phase full wave bridge rectifier with RL – load and parallel input resonance filter at $\alpha=30^\circ$.

Figure 4.26 shows the simulation results, there is a little distortion in the input current waveform compared to smooth grid voltage, it is important to mention that the displacement angle is -32.6° (see Fig.(4.29)).

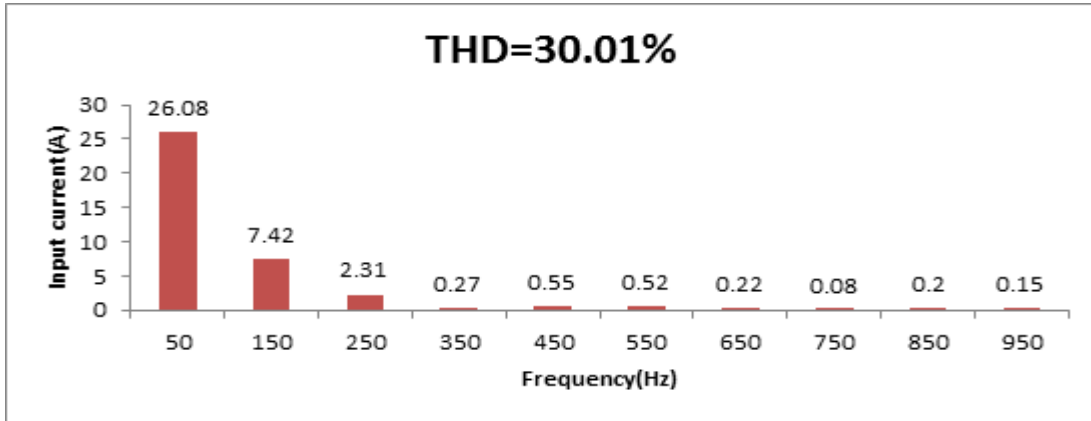
Table 4.8: Frequency spectrum of the input current.

Harmonic order	1 st	3 th	5 th	7 th	9 th	11 th	13 th	15 th	17 th	19 th
Frequency [Hz]	50	150	250	350	450	550	650	750	850	950
$I(\alpha=30^\circ)$ [A]	51.63	1.79	1.09	0.78	0.62	0.52	0.45	0.39	0.35	0.32
$I(\alpha=90^\circ)$ [A]	26.08	7.42	2.31	0.27	0.55	0.52	0.22	0.08	0.2	0.15
$I(\alpha=120^\circ)$ [A]	12.09	6.44	0.76	1.6	0.14	0.41	0.05	0.22	0.06	0.12

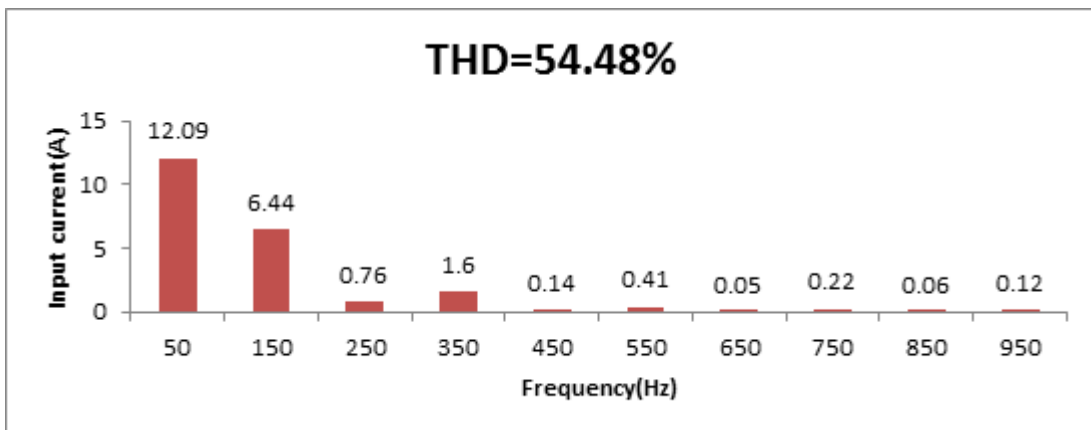
Fig.(4.27) shows the frequency spectrum of the input current with various firing angle.



(a)



(b)



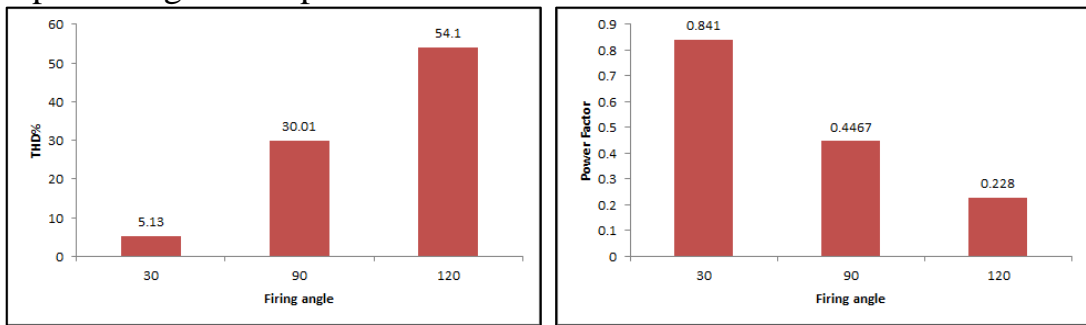
(c)

Figure 4.27: Frequency spectrum of the input current for controlled single phase full wave bridge rectifier with RL –load and parallel input resonance filter (a) at $\alpha=30^\circ$, (b) at $\alpha=90^\circ$, (c) at $\alpha=120^\circ$.

In this case the same inductor filter is used which equals (60 mH), but this circuit needs a heavy and bulky capacitor, so the capacitor used here is ten times larger than the one used previously (using 1.68mF instead of using 168 μ F) according to equ.(4.9). The aim of using such capacitor is to eliminate the third harmonic order of input current and to improve the shape of line current.

From simulation results of the line current spectrum, the lower odd harmonics at 3rd, 5th, 7th and 9th have the highest values compared to the rest values. When the firing angle increases, THD of the input current increases. At the same time the value of the input current decreases immediately with considerable reduction. These results are shown in Fig.(4.28).

Finally, it is noticed that the power factor has been improved and varied from (0.2) to (0.8) depending on the firing angle. At small firing angle, the power factor will reach maximum value. This happen due to the high drawing of current and reduction of displacement angle between input voltage and input current.



(a)

(b)

Figure 4.28: (a) THD of input current (b) power factor for controlled single phase full wave bridge rectifier with RL-load and parallel input resonance filter at $\alpha=30^\circ, 90^\circ, 120^\circ$.

4.3.2 Determination of the circuit parameters.

From equ. (2.3), the R.M.S value of the input current is obtained:

$$I_{\text{prms}} = \left[\left(\frac{51.63}{\sqrt{2}} \right)^2 + \left(\frac{1.79}{\sqrt{2}} \right)^2 + \left(\frac{1.08}{\sqrt{2}} \right)^2 + \left(\frac{.78}{\sqrt{2}} \right)^2 + \left(\frac{.62}{\sqrt{2}} \right)^2 + \left(\frac{.52}{\sqrt{2}} \right)^2 + \left(\frac{.45}{\sqrt{2}} \right)^2 + \right. \\ \left. \left(\frac{.39}{\sqrt{2}} \right)^2 + \left(\frac{.35}{\sqrt{2}} \right)^2 + \left(\frac{.32}{\sqrt{2}} \right)^2 + \left(\frac{.3}{\sqrt{2}} \right)^2 + \left(\frac{.28}{\sqrt{2}} \right)^2 + \left(\frac{.27}{\sqrt{2}} \right)^2 + \left(\frac{.25}{\sqrt{2}} \right)^2 + \left(\frac{.24}{\sqrt{2}} \right)^2 + \right. \\ \left. \left(\frac{.23}{\sqrt{2}} \right)^2 + \left(\frac{.22}{\sqrt{2}} \right)^2 + \left(\frac{.21}{\sqrt{2}} \right)^2 + \left(\frac{.21}{\sqrt{2}} \right)^2 + \left(\frac{.2}{\sqrt{2}} \right)^2 + \left(\frac{.2}{\sqrt{2}} \right)^2 + \left(\frac{.2}{\sqrt{2}} \right)^2 + \left(\frac{.19}{\sqrt{2}} \right)^2 + \right. \\ \left. \left(\frac{.2}{\sqrt{2}} \right)^2 + \left(\frac{.2}{\sqrt{2}} \right)^2 \right]^{1/2}$$

$$= 36.55\text{A}$$

From equ.(2.5), the THD is:

$$\text{THD} = \sqrt{\left(\frac{36.55}{36.50} \right)^2 - 1} = 4.8\%$$

From FFT analysis the THD of input current equals 5.13% and the theoretical value obtained from equ.(2.5) is 4.8%. The values are very closed.

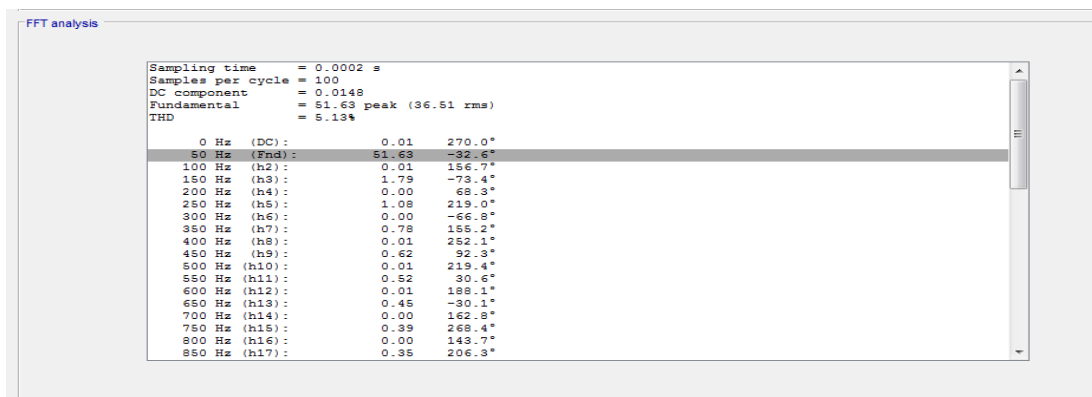


Figure 4.29: FFT analysis results of the input current for controlled single phase full wave bridge rectifier with RL –load and parallel input resonance filters at $\alpha=30^\circ$.

From the above simulation results, for $\alpha=30^\circ$, $L=60$ mH, $C=1.68$ mF, the rms value of the input current is:

$$I_{\text{prms}} = \frac{51.68}{\sqrt{2}} = 36.55\text{A}$$

Referring to equ.(4.1,4.2):

$$X_{L_2} = 18.84\Omega$$

$$Q_{L_2} = (4.051)^2 * 18.84 = 0.2366 \text{ kVAr}$$

Referring to equ. (4.6,4.7):

$$X_{C_1} = \frac{1}{2 * \pi * f * c_1} = \frac{1}{2 * \pi * 50 * .001688} = 1.885\Omega$$

$$Q_{C_1} = (40.6)^2 * 1.885 = 3.107 \text{ kVAr}$$

From equ. (2.6), the power factor is:

$$\text{PF} = \frac{36.51}{36.55} * \cos(-32.6) = 0.841$$

From the values above and as shown in Fig.(4.29), both values THD and input current have increased ($I_{\text{rms}}=36.51\text{A}$, $\text{THD}=5.13\%$) in comparison with their corresponding values of series LC- resonance filter ($I_{\text{rms}}=32.19$ A, $\text{THD} = 2.52 \%$). The power of parallel filter has performed better and has a higher value (0.841) in comparison with the series LC- filter with (0.745).

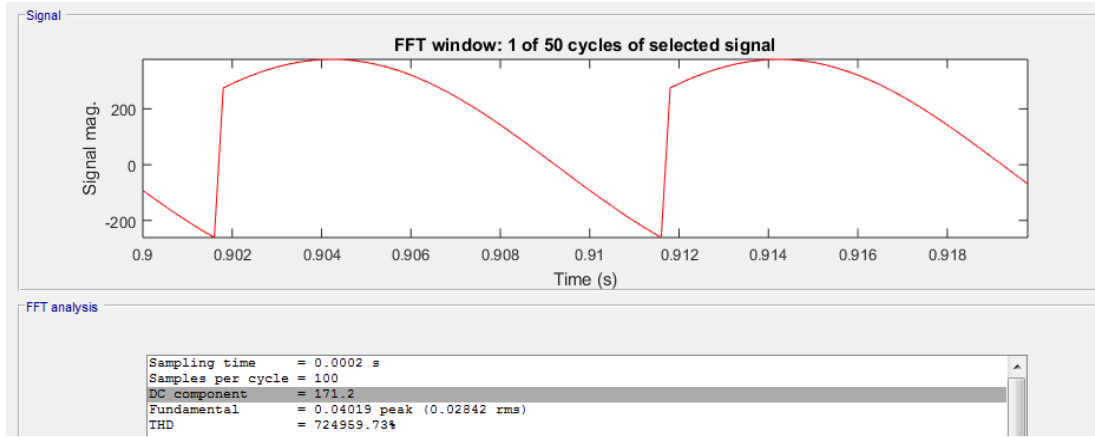


Figure 4.30: Output voltage waveform for controlled single phase full wave bridge rectifier with RL-load and parallel input resonance filter at $\alpha=30^\circ$.

The FFT analysis windows of the source voltage are given in Fig.(4.30) which shows the average output voltage of:

$$V_{dc} = 171.2 \text{ V}$$

From equ.(4.9), the reactance at 3rd order is:

$$Z_3 = \frac{3 * (18.84) * \frac{1.885}{3}}{j3 * (18.84) - \frac{j(1.885)}{3}} = -j.6287 \Omega$$

Substituting Z_3 in the equation for only the 3rd harmonic:

$$\Delta V = I * Z \quad (4.11)$$

$$\Delta V = 1.79 \angle -73.4^\circ * .6287 \angle -90^\circ \text{ V}$$

$$= 1.125 \angle -163.4^\circ \text{ V}$$

$$V_{in}(\text{new}) = \left(\sqrt{2} * 220 \angle 0^\circ - 1.125 \angle -163.4^\circ \right) = 312.07 \angle 058^\circ \text{ V}$$

$$V_{dc}(\text{after}) = \frac{2 * 312.07 * \cos 30}{\pi} = 172.05 \text{ V}$$

The simulated output voltage (DC component) obtained from FFT analysis Fig.(4.30) equals 171.2 V, while the theoretical value equals 172.05V. The two values are close. At resonance, the reactance is maximum for the parallel resonance filter, and so the voltage is at a peak because of it is proportional to the reactance ($V=I*Z$), the lack of drop voltage makes improvement in the voltage regulation and output voltage.

Applying the equ. (2.9), the average output current is:

$$I_{dc} = \frac{171.2}{5} = 34.24 \text{ A}$$

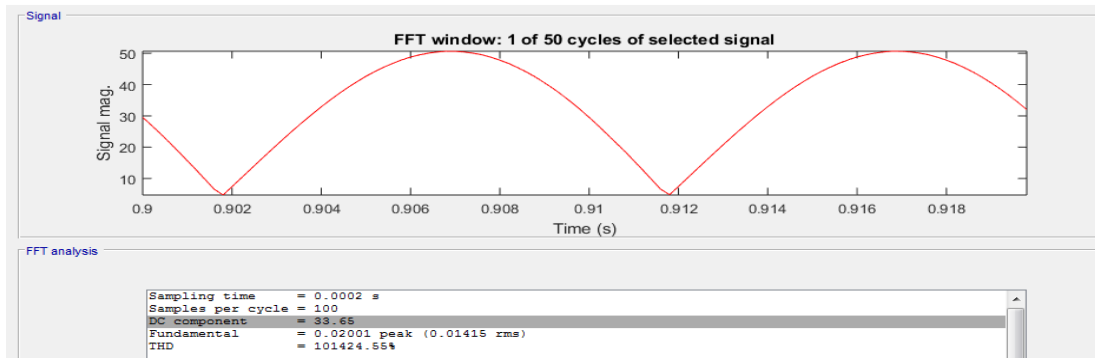


Figure 4.31:Output current waveform for controlled single phase full wave bridge rectifier with RL-load and parallel input resonance filter at $\alpha=30^\circ$.

4.3.3 Efficiency

From equ.(2.11,2.12,2.10) and according to simulation results obtained from MATLAB/SIMULINK:

$$P_{dc} = 171.2 * 33.65 = 5760 \text{ W}$$

$$P_{ac} = 220 * 36.69 = 8071 \text{ W}$$

$$\eta = \frac{5760}{8071} * 100\% = 71.35\%$$

The efficiency has increased to (71.35%) which is higher than the efficiency of series LC-filter (63.05%).

4.3.4 Representation in decibel form (dB)

Fig.(4.32) shows the frequency spectrum in (dB) for the input current of controlled single phase full wave bridge rectifier with parallel input resonance filter at $\alpha=30^\circ$.

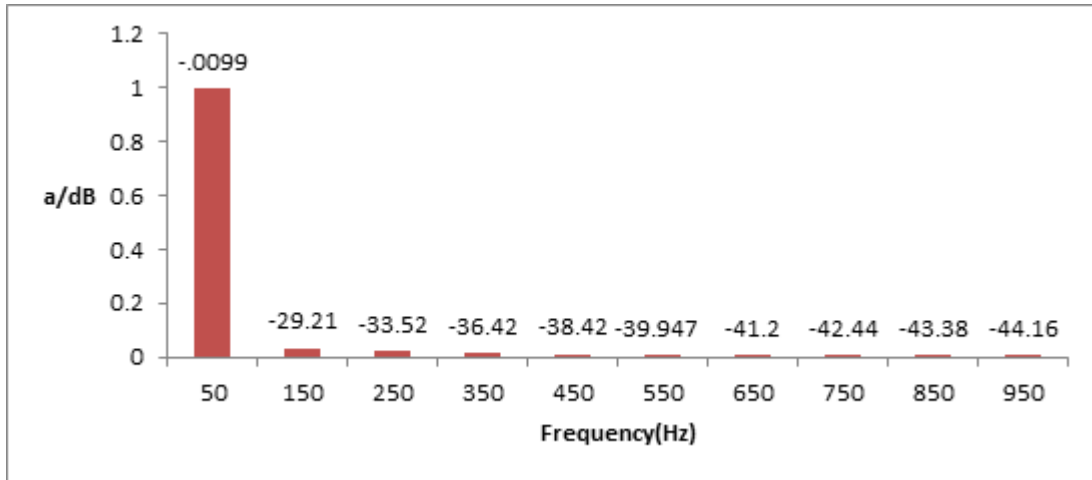
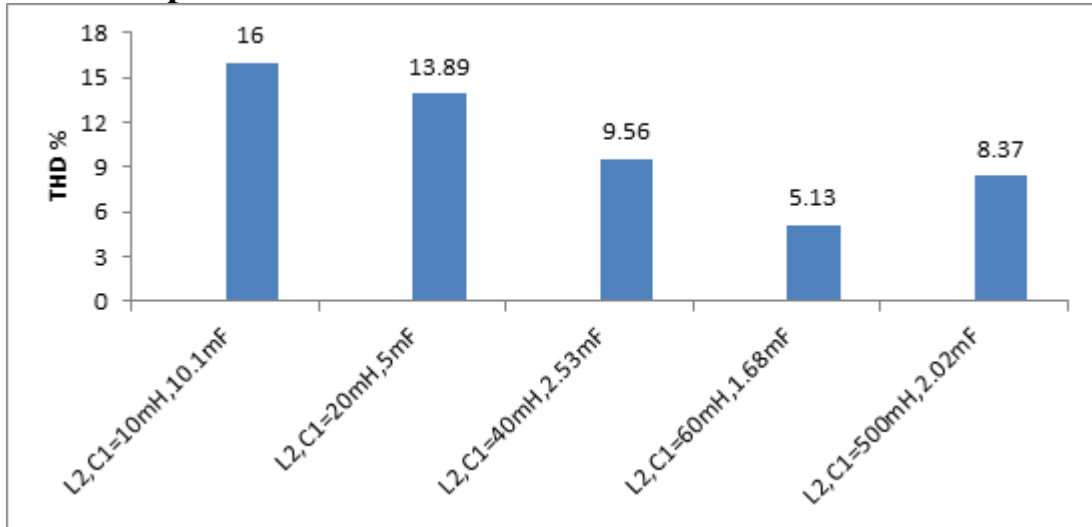
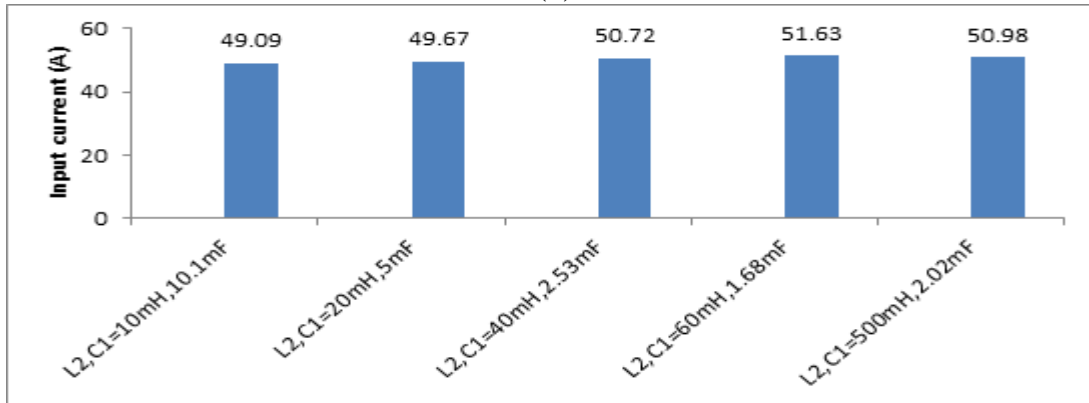


Figure 4.32: Frequency spectrum of input current in dB for controlled single phase full wave bridge rectifier with RL- load and parallel input resonance filter at $\alpha=30^\circ$.

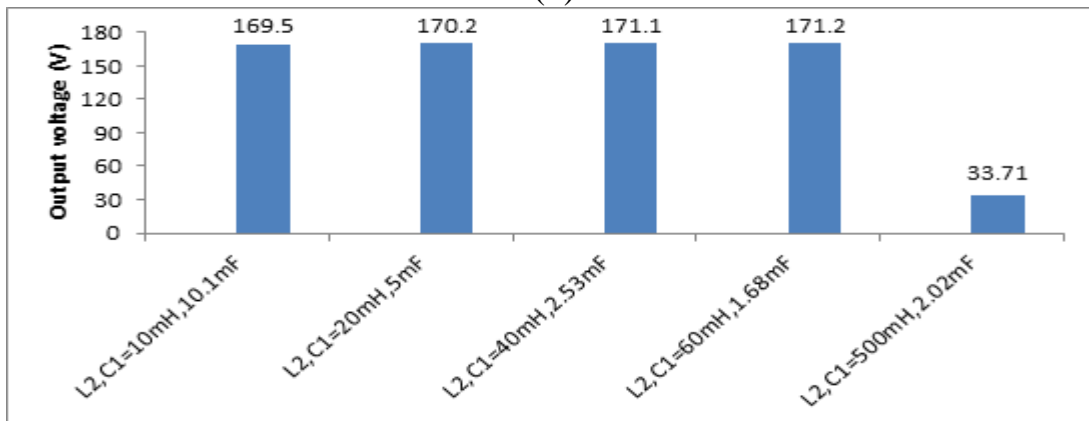
4.3.5 Comparison between the obtained results



(a)



(b)



(c)

Figure 4.33: (a)THD of input current (b) input current (c) output voltage for controlled single phase full wave bridge rectifier with RL- load and various parallel input resonance filter values at $\alpha=30^\circ$.

Fig.(4.33,a, b,c) shows the simulation results for THD, the input current and output voltage. To obtain better results for parallel resonance filter, the inductor must be increased and the capacitor must be kept within limited range .

The output voltage of DC component remains approximately constant for all values of filter parameter within the limits mentioned previously.

From the obtained results, it is allowed to increase the inductor until a limit. Otherwise, opposite results will be obtained such as decreasing the output voltage, increasing the THD and decreasing in the input current at fundamental frequency.

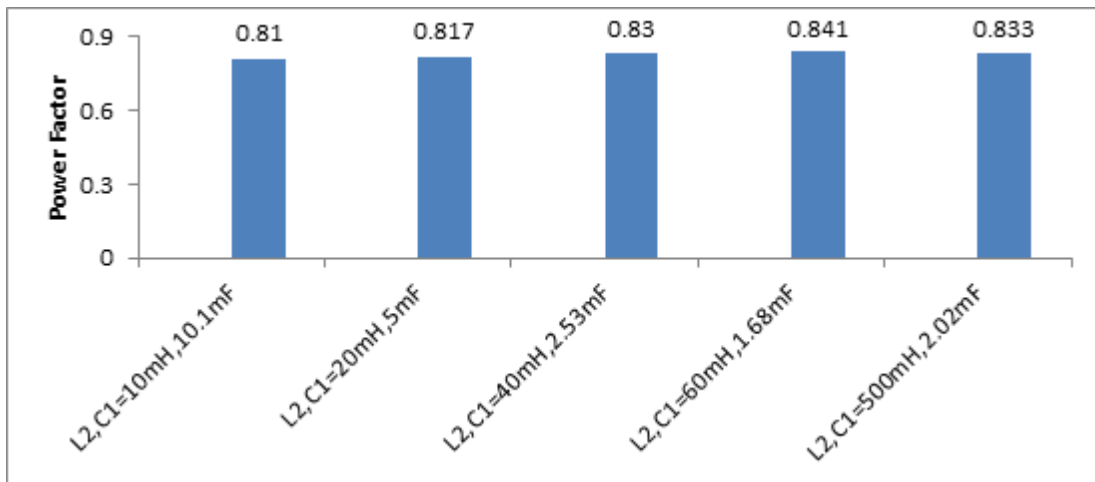


Figure 4.34: Power factor for controlled single phase full wave bridge rectifier with RL-load and various parallel input resonance filter values at $\alpha=30^\circ$.

Some of the privileges of this circuit are that the value of input power factor has been improved to a better extent compared with its value in the previous configuration. The limits of filters parameter contribute in

decreasing the value of the input power factor, but the third harmonic component is still the main reason for decreasing it.

4.3.6 Reactive power

For the parallel input resonance filter, the same calculations for the reactive power will be done as in the previous section.

Table 4.9: Example of calculated reactive power for different values of parallel input resonance filter.

L_2 [mH]	C_1 [μF]	X_L [Ω]	X_C [Ω]	I_{prms} [A]	I_{prms} [A]	Q_L [kVAr]	Q_C [kVAr]	Q_{total} [kVAr]
10	1010	3.14	0.3151	3.76	38.47	0.044	0.466	0.51
20	5000	6.283	0.6328	3.896	39.02	0.095	0.963	1.058
40	2530	12.566	1.2581	3.98	39.84	0.199	1.996	2.195
60	1680	18.849	1.89	4.051	40.6	0.2366	3.107	3.3436
500	2020	157.079	1.57079	.3637	36.41	0.020	2.08	2.1

Due to the nature of this filter and the selected values for the capacitor and inductor, the total value of reactive power will become smaller in comparison with the values obtained for series input resonance filter.

4.4 Parallel LC-Filter in Series with Inductor L

This method is considered to be the extension of the parallel input resonance filters. To overcome the high total harmonic distortion associated with the input parallel resonance filter, L_3 will be connected in series with the parallel input resonance filter which will cancel the harmonic components remaining in the line current from the previous method.

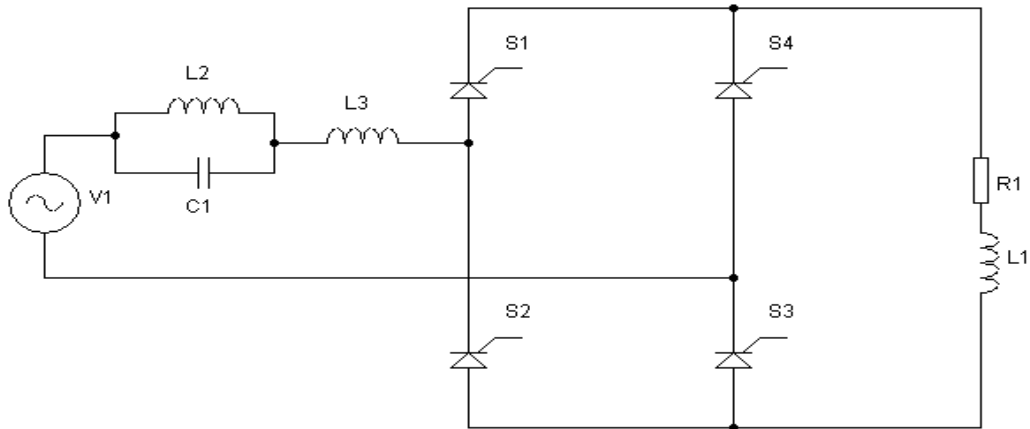


Figure 4.35: Simplified schematic of controlled single phase full wave bridge rectifier with RL- load and parallel LC-filter in series with inductor L.

4.4.1 System simulation using parallel LC-filter in series with inductor L

Similar simulations using MATLAB/Simulink has been carried out as shown in the previous section for another configuration.

Table 4.10: Simulation specifications of controlled single phase full wave bridge rectifier with parallel LC-filter in series with inductor L.

Parameter Name	Symbol	Value
Input voltage (V)	V supply	220 (R.M.S)
Load resistance (Ω)	R_1	5
Load Inductance (mH)	L_1	19
Line inductor filter (mH)	L_2	60
Line inductor filter (mH)	L_3	60
Capacitor (mF)	C_1	1.68
Supply Frequency (Hz)	f	50
Load angle	ϕ	50°
Firing angle	α	30°

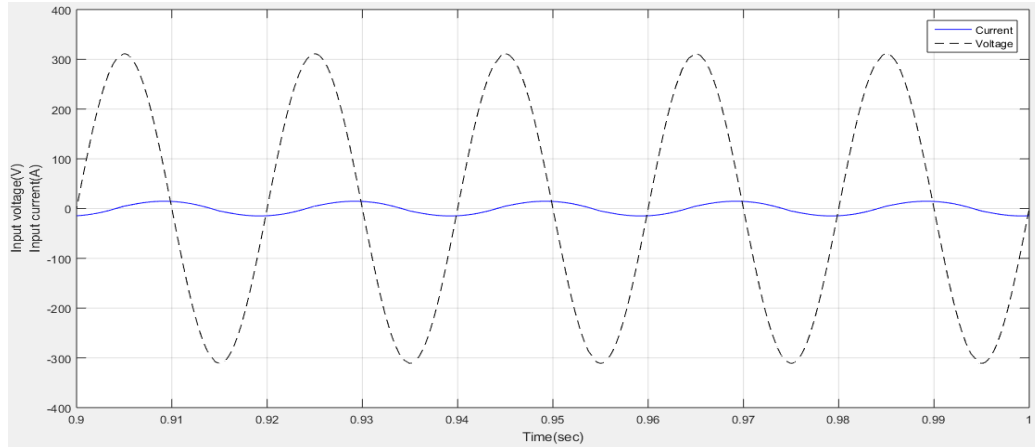


Figure 4.36: Input voltage and input current waveform for controlled single phase full wave bridge rectifier with RL- load and parallel LC-filter in series with inductor L at $\alpha=30^\circ$.

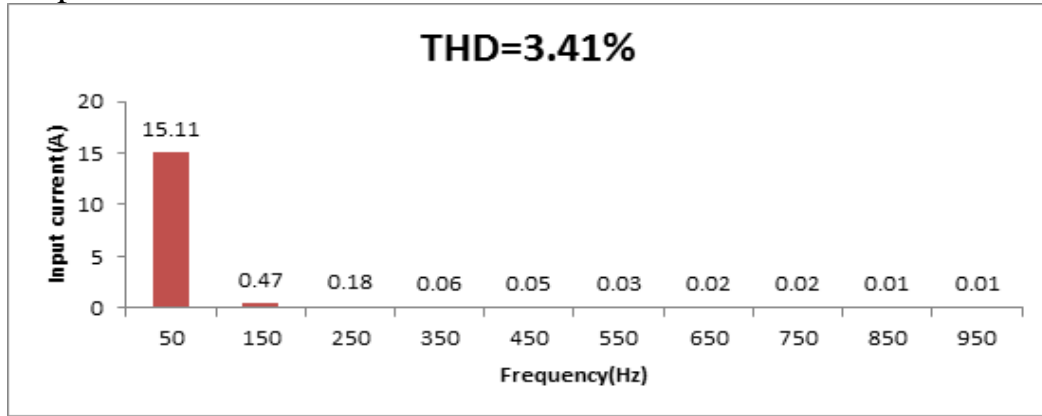
From Fig.(4.36) it is clear that the input current drawn by the utility becomes smooth, but it will be displaced in phase with respect to the grid voltage. Using this kind of filter configuration, harmonic current distortion will be improved by less than 5%, but power factor will still be low due to the large displacement angle as it will be observed later.

Table 4.11: Frequency spectrum of the input current.

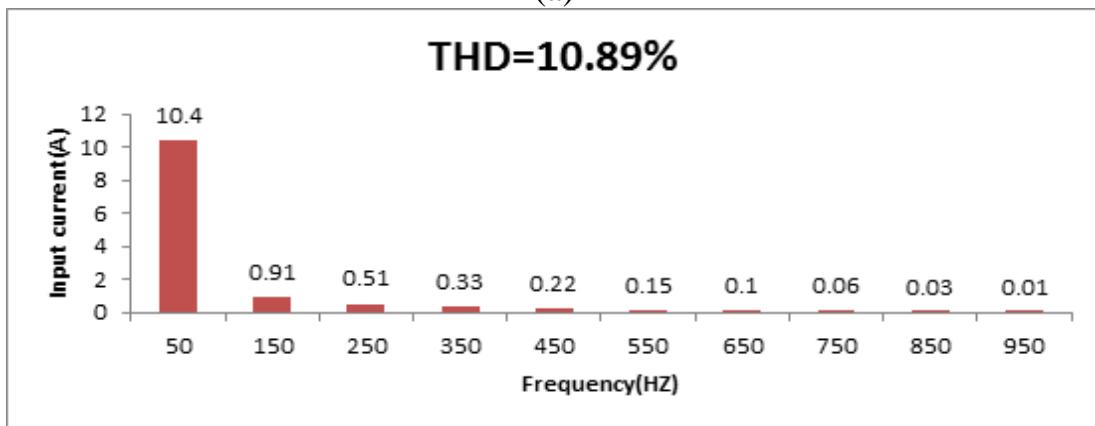
Harmonic order	1 st	3 th	5 th	7 th	9 th	11 th	13 th	15 th	17 th	19 th
Frequency [Hz]	50	150	250	350	450	550	650	750	850	950
$I(\alpha=30^\circ)$ [A]	15.11	.47	.18	.06	.05	.03	.02	.02	.01	.01
$I(\alpha=90^\circ)$ [A]	10.4	.91	.51	.33	.22	.15	.1	.06	.03	.01
$I(\alpha=120^\circ)$ [A]	4.38	1.77	0.22	0.22	0.17	0	.08	.06	.02	.05

Table 4.11 presents the simulation results of the input current, the higher odd harmonics at 7th, 9th... are mitigated to the lower values. It is also observed, that as firing angle increases, the peak of input current decreases.

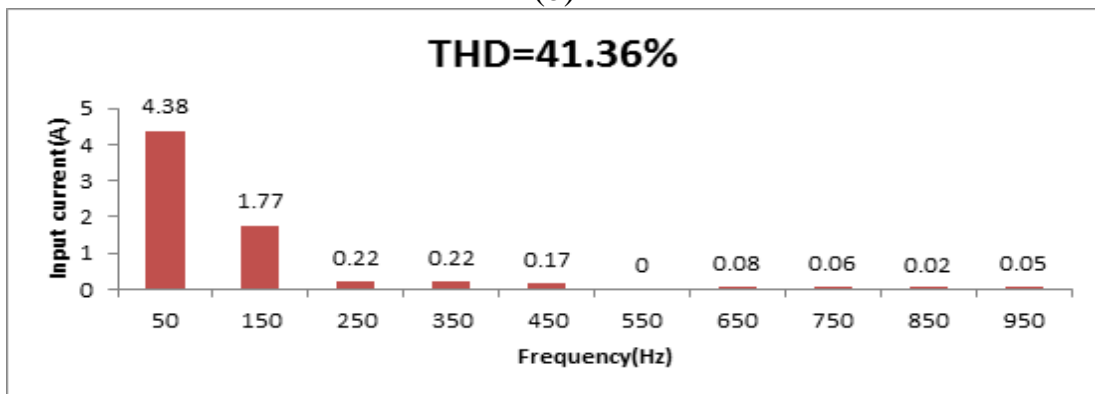
Fig.(4.37) shows the frequency spectrum of the input current with various firing angles for controlled single phase full wave bridge rectifier with parallel LC-filter in series with inductor L.



(a)

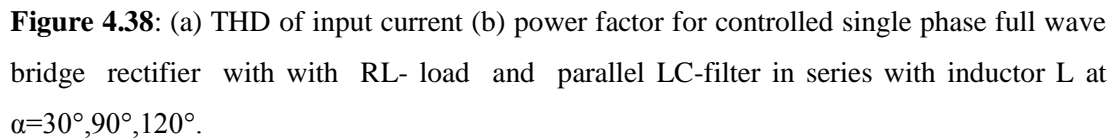


(b)



(c)

Figure 4.37: Frequency spectrum of input current for controlled single phase full wave bridge rectifier with RL-load and parallel LC-filter in series with inductor L at $\alpha=30^\circ$, 90° , 120° .



From equ. (2.3):

$$\begin{aligned} I_{\text{prms}} &= \left[\left(\frac{15.11}{\sqrt{2}} \right)^2 + \left(\frac{.47}{\sqrt{2}} \right)^2 + \left(\frac{.18}{\sqrt{2}} \right)^2 + \left(\frac{.06}{\sqrt{2}} \right)^2 + \left(\frac{.05}{\sqrt{2}} \right)^2 + \left(\frac{.03}{\sqrt{2}} \right)^2 + \left(\frac{.02}{\sqrt{2}} \right)^2 + \right. \\ &\quad \left. \left(\frac{.02}{\sqrt{2}} \right)^2 + \left(\frac{.01}{\sqrt{2}} \right)^2 + \left(\frac{.01}{\sqrt{2}} \right)^2 + \left(\frac{.01}{\sqrt{2}} \right)^2 + \left(\frac{.01}{\sqrt{2}} \right)^2 + \left(\frac{.01}{\sqrt{2}} \right)^2 + \left(\frac{.01}{\sqrt{2}} \right)^2 + \left(\frac{.01}{\sqrt{2}} \right)^2 + \right. \\ &\quad \left. \left(\frac{0}{\sqrt{2}} \right)^2 + \left(\frac{0}{\sqrt{2}} \right)^2 + \left(\frac{0}{\sqrt{2}} \right)^2 + \left(\frac{0}{\sqrt{2}} \right)^2 + \left(\frac{0}{\sqrt{2}} \right)^2 + \left(\frac{0}{\sqrt{2}} \right)^2 + \left(\frac{0}{\sqrt{2}} \right)^2 + \left(\frac{0}{\sqrt{2}} \right)^2 + \right. \\ &\quad \left. \left(\frac{0}{\sqrt{2}} \right)^2 + \left(\frac{0}{\sqrt{2}} \right)^2 \right]^{\frac{1}{2}} \\ &= 10.690 \text{ A} \end{aligned}$$

From equ.(2.5):

$$\text{THD} = \sqrt{\left(\frac{10.69}{10.684}\right)^2 - 1} = 3.35\%$$

From FFT analysis THD of the input current equals 3.41%, and the true value obtained from equ. (2.5) equals 3.35%. The two values are very close.

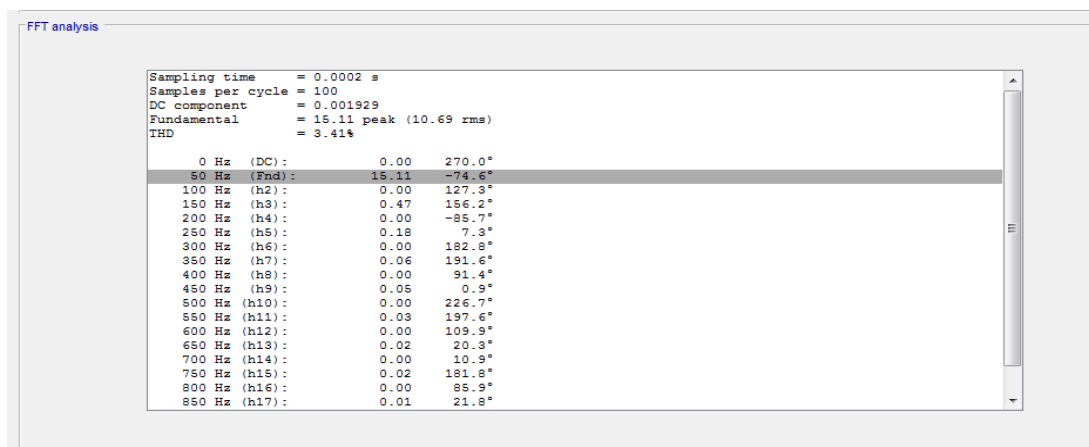


Figure 4.39: FFT analysis results of the input current for controlled single phase full wave bridge rectifier with RL- load and parallel LC-filter in series with inductor L at $\alpha=30^\circ$.

From above simulation results:

$$I_{\text{prms}} = \frac{15.117}{\sqrt{2}} = 10.69\text{A}$$

According to equ.(4.1,4.2):

$$X_{L_1} = X_{L_2} = \omega * L$$

$$= 2 * \pi * f * L = 2 * \pi * 50 * .06 = 18.84\Omega$$

$$Q_{L_1} = I^2 * X_L$$

$$=(1.187)^2 * 18.84 = 0.0265 \text{ kVAr}$$

$$Q_{L3} = I^2 * X_L$$

$$=(10.69)^2 * 18.84 = 2.152 \text{ kVAr}$$

According to equ. (4.6,4.7):

$$X_C = \frac{1}{2 * \pi * 50 * .001688} = 1.885 \Omega$$

$$Q_C = (11.87)^2 * 1.885 = 0.265 \text{ kVAr}$$

From equ. (2.6), the power factor is:

$$PF = \frac{10.684}{10.69} * \cos(-74.6) = 0.265$$

The large phase displacement of the fundamental component is (-74.4°) leads to the poor power factor that equals at 0.265. With respect to previous topology, phase displacement was -32.6° and the power factor was 0.841.

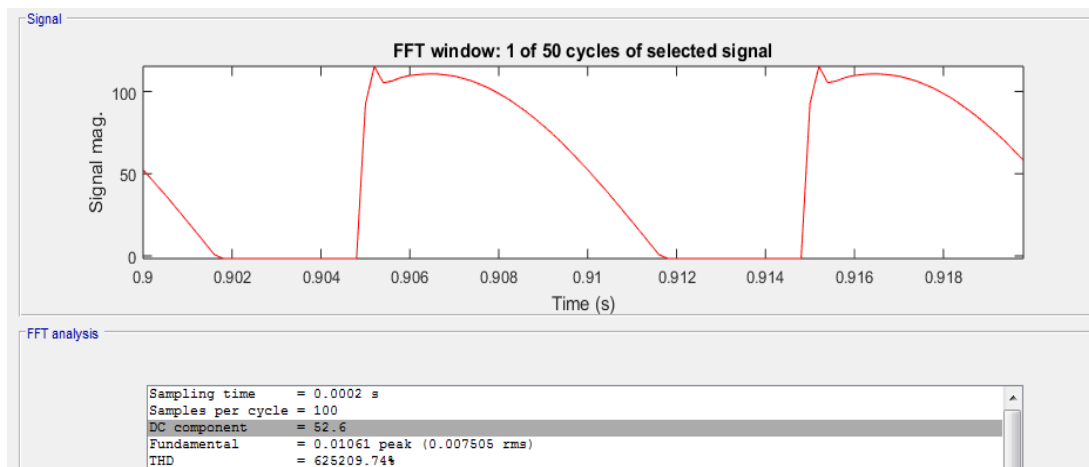


Figure 4.40: Output voltage waveform for controlled single phase full wave bridge rectifier with RL- load and parallel LC-filter in series with inductor L at $\alpha=30^\circ$.

From FFT analysis tool in MATLAB/SIMULINK, the average output voltage is $V_{dc} = 52.6 \text{ V}$

For the previous of parallel input resonance filter, the output voltage was 171.2 V.

The equivalent reactance of the filter in Fig.(4.35) is:

$$Z_3 = \frac{3(18.84) * \frac{1.885}{3}}{j3(18.84) - \frac{j(1.885)}{3}} = -j.6287\Omega \quad (4.9)$$

$$Z_{Lseries} = j18.84\Omega$$

$$Z_{total} = Z_3 + Z_{Lseries}$$

$$= -j.6287 + j18.84 \Omega$$

$$= 18.21 \angle 90^\circ \Omega$$

This type of filter configuration provides relatively high reactance. This has a great effect in reducing the value of DC component of the output voltage (52.6 V). In the previous filter where $Z_{total} = j.6287\Omega$. The output voltage was much higher (171.2V).

According to equ. (4.11), the voltage drop for this filter is:

$$\Delta V = I * Z$$

$$= 10.69 \angle -74.6^\circ * 18.21 \angle 90^\circ \text{V}$$

$$= 194.66 \angle 15.4^\circ \text{V}$$

$$V_{in}(\text{new}) = \left(\sqrt{2} * 220 \angle 0^\circ - \sqrt{2} * 194.66 \angle 15.4^\circ \right) = 86.42 \angle 57.44^\circ \text{V}$$

$$V_{dc}(\text{after}) = \frac{2 * 86.42 * \cos(30)}{\pi} = 47.64 \text{ V.}$$

As seen, there is a little difference between the simulated and calculated values of the average output voltage amounting to 52.6V, 47.64V respectively.

Applying the equ. (2.9), the average output current is:

$$I_{dc} = \frac{52.6}{5} = 10.52 \text{ A}$$

Fig.(4.41) shows the output current with the simulated value which is 10.46A.

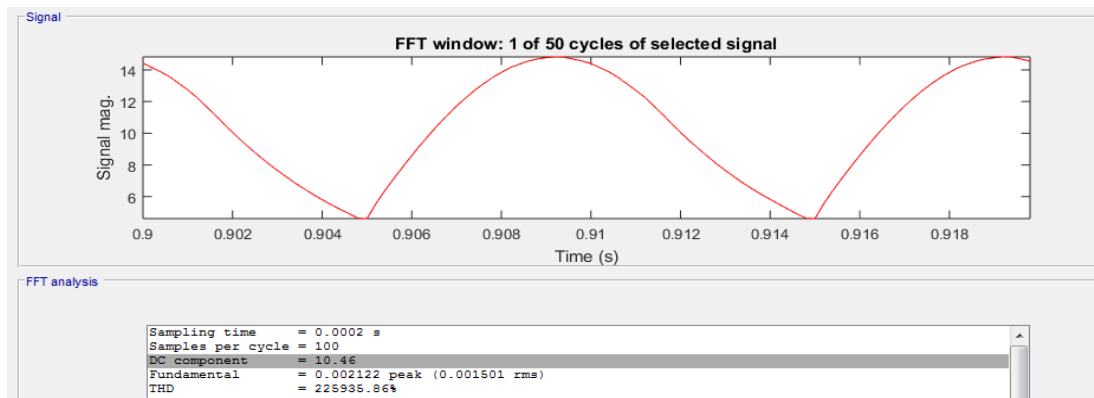


Figure 4.41: Output current waveform for controlled single phase full wave bridge rectifier with with RL- load and parallel LC-filter in series with inductor L at $\alpha=30^\circ$.

4.4.3 Efficiency

The following P_{out} , P_{in} and η are from previous mentioned equations:

$$P_{dc} = 52.6 * 10.46 = 550.1 \text{ W}$$

$$P_{ac} = 220 * 10.69 = 2351.8 \text{ W}$$

$$\eta = \frac{550.1}{2351.8} * 100\% = 23.39\%$$

From the above results, this topology has a low efficiency in comparison with input parallel resonance filter topology which was 71.35%.

4.4.4 Representation in decibel form (dB)

Fig.(4.42) shows the frequency spectrum in (dB) for the input current of single phase full wave bridge rectifier with parallel LC-filter in series with inductor L at $\alpha=30^\circ$.

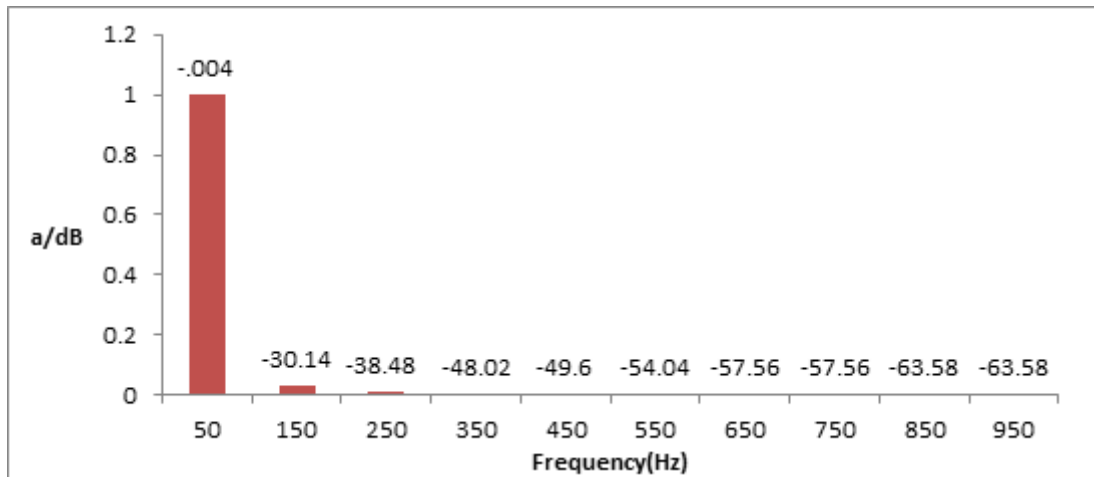


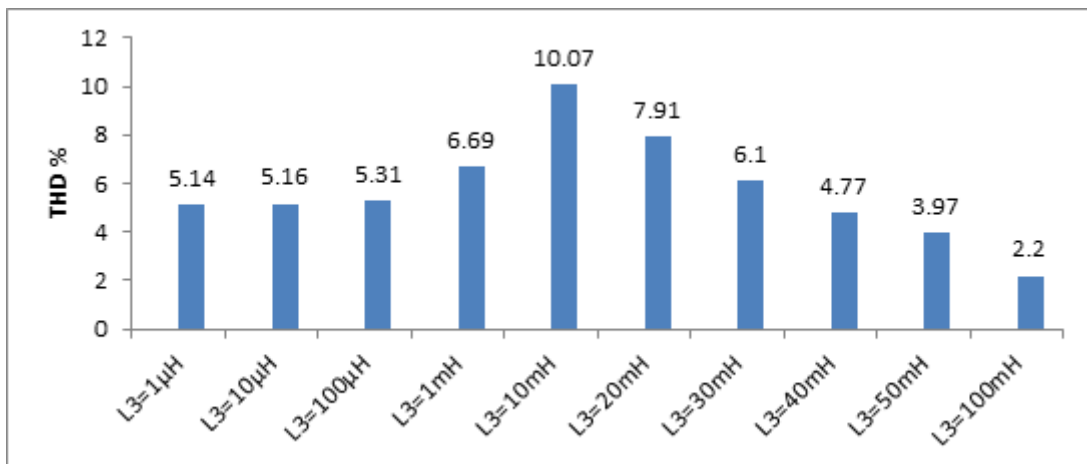
Figure 4.42: Frequency spectrum of input current in dB for controlled single phase full wave bridge rectifier with RL- load and parallel LC-filter in series with inductor L at $\alpha=30^\circ$.

Table 4.12: Calculated parameter values for different values of L_3 .

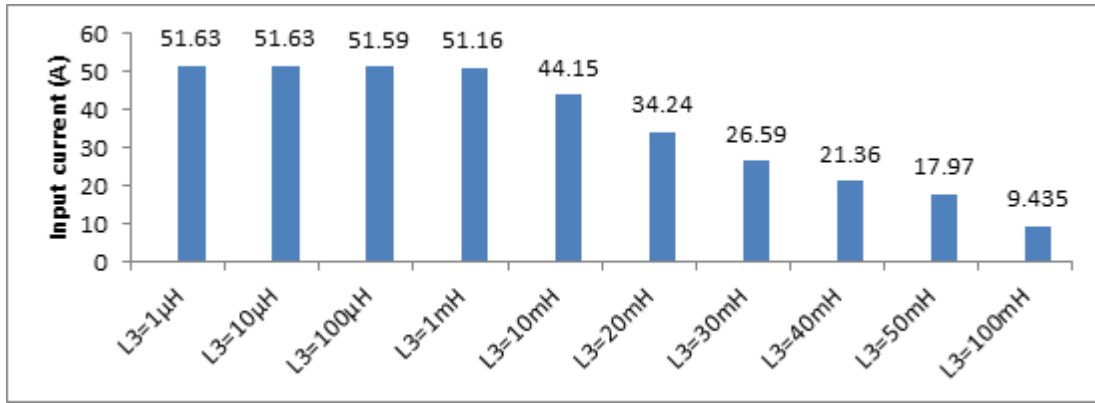
$L_2=60\text{ mH}$ Parallel $C_1=1.68\text{ mF}$						
L_3	THD%	I_s	I_{s1}	ϕ	V_{dc}	PF
$L=1\mu\text{H}$	5.14	36.55	36.51	-32.6°	171.2	0.841
$L=10\mu\text{H}$	5.16	36.55	36.51	-32.6°	171.3	0.841
$L=100\mu\text{H}$	5.31	36.53	36.48	-32.7°	171.3	0.84
$L=1\text{mH}$	6.69	36.26	36.18	-33.2°	170.1	0.834
$L=10\text{mH}$	10.07	31.37	31.22	-42.9°	149.6	0.729
$L=20\text{mH}$	7.91	24.27	24.21	-54.6°	118.2	0.577
$L=30\text{mH}$	6.1	18.82	18.8	-62.8°	92.46	0.456
$L=40\text{mH}$	4.77	15.12	15.1	-68.3°	74.48	0.369
$L=50\text{mH}$	3.97	12.546	12.54	-72°	61.68	0.308
$L=100\text{mH}$	2.2	6.669	6.669	-80.3°	32.54	0.168

Referring to Table 4.12, for the first four values of the inductor, the rms values of the input current remained high, while the THD values varied from (5.14-6.69)% .After the fourth value of the inductor, THD begins to increase and after the fifth value it begin to decrease again. The values of power factor are kept similar with acceptable value of 0.84. Finally, for the DC output voltage value, it is kept fixed at 171V.

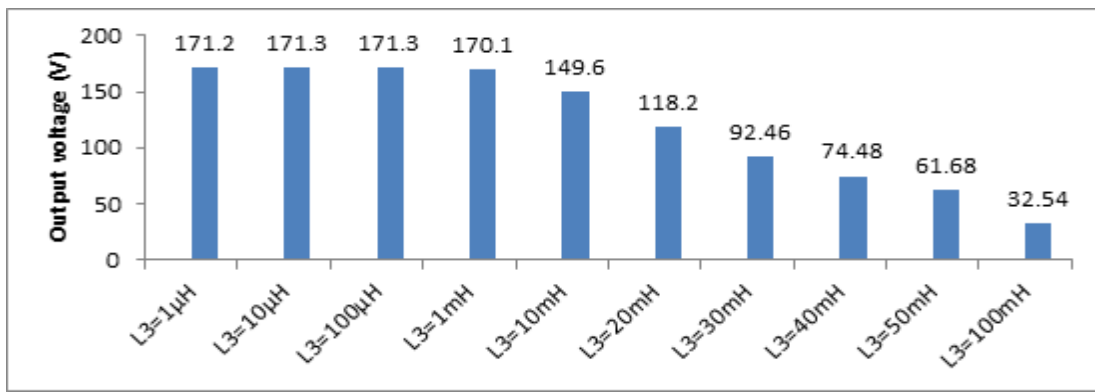
4.4.5 Comparison between the obtained results.



(a)



(b)



(c)

Figure 4.43: (a) THD of input current (b) input current (c) output voltage for controlled single phase full wave bridge rectifier with RL- load and various parallel LC-filter in series with inductor L values at $\alpha=30^\circ$.

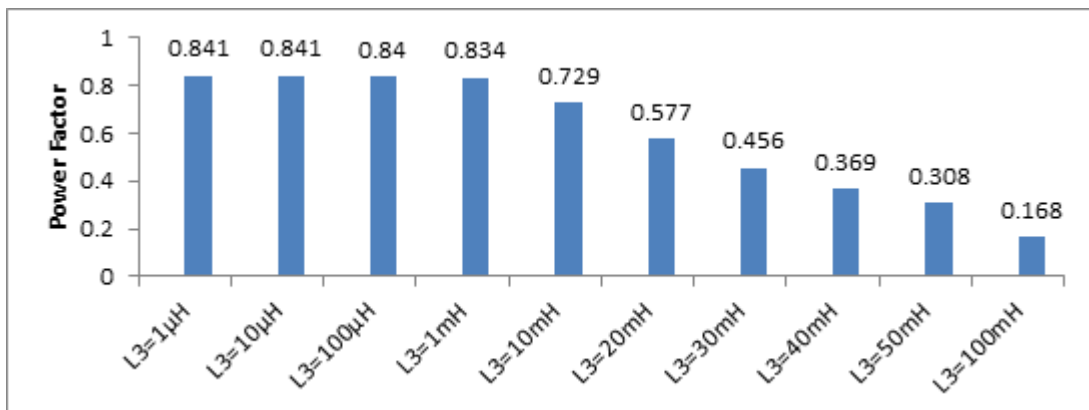


Figure 4.44: Power factor for controlled single phase full wave bridge rectifier with RL- load and various parallel LC-filter in series with inductor L values at $\alpha=30^\circ$.

The resulted voltage distortion is caused by the large value of inductor which leads to increasing the impedance and decreasing the current.

4.4.6 Reactive power

For the parallel LC-filter in series with inductor L, the cost to be estimated is associated with the total installed reactive power related to the change of filter parameters as shown in Table 4.13.

Table 4.13: Examples of calculated reactive power for different values of parallel LC-filter in series with inductor L.

L ₂ [mH]	60		C ₁ [μF]	1680				
X _{L2} [Ω]	18.849		X _C [Ω]	1.89				
L ₃ [mH]	X _{L3} [Ω]	Q _{L2} [kVAr]	Q _{C2} [kVAr]	Q _{L3} [kVAr]	Q _{total} [kVAr]	I _{prms} L ₂	I _{prms} C ₁	I _{prms} L ₃
.0001	3.14*10^-5	0.309	3.109	.000041	3.418	4.051	40.56	36.51
0.01	3.14*10^-3	0.309	3.109	.0004	3.418	4.051	40.56	36.51
0.1	0.0314	0.308	3.104	.0417	3.453	4.048	40.53	36.48
1	0.314	0.303	3.052	.411	3.766	4.015	40.19	36.18
10	3.14	0.226	2.244	3.06	5.53	3.465	34.68	31.22
20	6.283	0.135	1.366	3.68	5.181	2.686	26.89	24.21
30	9.424	0.082	0.823	3.33	4.235	2.086	20.88	18.8
40	12.566	0.052	0.532	2.86	3.444	1.675	16.78	15.1
50	15.70	0.036	0.366	2.46	2.862	1.39	13.93	12.54
60	18.849	0.026	0.262	2.15	2.438	1.186	11.87	10.69
100	31.41	0.010	0.103	1.39	1.503	.737	7.406	6.669

4.5 Second Order High Pass Filter

Another option is to use a harmonic trap filter. A mains supplied filter usually consists of series capacitor and an inductor in parallel to the AC source followed by the controlled single phase full wave bridge rectifier as shown in Fig.(4.45).

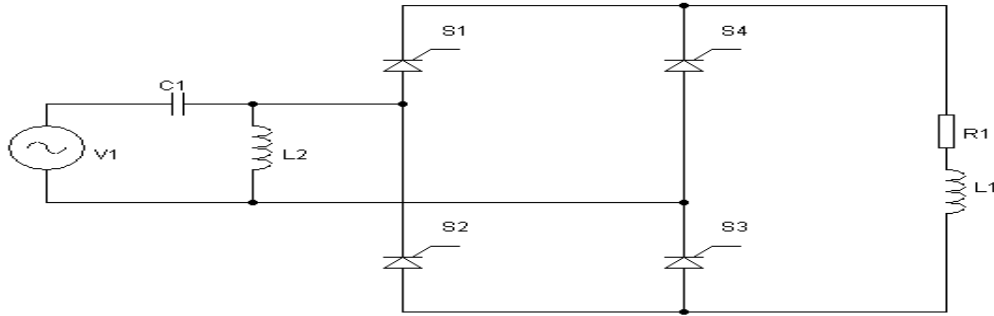


Figure 4.45: Simplified schematic of controlled single phase full wave bridge rectifier with RL- load and second order high pass filter.

4.5.1 System simulation using second order high pass filter

A similar simulation by using MATLAB/Simulink has been carried out as shown in the previous section for another configuration.

Table 4.14: Simulation specifications of controlled single phase full wave bridge rectifier with second order high pass filter.

Parameter Name	Symbol	Value
Input voltage (V)	V supply	220 (R.M.S)
Load resistance (Ω)	R_1	5
Load inductance (mH)	L_1	19
Line inductor filter (mH)	L_2	60
Capacitor (mF)	C_1	1.68
Supply frequency (Hz)	f	50
Load angle	ϕ	50°
Firing angle	α	30°

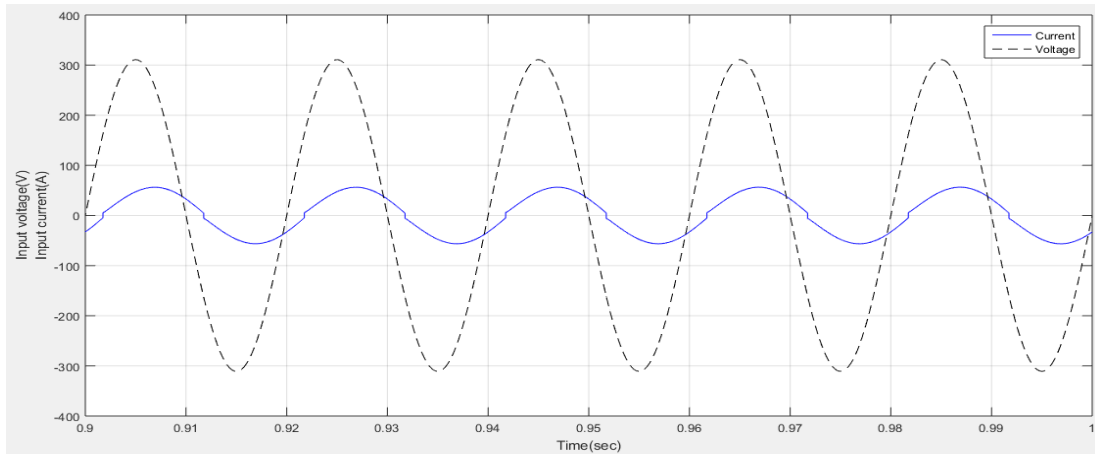


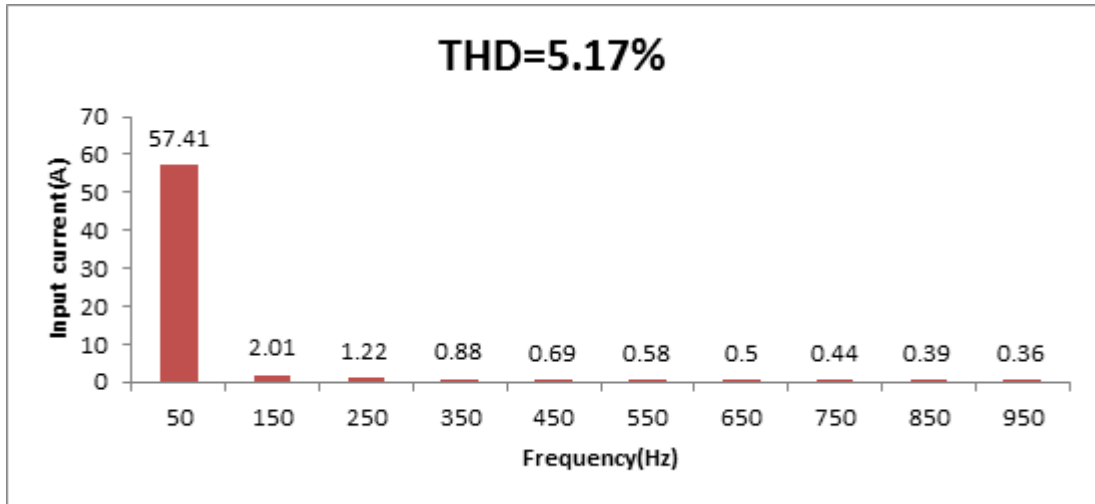
Figure 4.46: Input voltage, input current waveform for controlled single phase full wave bridge rectifier with RL- load and second order high pass filter at $\alpha=30^\circ$.

Simulation results of second order high pass filter are provided, where the input voltage is assumed to be sinusoidal, also the input current is almost pure sinusoidal with small distortion in its waveform. The current is phase-shifted from the voltage waveform with -32.6° as shown in Fig.(4.49). This phase shift results in reduction of power factor.

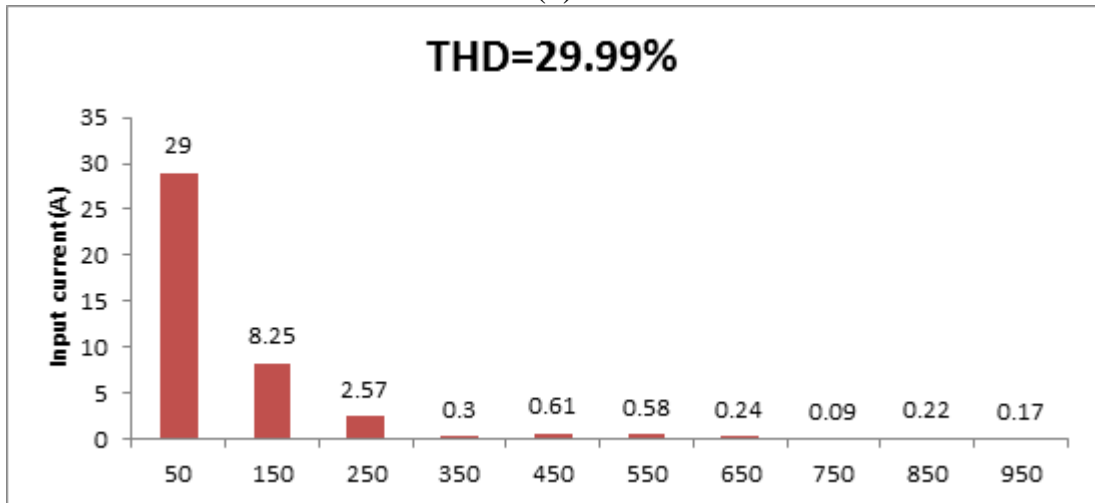
Table 4. 15:Frequency spectrum of the input current.

Harmonic order	1 st	3 th	5 th	7 th	9 th	11 th	13 th	15 th	17 th	19 th
Frequency [Hz]	50	150	250	350	450	550	650	750	850	950
$I(\alpha=30^\circ)$ [A]	57.41	2.01	1.22	.88	.69	.58	.5	.44	.39	.36
$I(\alpha=90^\circ)$ [A]	29	8.25	2.57	.3	.61	.58	.24	.09	.22	.17
$I(\alpha=120^\circ)$ [A]	13.45	7.16	.84	1.17	.16	.46	.06	.24	.06	.14

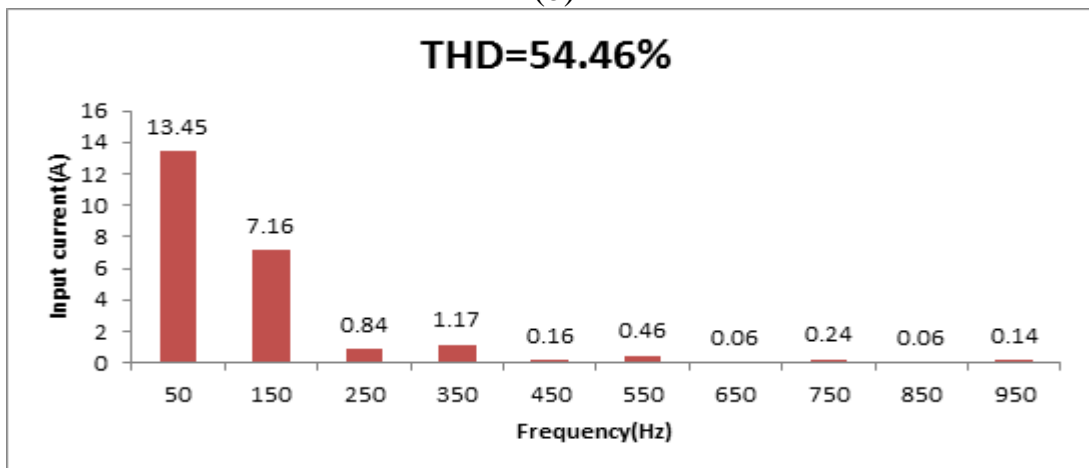
Table 4.15 shows the frequency spectrum of the input current with various firing angle for controlled single phase full wave bridge rectifier with the second order high pass filter.



(a)



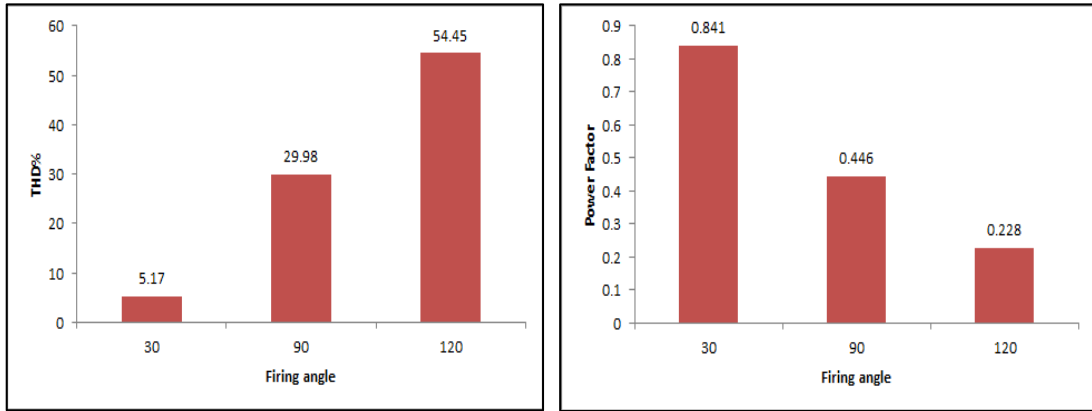
(b)



(c)

Figure 4.47: Frequency spectrum of the input current for controlled single phase full wave bridge rectifier with RL-load and second order high pass filter (a) at $\alpha=30^\circ$, (b) at $\alpha=90^\circ$, (c) at $\alpha=120^\circ$.

Fig.(4.48) shows the THD of the input and the corresponding power factor at three different firing angles. As the firing angle increases, the THD increases highly while the peak of the power factor decreases. Note that THD can be slightly higher than 5% with a small firing angle ($\alpha=30^\circ$).



(a)

(b)

Figure 4.48: (a) THD of input current (b) power factor for controlled single phase full wave bridge rectifier with RL- load and second order high pass filter at $\alpha=30^\circ, 90^\circ, 120^\circ$.

4.5.2 Determination of the circuit parameters

Repeating of the calculation by using equ.(2.3):

$$I_{\text{prms}} = \left[\left(\frac{57.41}{\sqrt{2}} \right)^2 + \left(\frac{2.01}{\sqrt{2}} \right)^2 + \left(\frac{1.21}{\sqrt{2}} \right)^2 + \left(\frac{.87}{\sqrt{2}} \right)^2 + \left(\frac{.69}{\sqrt{2}} \right)^2 + \left(\frac{.58}{\sqrt{2}} \right)^2 + \left(\frac{.5}{\sqrt{2}} \right)^2 + \left(\frac{.44}{\sqrt{2}} \right)^2 + \left(\frac{.39}{\sqrt{2}} \right)^2 + \left(\frac{.36}{\sqrt{2}} \right)^2 + \left(\frac{.33}{\sqrt{2}} \right)^2 + \left(\frac{.31}{\sqrt{2}} \right)^2 + \left(\frac{.3}{\sqrt{2}} \right)^2 + \left(\frac{.28}{\sqrt{2}} \right)^2 + \left(\frac{.27}{\sqrt{2}} \right)^2 + \left(\frac{.25}{\sqrt{2}} \right)^2 + \left(\frac{.25}{\sqrt{2}} \right)^2 + \left(\frac{.24}{\sqrt{2}} \right)^2 + \left(\frac{.23}{\sqrt{2}} \right)^2 + \left(\frac{.23}{\sqrt{2}} \right)^2 + \left(\frac{.22}{\sqrt{2}} \right)^2 + \left(\frac{.22}{\sqrt{2}} \right)^2 + \left(\frac{.22}{\sqrt{2}} \right)^2 + \left(\frac{.22}{\sqrt{2}} \right)^2 \right]^{\frac{1}{2}}$$

$$= 40.649 \text{ A}$$

From equ. (2.5):

$$\text{THD} = \sqrt{\left(\frac{40.649}{40.595}\right)^2 - 1} = 5.15\%$$

From the simulation results, $\text{THD} = 5.16\%$

In conclusion, the two values above are almost the same but they don't meet the requirements of standards.

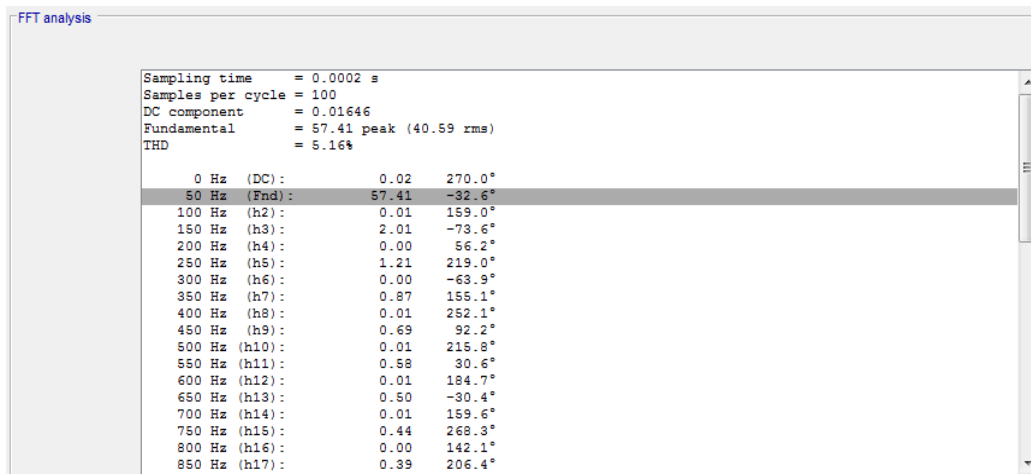


Figure 4.49: FFT analysis results of the input current for controlled single phase full wave bridge rectifier with second order high pass filter at $\alpha=30^\circ$.

From the above simulation results:

$$I_{\text{rms}} = \frac{57.41}{\sqrt{2}} = 40.595 \text{ A}$$

Referring to the equ.(4.1, 4.2):

$$X_{L_2} = 2 * \pi * f * L_2 = 2 * \pi * 50 * .06 = 18.84 \Omega$$

$$Q_{L_2} = (15.85)^2 * 18.84 = 4.733 \text{ kVAr}$$

Referring to the equ. (4.6,4.7):

$$X_C = \frac{1}{2 * \pi * 50 * .001688} = 1.885 \Omega$$

$$Q_C = (53.25)^2 * 1.885 = 5.345 \text{ kVar}$$

From equ. (2.6), the power factor is:

$$\text{PF} = \frac{40.595}{40.649} * \cos(-32.6) = 0.841$$

The input power factor can be improved to 0.841 by using the second order high pass filter.

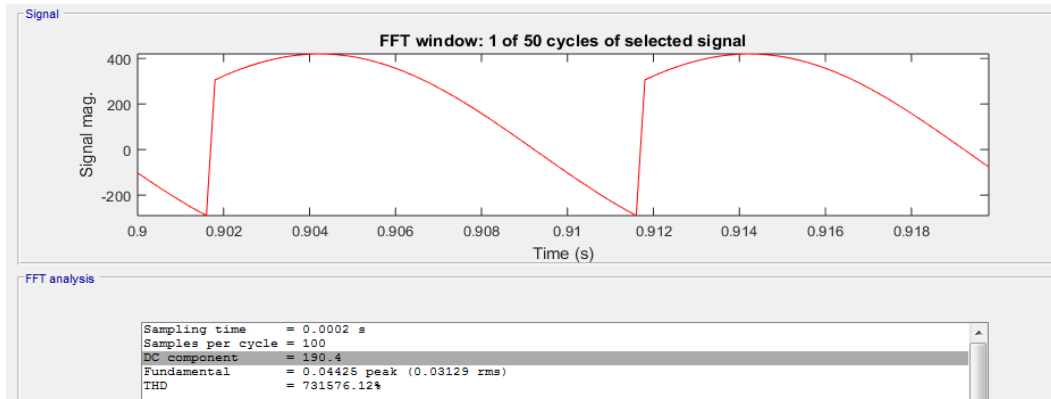


Figure 4.50: Output voltage waveform for controlled single phase full wave bridge rectifier with RL-load and second order high pass filter at $\alpha=30^\circ$.

The voltage drop for the second order high pass filter is given by:

$$\Delta V = I * Z_C$$

$$= 57.41 \angle -32.6^\circ * 1.89 \angle -90^\circ = 108.5 \angle -122.6^\circ \text{ V}$$

$$V_{in}(\text{new}) = \left(\sqrt{2} * 220 \angle 0^\circ - 108.5 \angle -122.6^\circ \right) = 380.58 \angle 13.89^\circ \text{ V}$$

$$V_{dc}(\text{after}) = \frac{2 * 380.58 * \cos 30}{\pi} = 209.8 \text{ V}$$

Clearly, there is variety between the calculated value of the average output voltage and the simulated voltage which is $V_{dc} = 190.4V$ that obtained from the FFT analysis windows.

Applying equ. (2.9), the output current is:

$$I_{dc} = \frac{190.4}{5} = 38.08 \text{ A}$$

However, the simulated value is 37.42 A, as shown in Fig.(4.51)

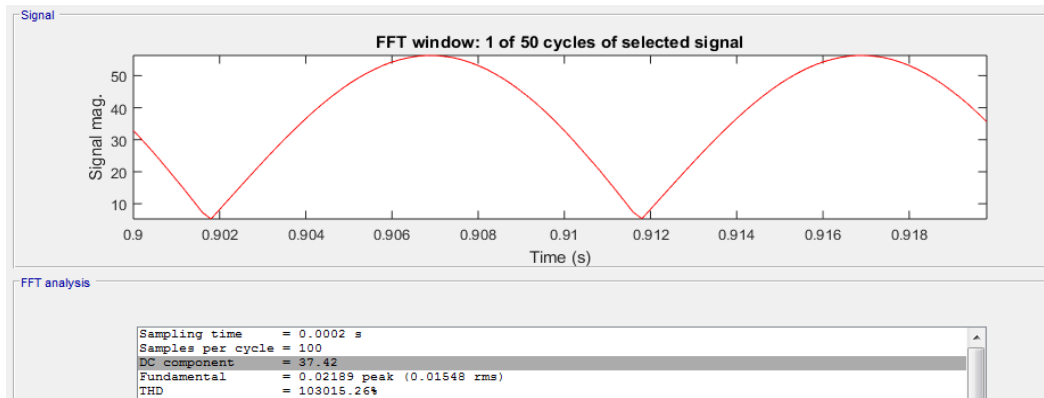


Figure 4.51: Output current waveform for controlled single phase full wave bridge rectifier with RL- load and second order high pass filter at $\alpha=30^\circ$.

4.5.3 Efficiency

The same previous procedure is used to calculate the efficiency:

$$P_{dc} = 190.4 * 37.42 = 7124 \text{ W}$$

$$P_{ac} = 220 * 40.649 = 8942.78 \text{ W}$$

$$\eta = \frac{7124}{8942.78} * 100\% = 79.66\%$$

This filter is considered to be the most efficient topology over the entire mentioned topology configurations, the maximum efficiency that can be obtained is 79.66%.

4.5.4 Representation in decibel form (dB)

Fig.(4.52) shows the frequency spectrum for the input current of controlled single phase full wave bridge rectifier with second order high pass filter.

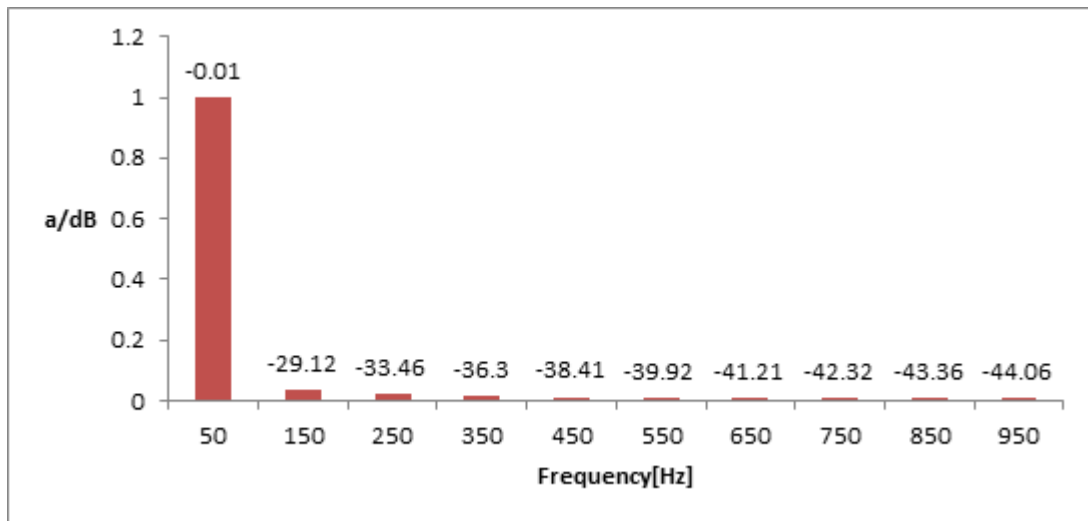
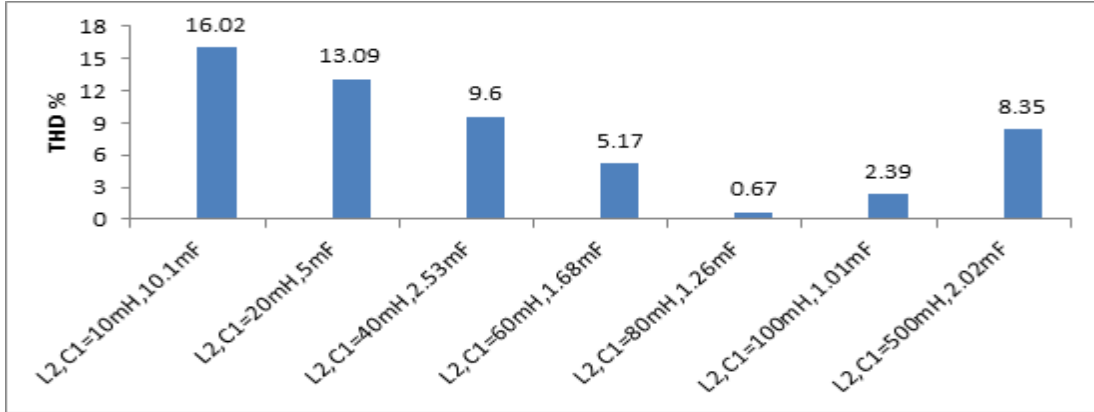
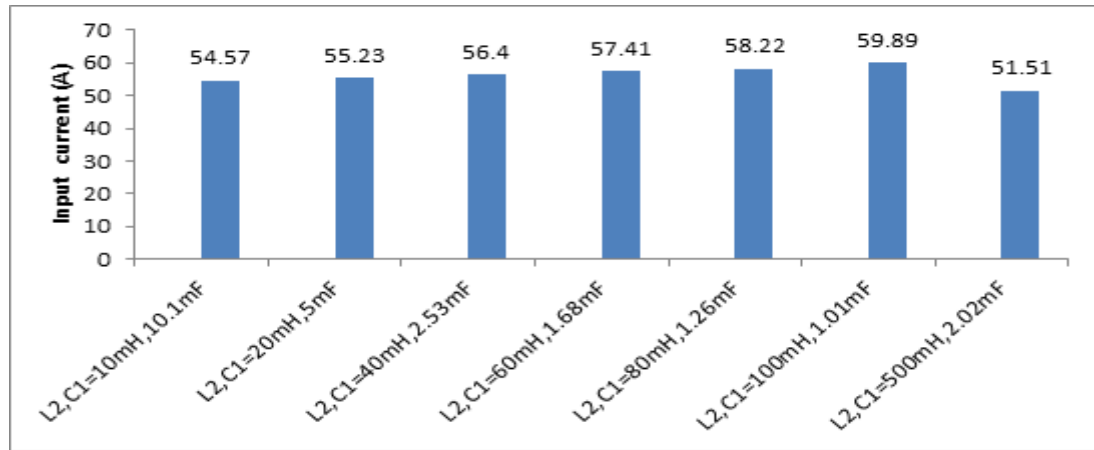


Figure 4.52: Frequency spectrum of input current in dB for controlled single phase full wave bridge rectifier with RL- load and second order high pass filter at $\alpha=30^\circ$.

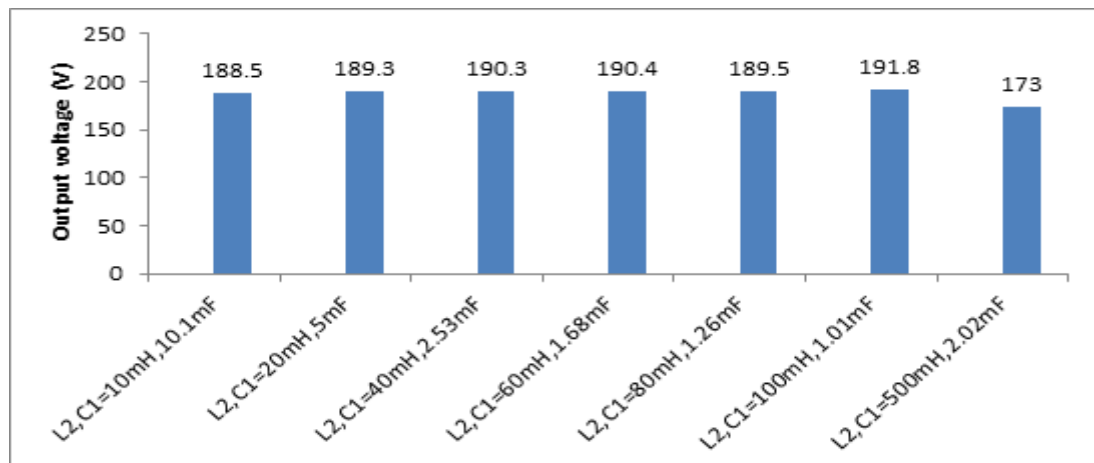
4.5.5 Comparison between the obtained results



(a)



(b)



(c)

Figure 4.53: (a)THD of input current (b) input current (c) output voltage for controlled single phase full wave rectifier with RL-load and second order high pass filter at $\alpha=30^\circ$.

It is important to emphasize that the selection of the filter depends on:

- Peak current should be as large as possible.
- THD should be minimized least as possible.

To achieve the best result, inductor must be increased and capacitor decreased to a limited value and after that, increasing the inductor value will contribute in the decreasing the THD and increasing the peak current, as shown in the Fig.(4.53,a, b).

The output voltage across the RL- load is approximately high which means that there is a small voltage drop which maintains the output DC voltage within acceptable range as shown in the Fig.(4.53,c).

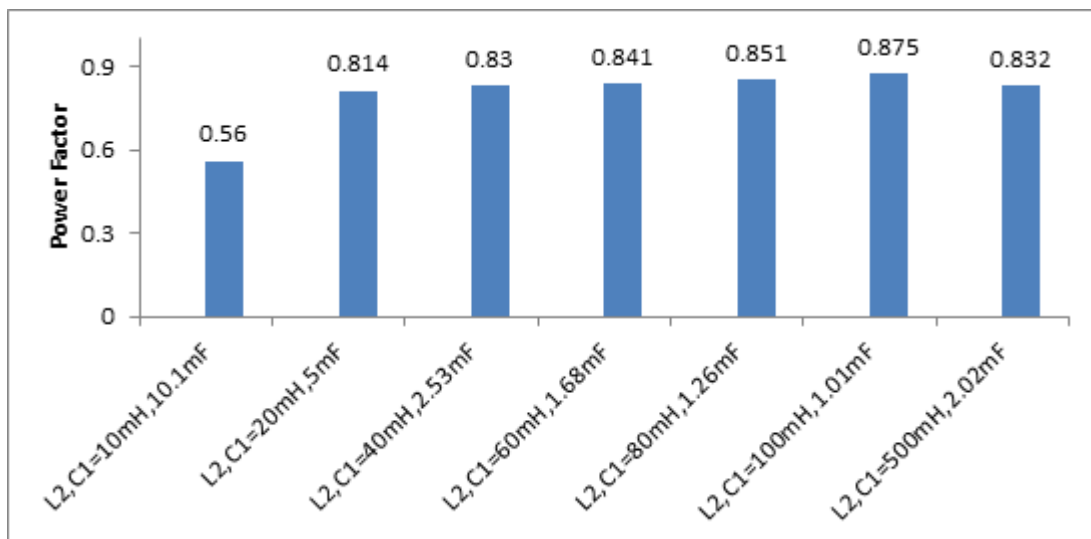


Figure 4.54: Power factor for controlled single phase full wave bridge rectifier with RL-load and second order high pass filter at $\alpha=30^\circ$.

As shown in Fig.(4.54), the power factor doesn't exceed 0.875.

4.5.6 Reactive Power

Table 4.16: Examples of calculated reactive power for different values of second order high pass filter.

L [mH]	C [μF]	I_{prms} L_2	I_{prms} C_1	X_L [Ω]	X_C [Ω]	Q_L [kVAr]	Q_C [kVAr]	Q_{total} [kVAr]
10	10100	80.26	108.1	3.14	.3151	20.226	3.682	23.908
20	5000	41.48	72.79	6.283	.6328	10.810	3.352	14.162
40	2530	22.2	57.38	12.566	1.2581	6.193	4.142	10.335
60	1680	15.85	53.21	18.849	1.89	4.735	5.351	10.086
500	2020	1.645	37.59	157.079	1.57079	.425	2.219	2.644

From the tabulated results, the value of the total installed reactive power is in middle range which means a reasonable cost.

4.6 Third Order High Pass T- Filter

The capacitive reactance in the series arm of T-filter offers lower reactance to the harmonics present in the line current, and thereby passes these harmonics. The inductive reactance in the shunt offers high reactance to the harmonics which rejects them. This will improve the power factor and reduce the THD. Also, " C_2 " is added over to the previous circuit in order to improve the response of the filter.

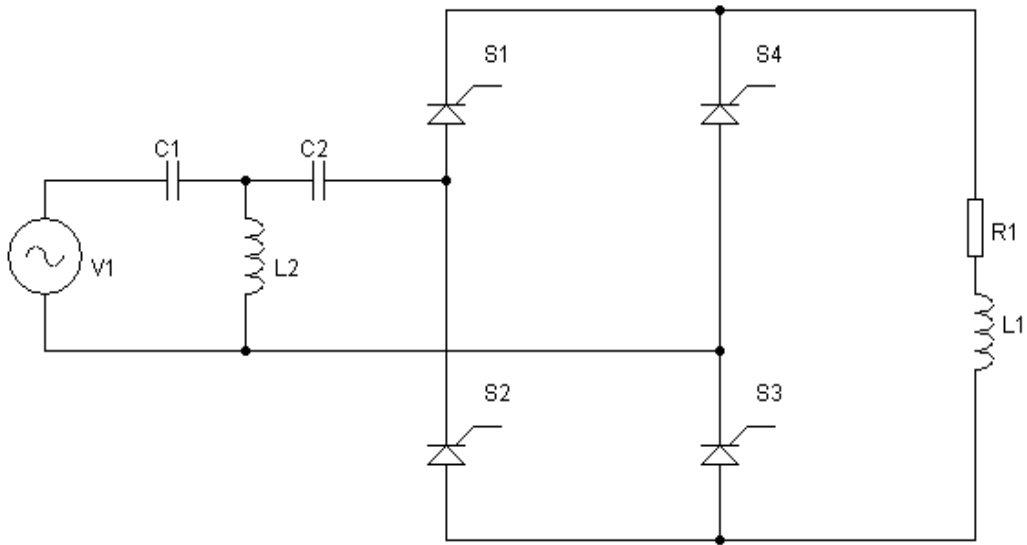


Figure 4.55: Simplified schematic of controlled single phase full wave bridge rectifier with RL- load and third order high pass T- filter.

4.6.1 System simulation using third order high pass filter

Similar simulations using MATLAB/Simulink has been carried out as shown in the previous section for another configuration.

Table 4.17: Simulation specifications of controlled single phase full wave bridge rectifier with third order high pass T- filter rectifier.

Parameter Name	Symbol	Value
Input voltage (V)	V _{supply}	220 (R.M.S)
Load resistance (Ω)	R ₁	5
Load inductance (mH)	L ₁	19
Line inductor filter (mH)	L ₂	60
Capacitor (mF)	C ₁	1.68
Capacitor (mF)	C ₂	1.68
Supply frequency (Hz)	f	50
Load angle	ϕ	50°
Firing angle	α	30°

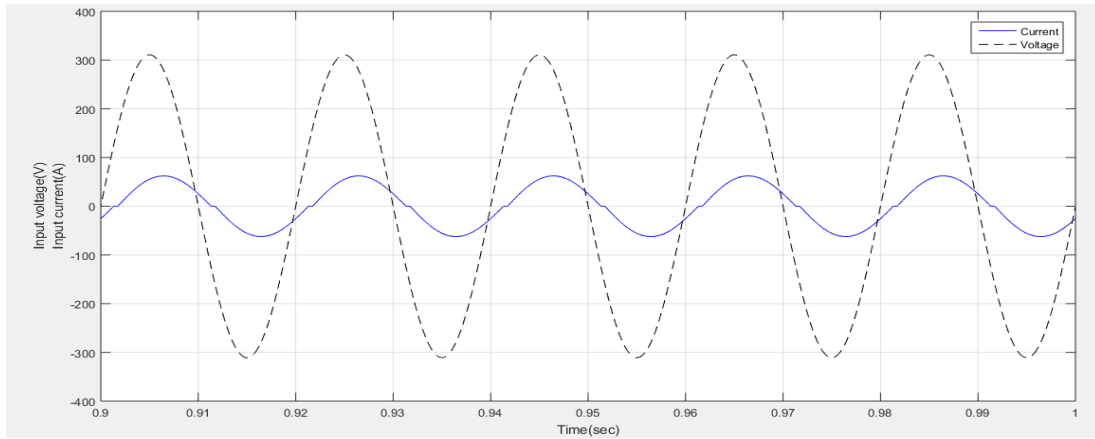


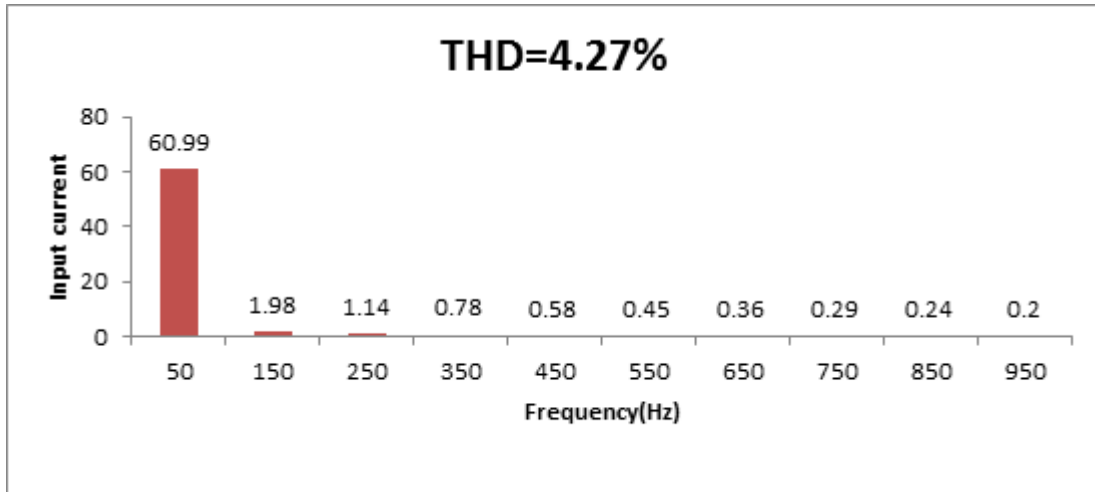
Figure 4.56: Input voltage and input current waveform for controlled single phase full wave bridge rectifier with RL-load and third order high pass T-filter at $\alpha=30^\circ$.

It can be observed from the Fig.(4.56) that the input current is nearly in phase with the input voltage.

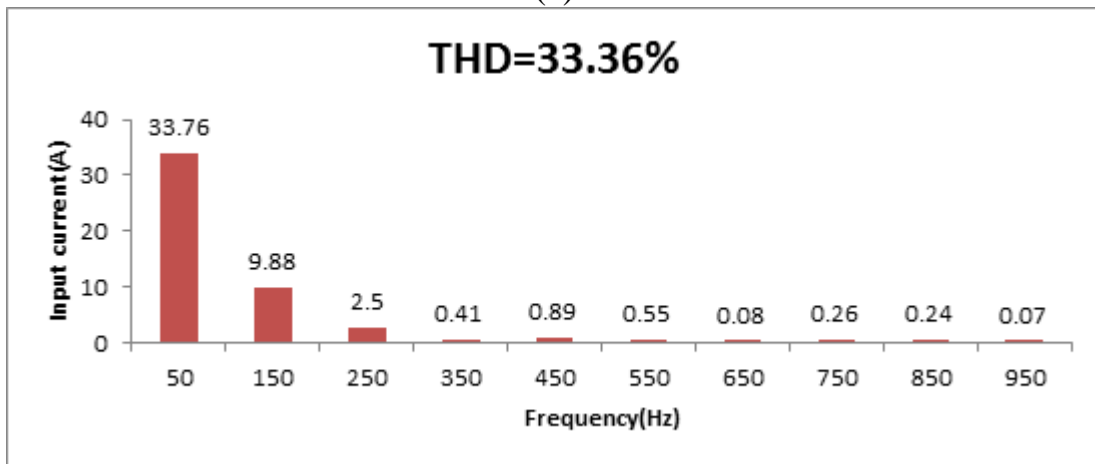
Table 4.18: Frequency spectrum of the input current.

Harmonic order	1 st	3 th	5 th	7 th	9 th	11 th	13 th	15 th	17 th	19 th
Frequency [Hz]	50	150	250	350	450	550	650	750	850	950
$I(\alpha=30^\circ)$ [A]	60.99	1.98	1.14	0.78	0.58	0.45	0.36	0.29	0.24	0.2
$I(\alpha=90^\circ)$ [A]	33.76	9.88	2.5	0.41	0.89	0.55	0.08	0.26	0.24	0.07
$I(\alpha=120^\circ)$ [A]	14.03	7.67	1.09	1.22	0.25	0.48	0.06	0.26	0.02	0.15

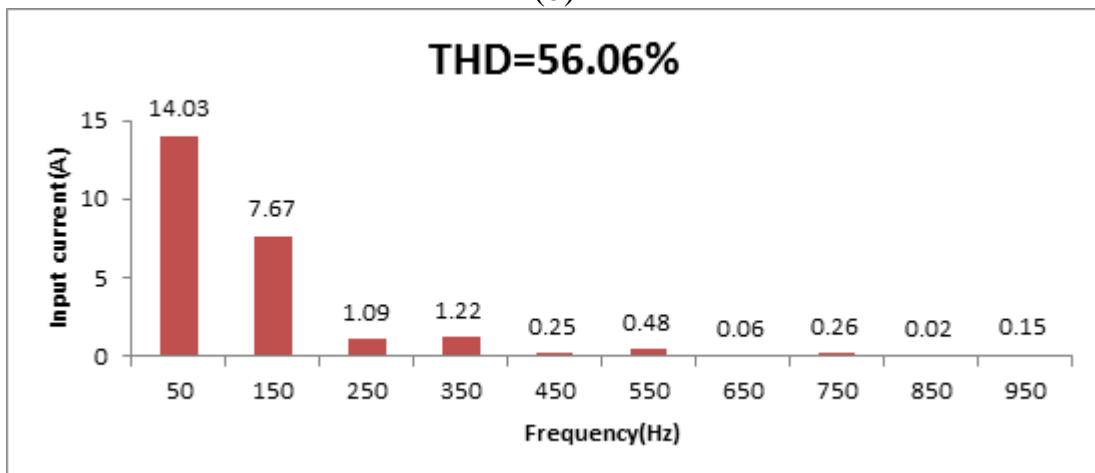
Table 4.18 shows the frequency spectrum of the input current with various firing angle for controlled single phase full wave bridge rectifier with third order high pass T-filter.



(a)



(b)



(c)

Figure 4.57: Frequency spectrum of the input current for controlled single phase full wave bridge rectifier with RL- load and third order high pass T- filter (a) at $\alpha=30^\circ$, (b) at $\alpha=90^\circ$, (c) at $\alpha=120^\circ$.

Fig.(4.57) shows the frequency spectrum of the input current produced during the rectification process in function of the firing angle. THD of the input current is undervalued which is less than 5% at small firing angle which is 30° . Good harmonic treating performance could be obtained when keeping the input current at high level and improving both the power factor and efficiency. However, as shown in Fig.(4.58) as the firing angle increases, the THD of the input current increases highly while the peak of the input current is reduced. For achieving the best results, the third harmonic needed to be reduced as it has relatively a large value.

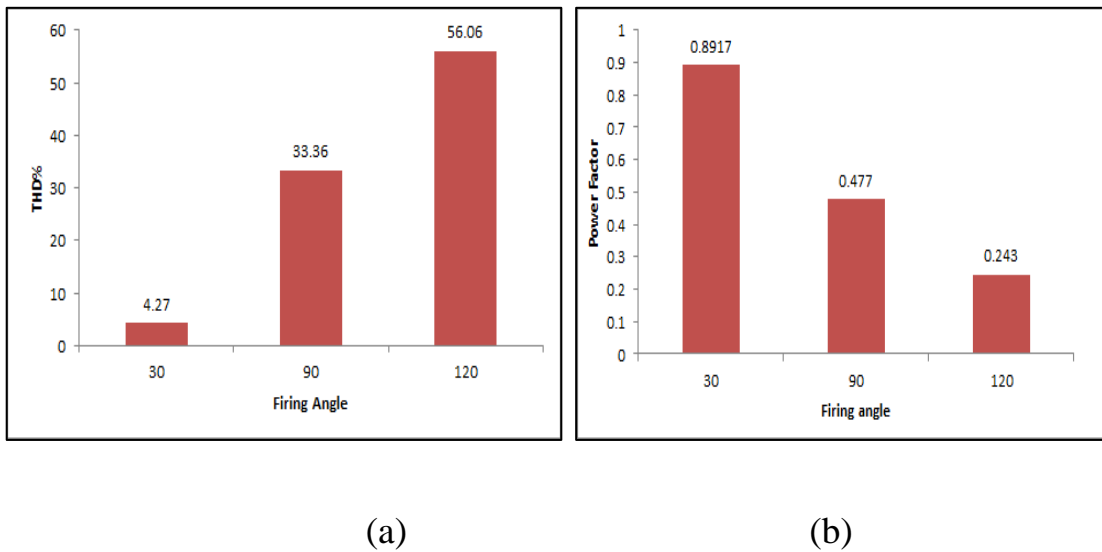


Figure 4.58: (a) THD of input current (b) power factor for controlled single phase full wave bridge rectifier with RL-load and third order high pass T-filter at $\alpha=30^\circ, 90^\circ, 120^\circ$.

4.6.2 Determination of the circuit parameters

From equ.(2.3), the following result for the R.M.S value of the input current is obtained:

$$I_{\text{prms}} = \left[\left(\frac{60.98}{\sqrt{2}} \right)^2 + \left(\frac{1.99}{\sqrt{2}} \right)^2 + \left(\frac{1.14}{\sqrt{2}} \right)^2 + \left(\frac{.78}{\sqrt{2}} \right)^2 + \left(\frac{.58}{\sqrt{2}} \right)^2 + \left(\frac{.45}{\sqrt{2}} \right)^2 + \left(\frac{.36}{\sqrt{2}} \right)^2 + \right. \\ \left. \left(\frac{.29}{\sqrt{2}} \right)^2 + \left(\frac{.24}{\sqrt{2}} \right)^2 + \left(\frac{.19}{\sqrt{2}} \right)^2 + \left(\frac{.17}{\sqrt{2}} \right)^2 + \left(\frac{.14}{\sqrt{2}} \right)^2 + \left(\frac{.1}{\sqrt{2}} \right)^2 + \left(\frac{.1}{\sqrt{2}} \right)^2 + \left(\frac{.07}{\sqrt{2}} \right)^2 + \right. \\ \left. \left(\frac{.07}{\sqrt{2}} \right)^2 + \left(\frac{.04}{\sqrt{2}} \right)^2 + \left(\frac{.04}{\sqrt{2}} \right)^2 + \left(\frac{.02}{\sqrt{2}} \right)^2 + \left(\frac{.02}{\sqrt{2}} \right)^2 + \left(\frac{.02}{\sqrt{2}} \right)^2 + \left(\frac{0}{\sqrt{2}} \right)^2 + \left(\frac{.01}{\sqrt{2}} \right)^2 + \right. \\ \left. \left(\frac{.01}{\sqrt{2}} \right)^2 + \left(\frac{.01}{\sqrt{2}} \right)^2 \right]^{\frac{1}{2}} \\ = 43.15 \text{ A}$$

Using third order high pass filter, the peak current is equals 61.03A and it equals 57.48 A by using the second order high pass filter.

From equ. (2.5):

$$\text{THD} = \sqrt{\left(\frac{43.15}{43.12} \right)^2 - 1} = 3.73\%$$

From the FFT analysis THD of the input current is equal 4.28% and the theoretical value obtained from the equ.(2.5) is 3.73%. In conclusion, there is little difference between the two values, but these two values are still smaller than the value obtained using second order high pass filter under the same conditions.

Ideally the input current should be sinusoidal and in phase with the input voltage .In this way a unity power factor is achieved. In this case, the phase angle is -26.8° while it was -32.6° in the previous configuration.

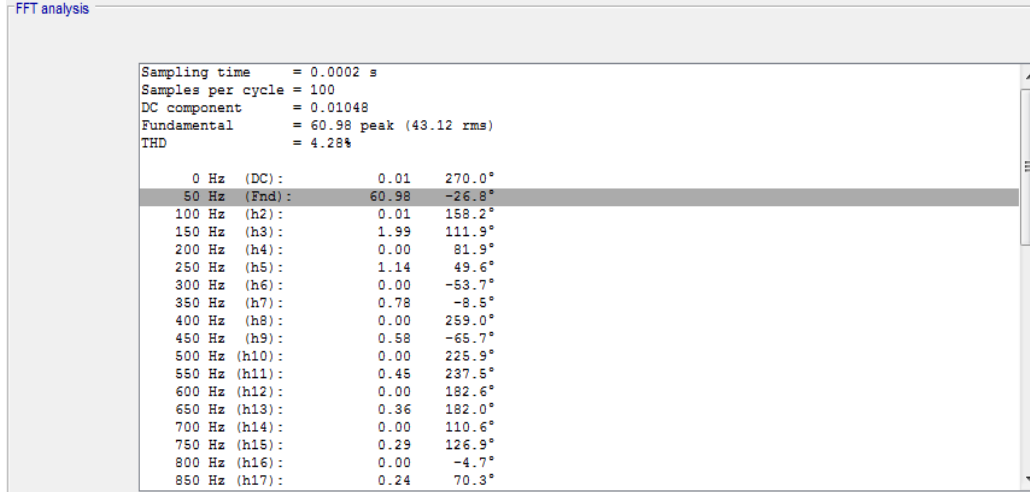


Figure 4.59: FFT analysis results of the input current for controlled single phase full wave bridge rectifier with RL- load and third order high pass T- filter at $\alpha=30^\circ$.

From the above simulation results, we obtain:

$$I_{\text{prms}} = \frac{60.98}{\sqrt{2}} = 43.11 \text{ A}$$

According to equ. (4.1,4.2):

$$X_{L_2} = 2 * \pi * f * L_2 = 2 * \pi * 50 * .06 = 18.84 \Omega$$

$$Q_{L_2} = (15.7)^2 * 18.84 = 4643.8 \text{ kVAr}$$

From equ. (4.6,4.7):

$$Q_{C1} = (54.97)^2 * 1.885 = 5695.9 \text{ kVAr}$$

$$Q_{C2} = (43.12)^2 * 1.885 = 3504.8 \text{ kVAr}$$

From equ. (2.6), the power factor is:

$$PF = \frac{43.12}{43.15} * \cos(-26.8) = 0.891$$

Comparing the power factor of this configuration with the corresponding factor of the second order high pass filter, it is clear that the power factor has been improved by third order high pass T-filter.

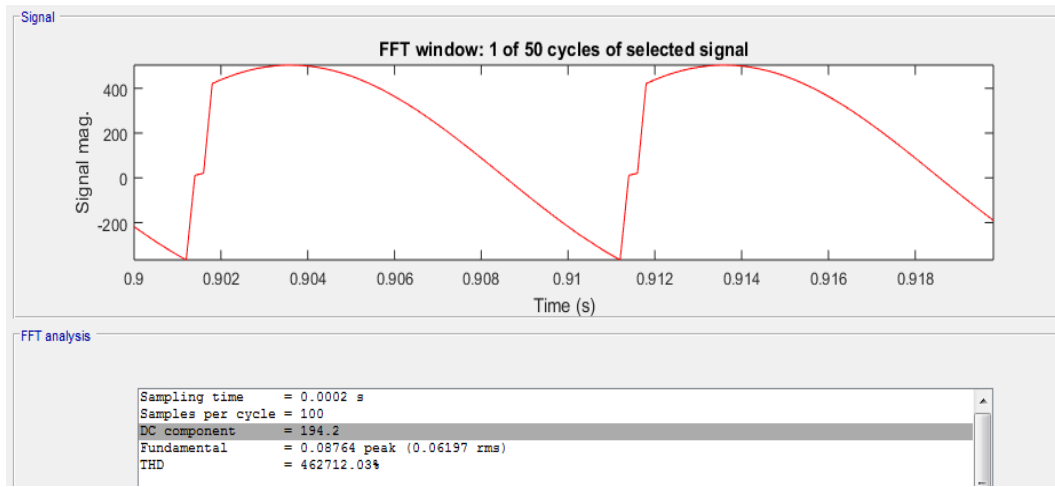


Figure 4.60: Output voltage waveform for controlled single phase full wave bridge rectifier with RL- load and third order high pass T- filter at $\alpha=30^\circ$.

From the above FFT analysis we obtain an average output voltage $V_{dc} = 194.2$ V by using third order high pass T- filter

The average output current is high and can be obtained by equ.(2.9)

$$I_{dc} = \frac{194.2}{5} = 38.84 \text{ A}$$

According to simulation results in Fig.(4.61) the value of this current is 38.07A.

Since the output voltage maintained at high level for both second and third high pass filter, the output current also maintained high.

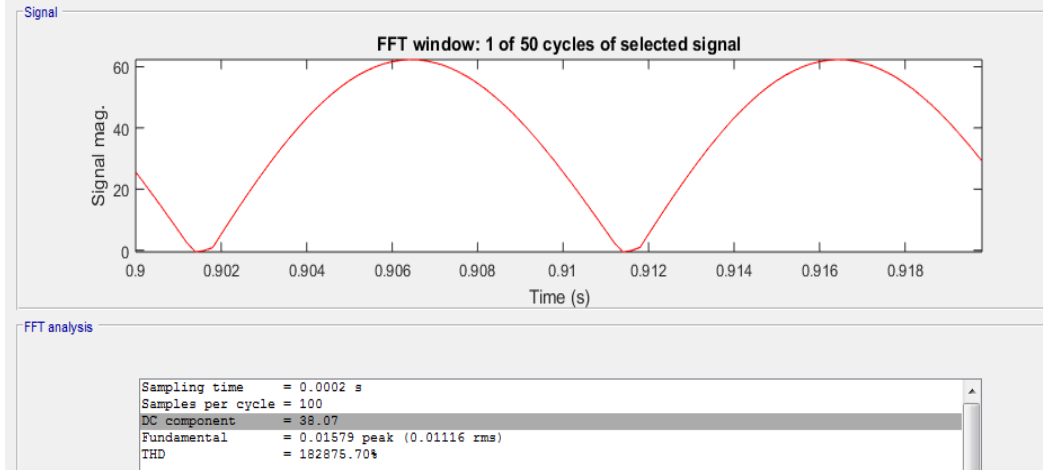


Figure 4.61: Output current waveform for controlled Single phase full wave bridge rectifier with RL-load and third order high pass T-filter at $\alpha=30^\circ$.

4.6.3 Efficiency

The same previous procedure is used to calculate the efficiency:

$$P_{dc} = 194.2 * 38.07 = 7393 \text{ W}$$

$$P_{ac} = 220 * 43.15 = 9493 \text{ W}$$

$$\eta = \frac{7393}{9458} * 100\% = 77.87\%$$

Comparing the efficiency for different configurations, the efficiency of using third order high pass T-filter is better than the efficiency of other configurations, but it is still less than the efficiency for the topology of second order high pass filter.

4.6.4 Representation in decibel form (dB)

Fig.(4.62) shows the frequency spectrum in (dB) for the input current of controlled single phase full wave bridge rectifier with third order high pass T- filter.

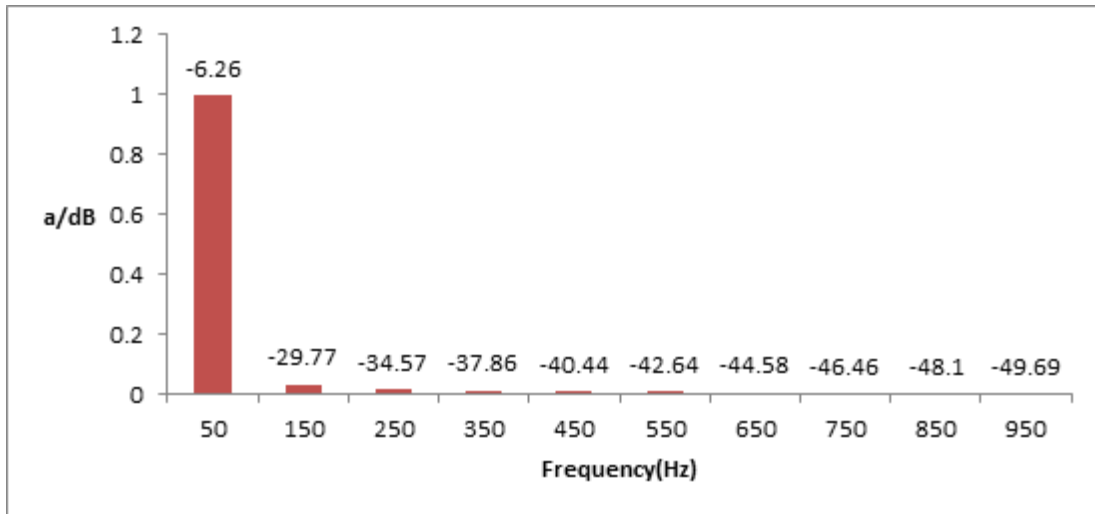
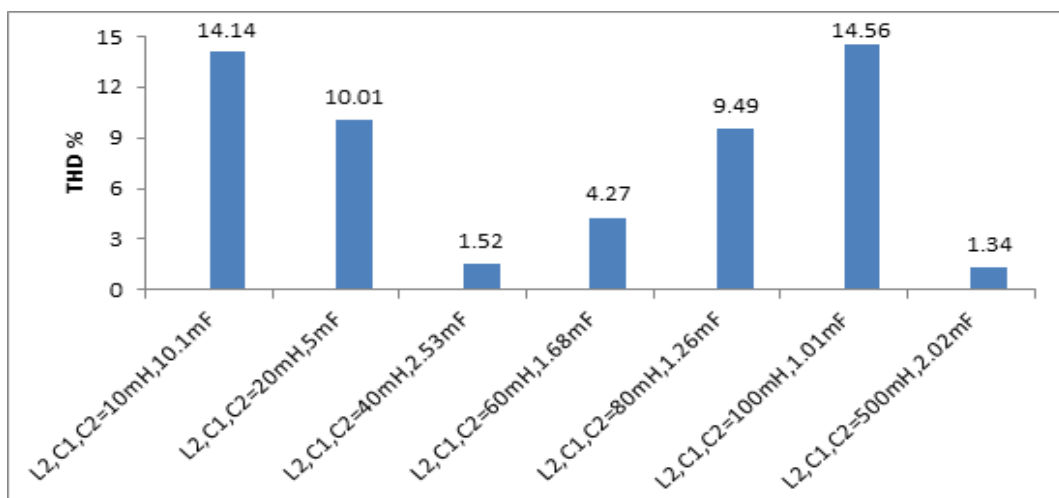
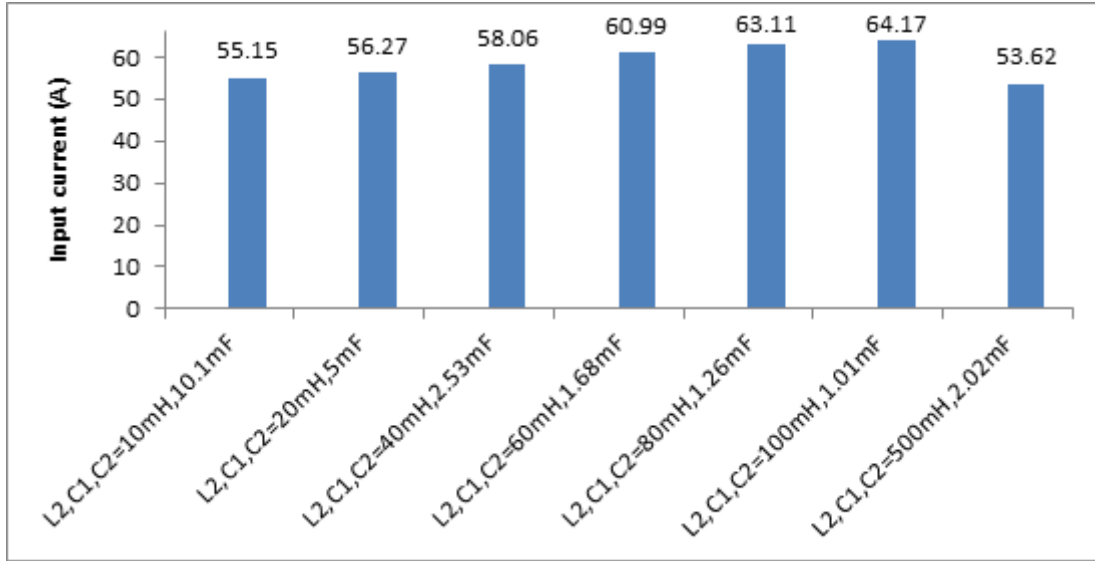


Figure 4.62: Frequency spectrum of input current spectrum in dB for controlled single phase full wave bridge rectifier with RL- load and third order high pass T- filter at $\alpha=30$.

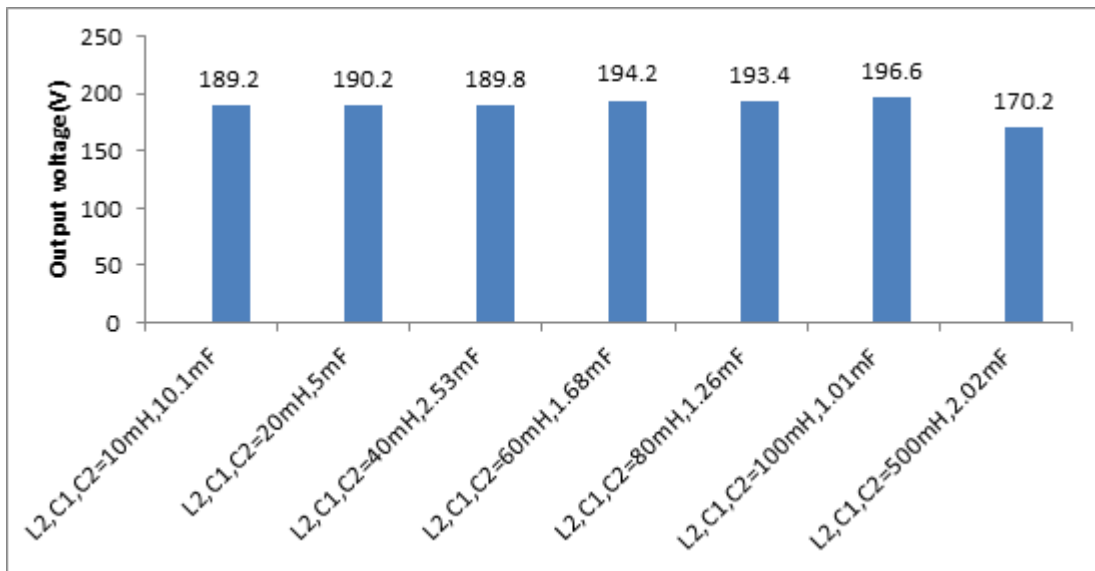
4.6.5 Comparison between the obtained results.



(a)



(b)



(c)

Figure 4.63: (a)THD of input current (b) input current (c) output voltage for controlled single phase full wave bridge rectifier with RL- load and various third order high pass T-filter values at $\alpha=30^\circ$.

If the values of the filter parameters increase, the THD of the input current will automatically fall down as shown in Fig.(4.63,a). The values of the output voltage are very high and nearly constant which means that

there is small voltage drop across the third order high pass T- filter. This is the reason why the output current has maintained its value to be high, as shown in the Fig.(4.63,c).

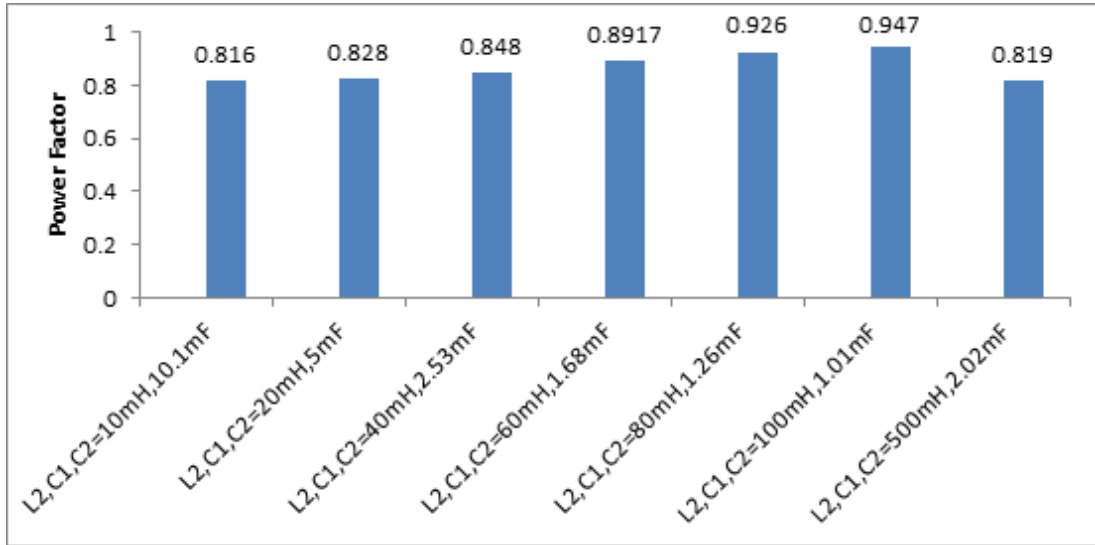


Figure 4.64: Power factor for controlled single phase full wave bridge rectifier with RL-load and various third order high pass T- filter values at $\alpha=30^\circ$.

By selecting the components of the filter, the power factor can be improved to achieve a maximum value of 0.94 that can be obtained by choosing: $L=100\text{ mH}$, $C_1, C_2 = 1.01\text{ mF}$.

4.6.6 Reactive power

Table 4.19: Examples of calculated reactive power for different values of third order high pass T- filter.

C_1 [μF]	L_1 [mH]	C_3 [μF]	I_{prms} C_1	I_{prms} L_1	I_{prms} C_3	X_C [Ω]	X_L [Ω]	X_C [Ω]
10100	10	10100	108.3	80.24	39	0.3151	3.14	0.3151
5000	20	5000	73.27	41.48	39.79	0.6328	6.283	0.6328
2530	40	2530	58.25	22.17	41.05	1.2581	12.566	1.2581
1680	60	1680	59.97	15.7	43.12	1.89	18.849	1.89
2020	500	2020	39.01	1.637	37.92	1.57079	157.079	1.57079
Q_C [kVAr]	Q_L [kVAr]		Q_C [kVAr]		Q_{total} [kVAr]			
3.695	20.216		.479		24.39			
3.397	10.810		1.001		15.208			
4.268	6.176		2.120		12.564			
6.797	4.646		3.514		14.957			
2.390	.420		2.258		5.098			

As shown in Table 4.19, the total reactive power has been increased in comparison with the previous configurations, which will increase the cost.

4.7 Third Order High Pass π - Filter

In this case, the third order high pass π -filter is employed with controlled single phase full wave bridge rectifier supplying R-L load. This model is shown in the Fig.(4.65).

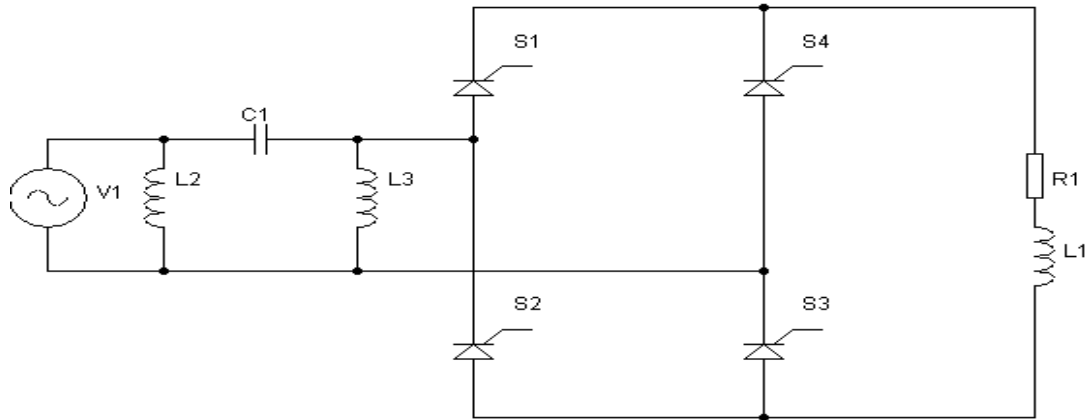


Figure 4.65: Simplified schematic of controlled single phase full wave bridge rectifier with RL- load and third order high pass π - filter.

The obtained results from this configuration are similar to those in the second order high pass filter in condition of using the same parameter values of filter configuration, only the reactive power in both cases are not similar because third order high pass π - filter has three elements.

4.7.1 Reactive power

Table 4.20: Examples of calculated reactive power for different values of third order high pass π -filter.

L_1 [mH]	C_1 [μ F]	L_3 [mH]	I_{prms} L_1 [A]	I_{prms} C_1 [A]	I_{prms} L_3 [A]	X_L [Ω]	X_C [Ω]	X_L [Ω]
10	10100	10	69.96	108.1	80.26	3.14	0.3151	3.14
20	5000	20	34.98	72.78	41.48	6.283	0.6328	6.283
40	2530	40	17.49	57.37	22.19	12.566	1.2581	12.566
60	1680	60	11.66	53.2	15.85	18.849	1.89	18.849
500	2020	500	1.399	37.58	1.645	157.079	1.57079	157.079
Q_L [kVAr]			Q_C [kVAr]			Q_L [kVAr]	Q_{total} [kVAr]	
15.368			3.682			20.226	39.276	
7.687			3.351			10.810	21.848	
3.843			4.140			6.187	14.17	
2.562			5.349			4.735	12.646	
0.307			2.218			0.425	2.95	

From the tabulated results, the values of the total installed reactive power are in the middle of the range which corresponds to a reasonable cost. In all these resonant filter designs, the selectivity depends greatly upon the “purity” of the inductance and capacitance used. If there is any stray resistance (especially likely in the inductor), this will diminish the filter’s ability to finely discriminate frequencies, as well as introduce anti-resonant effects that will skew the peak/notch frequency [54].

4.8 Conclusion

Table 4.21 reveals the results of the simulated passive filter configurations. The effectiveness of the study will help the researchers to choose the proper configuration from other passive power filter configurations.

Table 4.21: Comparison between the results obtained from the various analyzed filter circuits.

Type of Configuration	I_{rms} [A]	I_{rms1} [A]	V_{dc}	I_{dc}	ϕ	$\cos(\phi)$
Without filter	34.83	34.28	168.7	33.4	-35.2°	.817
L-filter ($L_2=60\text{mH}$)	9.728	9.722	47.25	9.513	-76°	.241
Series input resonance ($L_2, C_1=60\text{mH}, 168\mu\text{F}$)	32.19	32.18	150.2	29.73	-41.8°	.745
Parallel input resonance ($L_2, C_1=60\text{mH}, 1.68\text{mF}$)	36.55	36.5	171.2	33.65	-32.6°	.842
Parallel LC-filter in series with inductor L ($L_2, C_1=60\text{mH}, 1.68\text{mF}$) with series($L_3=60\text{mH}$)	10.69	10.684	52.6	10.46	-74.6°	.265
Second order high pass ($L_2, C_1=60\text{mH}, 1.68\text{mF}$)	40.649	40.595	190.4	37.42	-32.6°	0.842
Third order high pass-T ($L_2, C_1, C_2=60\text{mH}, 1.68\text{mF}$)	43.158	43.119	194.2	38.07	-26.8°	0.892
Third order high pass- π ($L_2, L_3, C_1=60\text{mH}, 1.68\text{mF}$)	40.641	40.587	190.4	37.41	-32.6°	0.842

In order to compare different topologies of the passive filter, it is also important to take into consideration some parameters that related to different topologies, such as: distortion factor, ripple factor, form factor, transformer utilization factor and finally reactive power shown in Table 4.22

4.8.1 Performance parameters

Before starting to examine different topologies for controlled single phase full wave bridge rectifiers, we should define some parameters which are included in appendix [B]. These parameters are required to compare performances among different structures of the passive filter.

Table 4.22: The performance parameters of controlled full wave rectifier with RL- load and different input LC- filter topologies at a firing angle of $\alpha=30^\circ$.

Type of Configuration	PF	THD	η	RF	FF	TUF	Q
Without Filter	.804	18.04	73.53	0.83	1.304	0.73	-
L-Filter ($L_2=60\text{mH}$)	.241	3.37	20.98	4.54	4.65	0.21	1.78
Series input resonance ($L_2, C_1=60\text{mH}, 1.68\mu\text{F}$)	.745	2.52	63.05	1.06	1.46	.63	39.053
Parallel input resonance ($L_2, C_1=60\text{mH}, 1.68\text{mF}$)	.841	5.13	71.35	0.79	1.28	0.71	3.3436
parallel LC-filter in series with inductor L ($L_2, C_1=60\text{mH}, 1.68\text{mF}$) with series($L_3=60\text{mH}$)	.265	3.41	23.39	4.05	4.18	0.23	2.438
Second order high pass ($L_2, C_1=60\text{mH}, 1.68\text{mF}$)	.841	5.17	79.66	0.56	1.15	0.8	10.086
Third order high pass -T ($L_2, C_1, C_2=60\text{mH}, 1.68\text{mF}$)	0.8917	4.27	77.87	0.52	1.13	0.77	14.957
Third order high pass- π ($L_2, L_3, C_1=60\text{mH}, 1.68\text{mF}$)	0.841	5.15	79.66	0.56	1.15	0.8	12.646

4.8.2 Proper selection of filter configuration

The simulation results fall in the area of controlled single phase full wave bridge rectifier, that contain seven different filter configurations, which are tabulated in Table 4.22. From the table and after inspecting the results, it can be now concluded that the third order high pass T-filter, the second order high pass, the third order high pass π -filter, the parallel resonance filter arrangement are desirable to produce the best results in terms of important parameters as small THD, high power factor and maximum efficiency in comparison with the other configuration. In addition harmonic values are undervalued with the allowable harmonic limits, the output voltage is maintained at high value for all the values and as well as the input current is kept high.

The Third Order High Pass T- Filter

The advantages of this filter are as follows:

- High average DC output voltage (194.2 V).
- The phase angle between the input voltage and the current $\phi_{i,v}$ is reduced to small value (-26.8°).
- Significant improvement in the power factor reaches to (0.891).
- Efficient circuit for input current wave form as the THD is low (4.27%).
- Increased rms current rating (43.158A).

The disadvantages of this filter are:

- Poor efficiency of the converter and that needs to be improved to (77.78%).
- Moderate installed reactive power (14.957 kVAr)
- Moderate cost that related to reactive power.

Second Order High Pass and Third Order High Pass π - Filter

In this work, the second order high pass and third order high pass filters are considered to provide similar results. The advantages of both topologies over the conventional method are:

- Provide high value the output voltage (190.4 V)
- Small phase angle between both input current and voltage $\phi_{i,v}$ (-32.6°)
- Give better PF on the input which equals (0.841).
- The most efficient configurations, where the efficiency for both filters reach to (79.66%).
- Increased rms current rating (40.649A).

The disadvantages of these filters are:

- Moderate reactive power installed (10.086 -12.646 kVAr).
- Moderate cost that related to installed reactive power.

The remained topology is **Parallel Resonance Filter** which has the following advantages:

- Provides high output voltage equals (171.2 V).
- Increased rms current rating (33.65 A).
- Small phase angle between both input current and voltage $\phi_{i,v}$ (-32.6°)
- Gives good PF at the input which equals (0.842).
- Small amount of installed reactive power (3.3436kVAr).
- Cheap, since the cost is associated with the installed reactive power.

The disadvantages of this filter are:

- High THD relatively, the peak input current remains at highest value approximately. THD needed to be reduced to (5.13%) or even less.
- Moderate efficiency of the filter amounting to (71.35%).

On the contrary rectifier **without Input Filter**, the THD of rectifier is (18.04%) with little rippled output voltage. To obtain pure AC input current, we should use large **Series Inductor Filter** which is inserted at the input that has the following advantages:

- THD reduces to (3.37%).
- Small installed reactive power (1.78 kVAr).

- Low cost.

The disadvantages of this L-filter are:

- Minimize the rms input current to (9.728 A).
- Enlarge the phase angle between current and voltage (-76°).
- Reduce the output voltage to (47.25 V).
- Very poor efficiency is mounting to (20.98%).

To raise the value of the input current and to overcome the pervious filter problem, we should insert **Series Capacitor with Inductor** at the input-side of the rectifier. This filter has the following advantages:

- Minimizes THD of input current to (2.52%).
- Remains the peak input current at high value. (32.19 A)
- There is small drop voltage across the filter resulting in high average output voltage of (150.3 V).

The disadvantages of this filter are:

- Increase the phase angle between current and voltage (-41.8°)
- Poor power factor is (0.745)
- Poor efficiency is (63.05%).
- Large amount of the reactive power (39.053 kVAr).

- High cost resulted from the large installed reactive power.

Parallel LC-filter in series with inductor L configuration.

This filter has the following advantages:

- Reduce the THD (3.41%).
- Small amount of installed reactive power (2.438 kVAr).
- Cheap, since the cost associated with the installed reactive power

The disadvantages of this filter are:

- Minimize the rms input current to (10.69 A)
- Increase the phase angle $\phi_{i,v}$ (-74.6°).
- Create large drop voltage, the distorted average of DC output voltage decreases to (52.6 V)
- The efficiency is very poor (23.39%)

4.8.3 The Summarized comparative results

The following numbers represent the values on X-axis representing the type of filter presented in Fig.(4.66 - 4.69)

1: Third order high pass T-filter

2: Second order high pass filter

3: Third order high pass π -filter

4: Parallel input resonance filter

5: Without filter

6: Series input resonance filter

7: Parallel LC-filter in series with inductor L-filter

8: L- filter

Fig.(4.66) shows the variation of the input displacement factor for the various passive filter topologies.

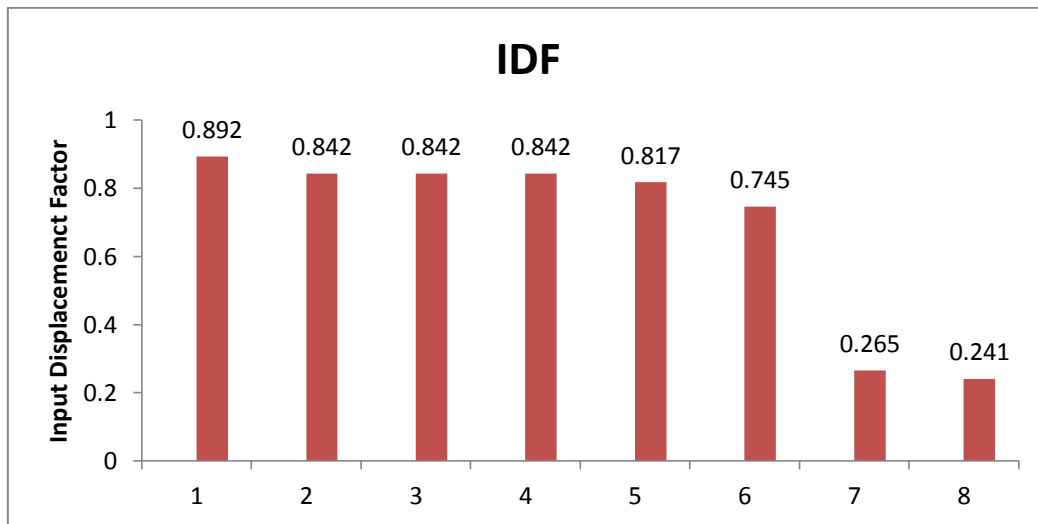


Figure 4.66: Variation of IDF for various input passive filter topologies.

The input displacement factor (IDF) is very important factor to determine the power factor, ideally its value should be close to one. The third order high pass T- filter configuration has value close to one.

Fig.(4.67) shows the variation of power factor for various input passive filter topologies.

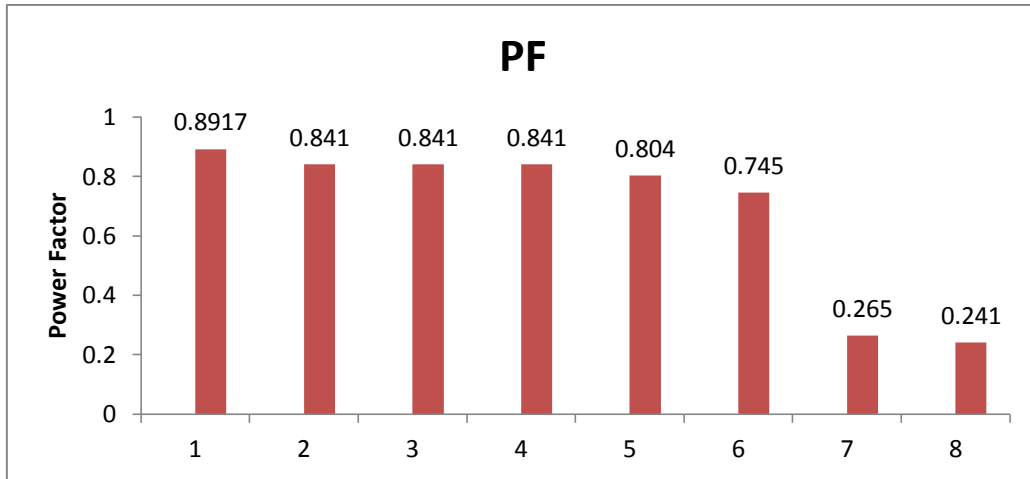


Figure 4.67: Variation of PF for various input passive filter topologies.

Power factor should be unity, but there is inability to achieve unity power factor by using various passive filter configurations, so it should be closed to one. For controlled single phase full wave rectifier circuit with the third order high pass T-filter, its value is (0.89) which is the best among all the topologies.

Fig.(4.68) shows the variation of the total harmonic distortion for various passive filter topologies.

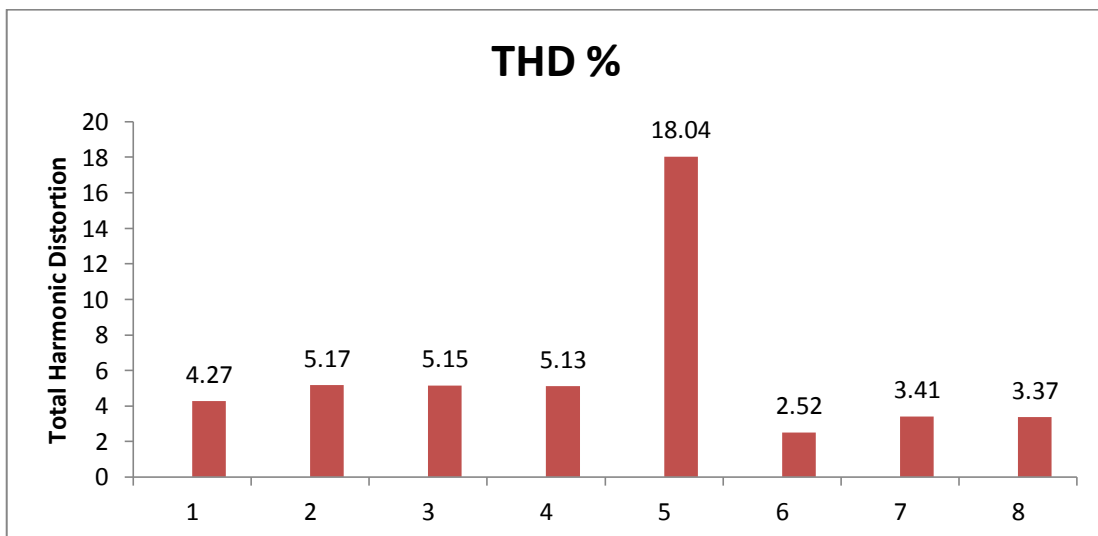


Figure 4.68: Variation of THD for various input passive filter topologies.

The value of THD should be zero. It is difficult to achieve zero value so it is tried to achieve minimum value of $\text{THD} < 5\%$. For controlled single phase full wave rectifier circuit with the third order high pass T-filter, THD is (4.27).

Fig.(4.69) shows the variation of efficiency for various passive filter topologies.

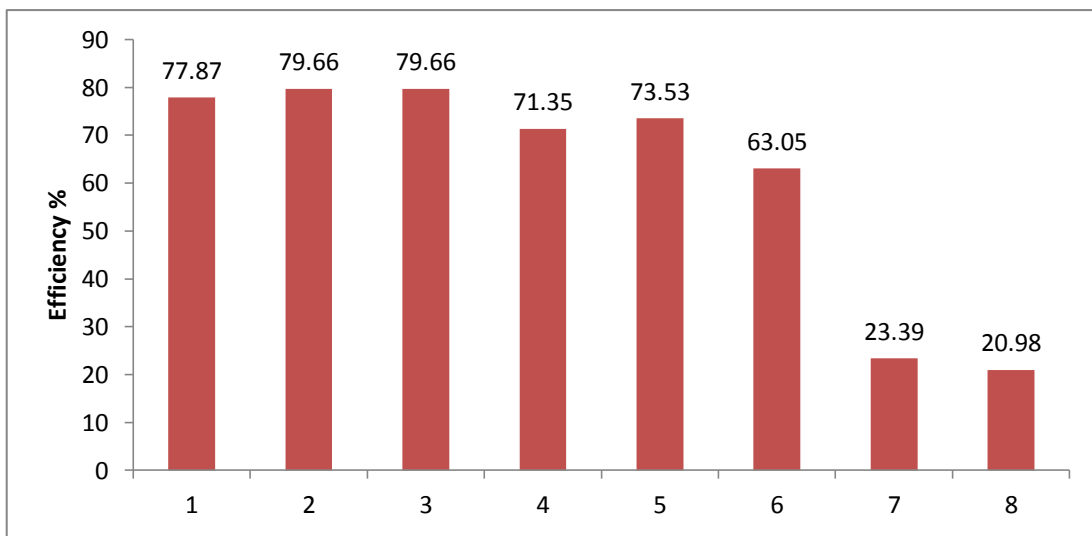


Figure 4.69: Variation of efficiency for various input passive filter topologies.

Ideally the value of the efficiency should be about 100%, it is difficult to achieve this value, and it was possible to achieve which is 79.66%. This is achieved by two filter configurations, second order high pass filter and third order high pass π - filter.

Ideal rectifier should have:

- $\eta = 100\%$
- $V_{AC} = 0$

- $RF=0$
- $PF=1$
- $DPF=1$
- $THD=0$
- $TUF=1$

With reference to this ideal case, and according to all tabulated simulated values ,if we want to recognize whether the parameters are good or not , we should compare the results with this ideal rectifier to resolve if the filter configuration parameters are good or not.

Chapter Five

Conclusions and Future Work

5.1 Conclusions

- The investigation in this study has shown that there is good possibility to improve the grid quality parameters by LC-power filters.
- Seven types of LC-filters have been tested by simulation, each one of these filters has shown different quality parameters.
- If the highest weight is given to low THD one should select the LC series resonance filter because it has the lowest THD amounting to 2.52%. In case of the highest weight is given to the PF one should select the third order high pass T-filter because it has the highest PF amounting to 0.891. If the highest weight is given to efficiency then the third order high pass π -filter or second order high pass filter should be selected since they result the highest efficiency amounting to 79.66%. Otherwise the remaining filter have lower corresponding values, therefore one should select the most appropriate filter according to his specific demand.
- The insertion of the mentioned filters affect the average output voltage of the rectifier due to the voltage drop associated with each filter. It should be emphasized that the highest output voltage is achieved by the least voltage drop in the filter which can be a measure helping in selection of the appropriate filter. The investigation in this thesis has

shown that the highest output voltage is achieved by series resonance and the minimum output voltage was obtained by using of L-filter.

- It should be considered that each one of the mentioned filters is associated with definite installed reactive power which represents the total necessary cost of the filter.

5.2 Recommendations and Future Work

The study has achieved the goals presented in the first chapter; yet, it was limited in scope and efficiency was less focused on. The filters need to be improved. In fact, there are many ways for this to be developed and it still remains some work to be done. The following points present the topics that need further research work

- Research is still required to look for analytical filter designing methods because the parameters of passive filter in this study are selected by trial and error.
- An extensive analyzed calculation and large effort investigation can be offered to find solutions to determine the value of filter parameters and carefully tuned by different optimization techniques.
- Using an active filter along with passive filter as a hybrid filter, which can alleviate shortcomings of conventional passive filter to meet the increasingly strict power quality requirement of modern technology. Leading unity power factor would be considered as a good idea. One should take into consideration varying highly reduction in main

harmonics to meet the increasingly strict power quality requirements of the modern technology. Finally, efficiency may still be improved; therefore, the most importantly optimized cost has to be developed and research in this area is highly recommended.

- Extending this work by using three phase fully controlled rectifiers with passive filters in order to overcome any problem connected with those systems. (If single phase full wave bridge rectifiers with passive filters don't produce current distortion of less than 5%, three phase fully controlled rectifiers with passive filters should be investigated).
- Verifying the obtained simulation results through inspecting the outlined rectifier system experimentally in the laboratory where the various passive filter configurations should be realized through hardware components. For implementing of such work a special spectrum analyzer is very necessary.

References

- [1] Pyakuryal, Sudeep and Mohammad Matin. "*Filter design for ac to dc converter.*" **International Refereed Journal of Engineering and Science (IRJES)** 2.6 (2013): 42-49

- [2] Vasireddy, Santhosh Kumar and G. Munfar Ali. "**Parallel Power Flow AC/DC Converter with Input Power Factor Correction and Tight Output Voltage Regulation for Universal Voltage Applications.**"

- [3] Bhattacharya, Mahasweta. "*Improvement of Power Quality Using PWM Rectifiers.*" **International Journal of Scientific and Research Publications** 4.7 (2014).

- [4] Yusoh, Mat and Mohd Abdul Talib. "**Development of a single phase active power filter for rectifier load.**" (2013).

- [5] Soomro, D. M., M. A. Omran, and S. K. Alswed. "**Design of a Shunt Active Power Filter to Mitigate the Harmonics Caused by Nonlinear Loads.**" (2006).

- [6] Purushothaman, S. K. "**HARMONICS ELIMINATION USING FILTER DESIGN.**"

- [7] Dugan, Roger C., Mark F. McGranaghan, and H. Wayne Beaty. "**Electrical power systems quality.**" New York, NY: McGraw-Hill,| c1996 (1996).

- [8] Anooja, C. L. and N. Leena. ***"Passive Filter For Harmonic Mitigation Of Power Diode Rectifier And SCR Rectifier Fed Loads."*** **International Journal of Scientific & Engineering Research** 4.6 (2013).
- [9] Mikkili, Suresh and Anup Kumar Panda. **Power Quality Issues: Current Harmonics**. CRC Press, 2015.
- [10] Hussien, Z. F., N. Atan, and I. Z. Abidin. **"Shunt Active Power Filter for Harmonic Compensation of Nonlinear Loads"**. IEEE, 2003.V 117-20.
- [11] Narmadha, T .V. **"Position sensor less speed control of permanent magnet brushless DC motor. "** (2013).
- [12] Rajashekara, Kaushik, Ashoka KS Bhat, and Bimal K. Bose. **"30.1 Power Semiconductor Devices."** (2000).
- [13] Tella, Pranavi Chowdari. **"The study of single phase diode rectifiers with high power factor and low total harmonic distortion."** (2008).
- [14] **"Introduction to power electronics lectures. "**
- [15] Eltamaly, Ali Mohamed. **"Power Electronics. "**
- [16] Tella, Pranavi Chowdari. **The Study of Single Phase Diode Rectifiers With High Power Factor and Low Total Harmonic Distortion**. University of Missouri-Columbia, 2008.

- [17] Visintini, Roberto. **"Rectifiers."** (2006).
- [18] Ellis, Robert G. and P. Eng. **"Power system harmonics reference guide to causes, effects and corrective measures."** An Allen-Brandley Series of Issues and Answers-Rockwell Automation (2001): 3.
- [19] Shah, Nikunj. **"Harmonics in power systems causes, effects and control."** Whitepaper design engineering low-voltage drives ,(2013).
- [20] <http://www.danfoss.com/drive>.
- [21] McCarty, Michael, et al. **"Harmonic Analysis of Input Current of Single-Phase Controlled Bridge Rectifier"**. IEEE, 2009.V 520-24.
- [22] **"Power electronics for elektroda."** 2001.[online] available <https://www.researchgate.net/file.PostFileLoader.html?id>.
- [23] **"Power factor correction."** [online] available <http://download.21dianyuan.com/download.php?dir=bbs&id>
- [24] Hoseini, Seyed Mohsen, Seyed Mohammad Sadeghzadeh, and Yousef Alinejad Beromi. *"A new method for active power factor correction using a dual-purpose inverter in a flyback converter."* **Turkish Journal of Electrical Engineering & Computer Sciences** 24.6 (2016).
- [25] **"Fourier analysis of complex sounds."** [online] available [http:// www.physics.indiana.edu/~courses/p109/P109fa08/10.pdf](http://www.physics.indiana.edu/~courses/p109/P109fa08/10.pdf)

- [26] Sadiku, Alexander and Charles K. Alexander. **"Fundamentals of electric circuits."** International Edition, Mc Graw Hill (2009).
- [27] Shaikh,R.A.,Lashari,A.B.,&Ansari,I. " **Harmonics Analysis and Mitigation Using Passive Filters.** "2015.
- [28] Das, J. C. **Power System Harmonics and Passive Filter Designs.** John Wiley & Sons, 2015.
- [29] Rao, R. Kameswara and S. S. Tulasiram. *"Harmonic modeling of residential and commercial loads with unified power quality conditioner."* **International Journal of Scientific & Engineering Research** 3.6 (2012): 1-7.
- [30] Iada, Musa Yusup, Ismadi Bugis, and Md Hairul Nizam Talib. **"Simulation a Shunt Active Power Filter Using MATLAB/Simulink"**. IEEE, 2010.V 371-75.
- [31] Sharaf, A. M. and Pierre Kreidi. **"Power Quality Enhancement Using a Unified Switched Capacitor Compensator"**. IEEE, 2003.V 331-33.
- [32] Chapman, David. **"Harmonics: Causes and Effects Power Quality Application Guide."** Copper Development Association, European Copper Institute (ECI) (2001).

- [33] Yildiz, Ali Bekir and Ezgi Unverdi. **"Simplified Harmonic Model for Full Wave Diode Rectifier Circuits."** *Automatika – ÇAE Journal for Control, Measurement, Electronics, Computing and Communications* 55.4 (2014).
- [34] Shukla, Amit Kumar. **"Studies on Power Quality and, an LSE & PSOPC based Harmonic Estimation to Real Time Data."** (2009).
- [35] Peng, Fang Z. **"Harmonic sources and filtering approaches."** *IEEE industry applications magazine* 7.4 (2001): 18-25.
- [36] Pyakuryal, Sudeep K. **"Control of harmonics in 6-pulse rectifiers."** (2013) .
- [37] **"Harmonic Distortion of the AC Power Line."** [online] available <https://www.researchgate.net/file.PostFileLoader.html?id>
- [38] Dagur, Y., Gupta, M.k. **"Single Phase AC-DC Converter Employing Power Factor Correction with High Frequency Isolation Using Buck-Boost PWM Converter ."** 2015.
- [39] Kumar, Shankar, Byaktiranjana Pattanayak, and Ravi Shankar Singh. **"Power Electronics: Computer Simulation and Analysis."** (2009).
- [40] Zubi, Hazem. **"Low Pass Broadband Harmonic Filter Design."** *lucrarea de dizertație, Department of Electrical and Electronics Engineering-MIT* (2005).

- [41] Acha, E., et al. **"General Frame of Reference for Analysis of Harmonic Distortion in Systems With Multiple Transformer Nonlinearities"**. IET, 1989.V 271-78.
- [42] Rudnick, Hugh, Juan Dixon, and Luis Moran. **"Delivering clean and pure power."** IEEE Power and Energy Magazine 99.5 (2003): 32-40.
- [43] Kuphaldt, R. and Tony R. Kuphaldt. **"2 Lessons In Electric Circuits, Volume II AC."** (2007).
- [44] Van Wyk, J.D. "Power Quality, Power Electronics and Control".1993
- [45] Peng, Fang Zheng, Hirofumi Akagi, and Akira Nabae. **"A new approach to harmonic compensation in power systems-a combined system of shunt passive and series active filters."** IEEE Transactions on industry applications 26.6 (1990): 983-90.
- [46] Vijayakumar, K., & Srihari, J. **"Investigation of Harmonic Content and Power Factor Improvement for Single Phase AC-DC Converter Topologies."** 2015.
- [47] Abdullah, Mohamad Nazir. **"Design Of A Single Phase Unity Power Factor Switch Mode Power Supply (SMPS) With Active Power Factor Correction [TK7881. 15. N335 2008 f rb]."** (2008).

[48] Tella, Pranavi Chowdari. **"The study of single phase diode rectifiers with high power factor and low total harmonic distortion."** (2008).

[49] Maheswaran, D., N. Rajasekar, and L. Ashok kumar. *"Design of passive filters for reducing harmonic distortion and correcting power factor in two pulse rectifier systems using optimization."* **Journal of Theoretical & Applied Information Technology** 62.3 (2014).

[50] Chou, Chih Ju, et al. **"Optimal planning of large passive-harmonic-filters set at high voltage level."** *IEEE Transactions on Power Systems* 15.1 (2000): 433-41.

[51] Wheeler, Patrick W. **"A matrix converter for variable speed AC motor drives."** (1993).

[52] Salomaki, Janne, Marko Hinkkanen, and Jorma Luomi. **"Cost-Effective Design of Inverter Output Filters for AC Drives"**. *IEEE*, 2007.V 1220-26.

[53] Sleuz. **"Designing Low-cost ,Multiple Output DC/DC Converter part I"**.2014.

[54] **"Resonant Filters. "** [online] available

<https://www.allaboutcircuits.com/textbook/alternating-current/chpt-8/resonant-filters/>

- [55] Kazem, Hussein A., et al. **"Simple and Advanced Models for Calculating Single-Phase Diode Rectifier Line-Side Harmonics"**. Citeseer, 2005.V 179-83.
- [56] Shukla, Tejashree R. and Paresh J. Shah. **"Simulation of Single Phase Digital PWM Inverter with Boost PFC Technique."** *Int.j.eng.sci* 4.3 (2015): 45-50.
- [57] Ingale, Rajesh. **"Harmonic analysis using FFT and STFT."** *International Journal of Signal Processing, Image Processing and Pattern Recognition* 7.4 (2014): 345-62.
- [58] Paul, Robinson P., et al. **"Performance Comparision of Single & 3phase Controlled and Uncontrolled Rectifier Using Matlab-Simulink."** *International Journal of Computer Science and InformationTechnologies* 5.2 (2014): 2107-11.

Appendix A

MATLAB Design

MATLAB is one of different simulating software applications that have been used to simulate the power electronic circuits.

Simulation of Environment

Electrical engineers require simple, powerful, and accurate software program to simulate that work in simplified way as soon as possible. MATLAB provides a powerful simulation environment for power electronics so that it is considered as simulation software. MATLAB is specifically designed for them and it drives with fast simulation and friendly user interface.

Designers are able to save their spent time in searching about required tools because of this SIMULINK. It is used to offer fully design and implemented simulation with easy access to components.

Features and Benefits

Software allows very easy redesign of the schematic and thus faster “re-running”. This way leads us not to waste much time and keep the effort which will be spent compared to find new mathematical equations. Simulink is useful, powerful, precise, flexible and reliable software tool in hand of the modern circuit designer for obtaining the response and results of circuits by implementation of real devices [55]. Some features of MATLAB/SIMULINK:

- It allows multiple plots to be displayed simultaneously, such as voltage, current, etc.
- It contains full libraries of specific components. So the user may achieve realistic simulation results.
- It simply represents any electrical circuit, in particular power-electronic circuits.
- It makes flexibility to change parameter values and view voltages/currents during simulation.
- It is like having a virtual test bench running on user's computer [39].

Methodology

In this study, MATLAB/SIMULINK is used as useful tool to implement the rectifier circuit with different filter configurations.

Basically, there are two simulations: the first one is without passive filter while the second one is with connected input passive filter configuration.

MATLAB Design of the Circuit

MATLAB is a software program to implement any hardware circuit. There are many various blocks can be using to simulate any system that is used from SIMULINK then power library and FFT tool [56].

Fourier analysis is used to convert waveforms in time domain into their frequency components and vice versa. When the waveform is periodical,

the Fourier series can be used to calculate the magnitudes and phases of the fundamental and its harmonic components in good way. It's considered to be fast computation to estimate fundamental amplitude and its harmonics with reasonable approximation. On the contrary, it does not perform well for sudden or fast changes in waveform

FFT spectrum distinguishes the harmonic components (odd and even harmonic component) and other waveform distortion components as DC offset [57].

THD analysis can be measured by FFT analysis method, the input /output waveform can be display on the scope.

MATLAB-Simulink for Power Electronics

Sim Power Systems contains libraries which offer components and tools for modeling and simulating electrical power systems. These libraries provide models of electrical power components. The electrical power components include various machines, electric drives, control and measurement for application [14].

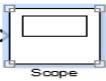


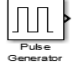
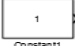
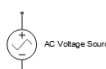




Sim Power Systems contains application libraries, Electrical Sources (Contains blocks that generate electric signals for single phase and three phases), Elements (Contains linear and nonlinear circuit elements such as R- L- C load.), Extra Library (Contains three-phase blocks and specialized measurement and control blocks, machines (Contains power machinery models.), measurements (Contains blocks for the current and

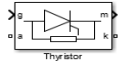
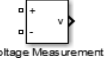

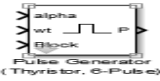

voltage measurements.), Power Electronics (Contains power electronics devices). And powerful libraries (used to decide supply; i.e. continues or discrete), the powerful libraries are used to design and stimulate different examples of power electronics circuits. One of these examples which use various library blocks is AC/DC controlled rectifier using thyristors [58].

The proposed rectifier system is single phase controlled full wave rectifier constructed in using MATLAB/SIMULINK tools and it was simulated to achieve the performance characteristics.

The elements which are used in the simulated prototypes that are designed for the controlled single phase full wave bridge rectifier with R- L Load , their symbols and libraries browser. All of these are tabulated in Table A.1.

Table A.1: The elements are used for passive filtering methods with rectifier circuit.

Simulink Library Browser	Block	Symbol Description
Simulink /Sink	Scope	
Simulink /Sink	Terminator	
Simulink /Signal routing	Mux	
Simulink /Source	Pulse Generator	
Simulink /Source	Constant	
Simscape/foundation library/Electrical/Electrical source	Ac Voltage Source	
Simscape/foundation library/Electrical/Electrical Element	Electrical Reference	
Simscape/SimPowerSystem/Specialized Technology/Fundamental Blocks	Powergui	
Simscape/SimPowerSystem/SpecializedTechnology/FundamentalBlocks/Element	Series RLC Branch	
Simscape/SimPowerSystem/SpecializedTechnology/FundamentalBlocks/PowerElectronic	Diode	

Simscape/SimPowerSystem/SpecializedTechnology/FundamentalBlocks/PowerElectronic	Thyristor	
Simscape/SimPowerSystem/SpecializedTechnology/FundamentalBlocks/Measurements	Voltage Measurement	
Simscape/SimPowerSystem/SpecializedTechnology/FundamentalBlocks/Measurements	Current Measurement	
Simscape/SimPowerSystem/SpecializedTechnology/Control&Measurement/pulse&Signal Generator	Pulse Generator(6-pulses)	
Simscape/SimPowerSystem/SpecializedTechnology/Control&Measurement/PLL	PLL	

1. Pulse Generator

Generate square wave pulses at regular intervals.

2. Pulse Generator(6-pulses)

The Pulse Generator (Thyristors) block generates two pulse trains. This block is controlled by alpha angle reference signal and synchronization signal ωt . The ωt signal is an angle varying between (0 and 2π) radians, it is synchronized on zero crossings of the fundamental (positive-sequence) of phase A of the primary voltage of the converter transformer. The ωt signal is normally obtained from a phase locked loop (PLL) system. It should be set in accordance with the following blocks as follows:

3. PLL

Determine frequency and fundamental component of signal phase angle. PLL block models are Phase Lock Loop (PLL) closed-loop control system, which track the frequency and phase of a sinusoidal signal by using an internal frequency oscillator. The control system adjusts the internal oscillator frequency to keep the phase's difference to 0.

4. Constant

The Constant block generates real or complex constant value.

5. AC Voltage Source

The AC voltage source is the supply voltage which supplies an AC voltage of 220V rms.

6. Thyristor

The thyristor is a semiconductor device that can be turned on via a gate signal.

7. Scope

Display signals generated during simulation with respect to simulation time.

8. Electrical Reference

The Electrical Reference block represents an electrical ground.

9. Series RLC Branch

The Series RLC Branch is block implements of single resistor, inductor, capacitor, or series combination of these. Use the Branch type parameter to select elements you want to include in the branch. A series R-L branch is used as output impedance with $R = 5\Omega$ and Inductance $= 0.018\text{mH}$ and it uses in selecting parameter of the passive filters with various configuration.

10. Current Measurement Block

Measures the instantaneous current between two electric nodes that flow through circuit, It has 3 terminals. First, (+) port which is kept in the side through which current enters the block. Second, (-) port through which the current exits the block. Another port named 'i' is connected to the scope which shows the measured current. The current measurement block must be connected in series with the circuit in the path where the current has to be measured [3].

11. Voltage Measurement Block

Measures the instantaneous voltage between two electric nodes. It has again 3 terminals. (+) port which is connected to the positive part of the circuit and (-) port which is connected to the negative part of the circuit.

The other port 'v' is connected to the scope which displays the measured voltage curve. The voltage measurement block must be connected to the circuit in parallel where the voltage has to be measured [3].

12.Mux

Combine several input signals into vector

13.Powergui Block

The Powergui block is necessary for simulation any Simulink model that contains SimPowerSystems blocks. This block is used to store the equivalent Simulink circuit that represents the state-space equations of the model. The Powergui block allows the users to choose one of the following methods to solve their circuit:

- Continuous method, which uses a variable step Simulink solver.
- Ideal switching continuous method.
- Discretization of the electrical system for a solution at fixed time steps.
- Phasor solution method [3].

Appendix B

Performance Parameters

Referring to Table 2.3 and assuming ideal switches and an inductive - resistive load, it is possible to calculate the expressions for the performance parameters of a single phase fully controlled bridge.

The R.M.S output voltage is equal to the R.M.S input supply voltage and is given by:

$$V_{\text{rms}} = \sqrt{\frac{1}{2\pi} \int_{\alpha}^{\alpha+2\pi} (\sqrt{2}V)^2 \sin^2 \omega t d\omega t} = V$$

B.1

The AC in the output voltage is:

$$V_{\text{ac}} = \sqrt{V_{\text{rms}}^2 - V_{\text{dc}}^2}$$

B.2

The load voltage form factor (ripple factor), is:

$$FF_V = \frac{V_{\text{rms}}}{V_{\text{dc}}} = \frac{\pi}{2\sqrt{2}\cos\alpha}$$

B.3

The harmonic factor or voltage ripple factor for the output voltage is:

$$RF_V = \frac{\sqrt{V_{\text{rms}}^2 - V_{\text{dc}}^2}}{V_{\text{dc}}} = \sqrt{\left(\frac{V_{\text{rms}}}{V_{\text{dc}}}\right)^2 - 1} = \left[\frac{\pi^2}{8} - \cos^2\alpha\right]^{\frac{1}{2}} = \sqrt{FF^2 - 1}$$

B.4

The transformer utilization factor (TUF) is:

$$\text{TUF} = \frac{P_{dc}}{(VA)_s}$$

B.5

Sample calculation:

In chapter 4 , for the single phase fully controlled rectifier with L-filter the simulation result reveals that the input current is (9.728) A ,fundamental input current is (9.722) A , the output voltage is (47.25) V, the output current is (9.513) A , the phase angle between the 1st harmonic of the input current , the voltage is (-76°) and total harmonic distortion is (3.37%).

Referring to equ. (B.3)

$$\text{FF}_V = \frac{220}{47.25} = 4.65$$

Referring to equ. (B.4)

$$\text{RF}_V = \frac{\sqrt{220^2 - 47.25^2}}{47.25} = 4.54$$

Referring to equ. (B.5)

$$\text{TUF} = \frac{47.25 * 9.513}{220 * 9.728} = 0.21$$

جامعة النجاح الوطنية

كلية الدراسات العليا

تحسين معاملات الجودة للشبكة الكهربائية بإستعمال فلاتر LC عند تغذية محولات القدرة الإلكترونية

إعداد

أسماء شرعب

إشراف

أ.د. مروان محمود

قدمت هذه الأطروحة استكمالاً لمتطلبات الحصول على درجة الماجستير في هندسة القوى
الكهربائية، بكلية الدراسات العليا، في جامعة النجاح الوطنية، نابلس - فلسطين.

2018

ب

تحسين معاملات الجودة للشبكة الكهربائية باستعمال فلاتر LC عند تغذية محولات القدرة الإلكترونية

إعداد

أسماء شرعب

إشراف

أ.د. مروان محمود

الملخص

الحصول على جهد وتيار كهربائي مستمر (ثابت) من الشبكة الكهربائية تعتبر حاجة ضرورية للعديد من الاجهزة الكهربائية والتطبيقات المختلفة مثل شحن البطاريات ،تغذية المحركات العاملة بالجهد الثابت وأعمال جلفنة المعادن وغيرها.

ولهذه الأغراض يتم استعمال المقومات الإلكترونية للجهد والتيار المتردد من الشبكة الكهربائية للحصول على جهد وتيار ثابتين. تتكون الدوائر الإلكترونية لهذه المقومات من صمامات السيلكون الثنائية أو من صمامات السيلكون المحكمة وبالرغم من سهولة بناء مثل هذه الدوائر وفوائدها العديدة إلا أنها تسبب موجات ثانوية ذات ترددات متفاوتة الذبذبة (موجات توافقية). حيث تسبب هذه الموجات مشاكل مختلفة في الشبكة الكهربائية المغذية للمقومات الإلكترونية مثل زيادة الفاقد ،تدني معامل القدرة، تشويه موجة الفولتية والتشويش على أجهزة الإتصالات وأجهزة التحكم المرتبطة مع الشبكة الكهربائية.

في هذه الرسالة تم استعراض ومناقشة بعض الحلول للحد والتقليل من مشكلة التوافقيات واضرارها على الشبكة الكهربائية ومن هذه الحلول استخدام مرشحات سعوية وحثية عند تغذية محولات القدرة الإلكترونية بأشكال مختلفة ووظائف متنوعة. أن استخدام مثل هذه المرشحات عمل على تحسين شكل موجة التيار والفولتية وبالتالي زيادة معامل القدرة والحد من التشويه لموجة التيار الوارد من الشبكة الكهربائية الامر الذي يؤدي الى تقليل الفاقد ورفع الكفاءة وتقليل معامل التشويش التوافقي .

ج

وللحصول على أفضل النتائج تم عمل محاكاة لهذه المرشحات بأشكالها المتعددة حيث
أقترنت أفضل النتائج بعدد معين من المعايير على رأسها وأهمها معامل التشوه التوافقي
الكلي لموجات التيار المزود من الشبكة وتوصلت الرسالة الى أن أفضل النتائج كانت مقرونة
بدوائر مرشحات تمرير الترددات العالية.

